Alma Mater Studiorum – University of Bologna

SCHOOL OF SCIENCE
Department of Industrial Chemistry "Toso Montanari"

Second cycle degree in

Low Carbon Technologies and Sustainable Chemistry

Classe LM-75 - Scienza e Tecnologie per l'Ambiente e il Territorio

Study on health status and remediation potential of *Phragmites australis* employed in an Emilia Romagna (IT) Constructed Wetland to assess zonal variability of the facility.

Experimental degree thesis

CANDIDATE
Francesco Chioggia

SUPERVISOR
Chiar.mo Prof. Stefano Del Duca

CO-SUPERVISOR
Dr. Iris Aloisi

Academic Year 2020-2021

Abstract

Phragmites australis (Cav.) Trin. ex Steud. is a hydrophyte particularly resistant to harsh conditions, *e.g.* drought, high salinity, contaminants, such as heavy metals and toxic molecules, and high nutrients concentrations. These resistances make the plant suitable for water depuration, where its particular metabolism is exploited to remove pollutants and excessive nutrients from the environment. In constructed wetlands, this principle is applied to purify wastewater of various origins. In the framework of a pre-existing project of the Department of Agricultural and Food Sciences (DiSTAl, University of Bologna), this work integrates the knowledge and data relative to a constructed wetland plant in Budrio (Emilia Romagna, Italy), in order to expand the knowledge about this particular facility and of the phytopurification systems in general. For this purpose, different specimens of *P.australis* were sampled along the route of the wastewater in the wetland, following a hypothetic contamination gradient. The health status and the elemental uptake of the plants sampled were investigated, evaluating antioxidants (both non-enzymatic and enzymatic) and chlorophylls content, net photosynthetic rates, the elemental composition of the specimens and structural differences through optical and SEM microscopy. To do so, the existing protocols published in literature were reviewed and compared, in order to optimise the procedure and to select the best conditions to perform the analyses, as well as to integrate information missing in literature or found as contradictory.

Eventually, the results were compared amongst the examined *P. australis* specimens with the aim to detect areas where there might be a higher stress due to a different wastewater composition.

Keywords: constructed wetland, phytoremediation, oxidative stress, antioxidant assays, antioxidant enzymes, spectrophotometry.

Abbreviations:

ABS, Absorbance; ABTS, 2,2'-Azino-bis(3-ethylbenzthiazoline-6-sulfonic acid); APX, Ascorbate Peroxidase; CAT, Catalase; DPPH, 2,2-Diphenyl-1-(2,4,6-trinitrophenyl)hydrazin-1-yl; EDTA, Ethylenediaminetetraacetic Acid; EDX, Energy-Dispersive X-ray Spectroscopy; FRAP, Ferric Ion Reducing Antioxidant Power; ICP, Inductively Coupled Plasma; OES, Optical Emission Spectroscopy; PBS, Phosphate buffer solution; PCA, Principal Component

Analysis; PRL, Phragmites, Reference, Leaves; ROS, Reactive Oxygen Species; SEM, Scansion Electron Microscopy; SOD, superoxide dismutase; TPTZ, tripyridyltriazine.

For samples names, refer to Table 1, Section 3.2.

Index

1. Introduction

1.1. Nonpoint Source Pollution and Water Resources

Nonpoint source pollution is a form of intermittent pollution whose origin is not ascribable to a specific, easily identifiable source, and deriving from many activities, such as agriculture, silviculture, urban activity, and mining [1].

In agriculture, nonpoint source pollution derives from the usage of fertilisers, phytochemicals and pesticides, washed away by rainfalls and irrigation water and, consequently, spread into the environment. Being water one of the most important resources, it is characterised by a high value, since it is fundamental for almost all human activities, ranging from domestic to industrial, and for the ecosystems in general [2,3]. Freshwater availability has a strong impact on crop production and food security, but it is often limited in quantity, and it is vulnerable to human activities, *e.g.* urbanisation, irrigation, agriculture, silviculture, urban activity, mining and industrialisation in general [1,4,5]. Water, in fact, can be contaminated by chemical species, including nutrients in excessive concentrations (C, N and P in particular), heavy metals, pesticides, hydrocarbons, microplastics and antibiotics, and by biological agents as well, such as pathogenic bacteria, viruses, protozoa and parasitic worms. When present in drainage water, these species and their derivatives could spread into the water bodies and to enter the food chain, constituting a serious threat to human health and ecologic balances: beside intoxication, contaminated water can lead to an imbalance in the ecosystem nutrients, consequently leading to eutrophication, *i.e.* favouring the proliferation of some species, as algae and water plants, up to a point where they no longer permit survival to others [6,7]. This contamination is most likely to occur as consequence of an improper crop management [8]. Additionally, being contaminated water not usable for most of the human activities anymore, the consequent water shortage can cause severe difficulties, and numerous nations are currently being socioeconomically affected by it [9].

It is therefore of utmost importance to apply a correct management plan and to implement, when possible, systems of restoration and reuse of effluents such as greywater, black water and agricultural and industrial sewage. The development and application of new approaches and technologies aiming to mitigate, if not resolve, the clean water shortage issue is of great interest. With the aim to reduce the anthropic impact on the Planet, it can help to preserve the delicate ecosystem equilibria and to maintain essential resources, as water and soil, available. [10,11,12]. Many solutions have been hitherto developed and studied for such purpose, ranging from physical and chemical to biotechnological, including their combinations, each

characterised by its own uniqueness, merits and demerits[10,12,13,14].

In a perspective of circular economy, a special and arising interest is also represented by the recycle of the contaminants, in particular nutrients, that can be recovered and employed anew, re-entering the agro-industrial and biotechnological production chains, *e.g.* as soil conditioners[15,16,17].

1.2. Phytoremediation

In the framework of renewable energies and green economy, biological and, in particular, sustainable technologies are gaining interest: cheaper, less economically impacting and more environmentally friendly in respect to the intensive technologies, such solutions take advantage of biological agents, *e.g.* nematodes, bacteria, algae and macrophytes, to employ them in applications including biofilters, bioreactors, composting and microbial fuel cells, to treat wastewater and to depollute the environment [18,19]. A particular case, phytoremediation involves the application of specific plants and associated microbial communities to remove contaminants from soil, air and water, by exploiting their metabolic pathways in a diversity of applications [20].

Depending on the physiology and metabolism of the employed organisms and on the nature of the pollutant, contaminants follow various pathways and are consequently processed in different manners:

- *Phytostabilisation* implies a fixation of the molecules at issue, performed by the root apparatus through immobilization or precipitation. This favours a reduction of the mobility of the pollutants in the soil and prevents, therefore, a spread in the adjoining areas.
- In *phytoextraction* the pollutants are absorbed from the environment and translocated within the plants tissues; this results in the sequestration of the molecules and their accumulation in different organs, depending on the plant metabolism.
- In *phytodegradation* the organic contaminants are transformed into less toxic or non-toxic forms either inside the plant or directly in the ground, via excreted enzymes.
- *Rhizofiltration* involves the use of the root apparatus to absorb, accumulate or precipitate pollutants from wastewater.

- *Phytovolatilisation* implies a transformation of the contaminants into volatile, less toxic and less concentrated forms which get eventually vented into the atmosphere [21,22,23].

In parallel to environmental depollution, phytoremediation concurs to reduce the greenhouse gasses: through photosynthesis, in fact, plants consume the atmospheric carbon dioxide, fixing it in their structures via the Calvin-Benson Cycle and, thus, removing it from the atmosphere [24]. Being driven by solar energy, this applied science particularly suits the current scientific efforts to follow and promote a green approach, in the attempt to decrease and resolve the anthropic impact on the planet [21].

Aside from having a reduced environmental impact, the employment of phytoremediation rather than physical and chemical treatments offers additional advantages, because the remediation activity can benefit from a synergy involving the local environment as a whole, leading to the constitution of a multifunctional ecosystem [25].

In addition, considering the constant increase in the overall land price, the restoration of contaminated areas may result an appealing strategy, with the dual advantage of returning value to contaminated areas and, thus, to reduce the land use change, making available areas otherwise unusable [26].

By selecting and growing adequate phytoremediating plants in the contaminated sites, especially when employing perennial species, the soil remains mostly undisturbed; it is thus possible to recover and even improve its properties, including texture, physiochemical balances and equilibria of microorganisms. This would help to promote revegetation and to establish or renovate the local fauna [27]. Furthermore, it is possible to employ a multitude of plant species which, apart from synergistically cooperate, can provide a spectrum of resources, such as biomass, biodiesel and herbalism material, depending on their phytoremediation-related metabolism [21].

The application of green technologies is an approach which arouses the acceptance of the public, since it meets its interests in sustainability, green solutions, economically viable alternatives to intensive treatments, low secondary waste production, low environmental impact, preservation of soil fertility, restoration of habitats and green areas, and increase in floral and faunal biodiversity [28,29]. Involving such a variety of factors, phytoremediation implies a synergy not only of ecosystem elements, but of diverse scientific fields as well, highlighting how cooperation amongst disciplines is fundamental for resolving the global

climatic issue [30]. Thus, it potentially constitutes a great opportunity for the enterprises to grow and ameliorate their public image, and, consequently, to increase their market competitiveness [31].

1.2.1. Phytodepuration

Due to the use of fertilisers, phytochemicals and pesticides, water deriving from agricultural activities might be characterised by a certain degree of contamination represented by nutrients, heavy metals and organic compounds.

Plant decontamination technology was proved to be suitable for restoring the quality of such contaminated water, and can be easily integrated in already-existing facilities, such as agricultural crops and industrial plants [32,33] . This type of phytoremediation it is named *phytodepuration*.

1.2.1.1. Phytodepuration Applied: Constructed Wetlands

One amongst the emerging green solutions that employ plants for depollution are constructed wetlands. They constitute an environmentally friendly, simple and relatively cheap technology, consisting in the establishment of an area where effluents, including landfill leachate, storm water, domestic sewage, industrial wastewater and mine drainage, are collected and treated with selected plant species and symbiotic bacteria [34,35]. One example of constructed wetland is the Budrio CER wetland, reported in the image; photo form Lavrnić *et al.* [36].

The systems are constituted by beds packed with substrate material of various nature, including natural materials, artificial media and industrial by-products, *e.g.* clay, sand, gravel, shells and/or stones of fruits, bricks, steel slag, concrete and biochar, which supports the growth of the plants and the microbial communities and which actively participates in decontamination of the effluents, forced to follow specific pathways [37,38,39].

Hydrologic feature and the type of vegetation determine the constructed wetland category (Figure 1). Respectively, constructed wetlands can be classified as open water surface flow (A) and sub-surface flow (B); the flow can be vertical (B) and horizontal (C); while the plant species can be free-floating (D), floating-leaved (E), submerged (F), and emergent (G) [40,41].

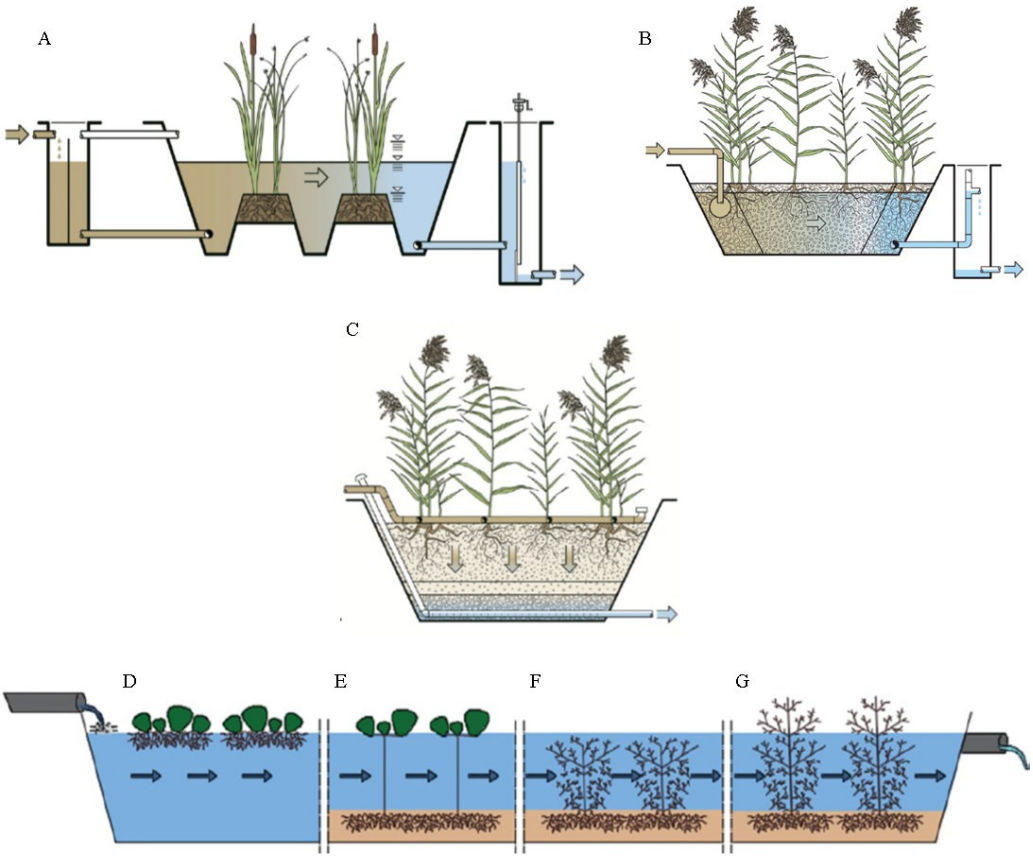

Figure 1: constructed wetlands classifications based on: hydrology (A,B), effluent flow path (B,C) and macrophyte types (D-G) [40,41].

These installations offer the additional possibility to recover the contaminants that can then re-enter the production chain as useful substances, such as nutrients and organic matter, with the synergistic effects of waste re-evaluation, resource preservation and recycle and environmental impact mitigation, in accordance with the current scientific efforts to follow and promote a green approach, in the attempt to decrease and resolve the anthropic impact on the planet [14,21,42]. Solar-energy driven, constructed wetlands constitute, therefore, an attractive and sustainable alternative to conventional water treatment systems, which can moreover result appealing to companies, by offering new market opportunities and increasing the business competitiveness, promoting thus the growth of this sector and attracting Governmental and Community subsidies; while representing an innovative and efficient solution to the water shortage, the pollution and the aforementioned environmental issues [43,44,45].

Some examples of applications are represented by the study of Sun *et al.* (2006), who focused in particular on spiked water, *i.e.* with added contaminants, mimicking the effluents deriving from an agroindustrial facility. In these studies, the facility decontamination efficiency was

assessed and a reduction of 80 % in dissolved oxygen depletion due to biochemical and chemical processes, and the formation of biofilms capable to degrade organic pollutants were highlighted [46]. Another investigation regarding agroindustrial wastewater treatment with constructed wetlands is represented by the study of Elsaesser *et al.*, who focused on the degradation of different common pesticides, assessing a mean reduction of 72 % in non-vegetative cells and of 92 % in vegetative cells. A retention of around 5 % within the facility and an uptake of 4 % by the plants was also estimated, leading to an net overall toxicity reduction of 95 % [47].

1.2.1.2. Surface Flow Constructed Wetlands

Cheap, easy to establish and maintain, the open water surface flow constructed wetland is proved to be suitable for agroindustrial wastewater treatment [48,49]. As shown in figure 1A, in this kind of wetlands, the water surface is exposed to the atmosphere, guaranteeing the formation and maintenance of an aerobic layer. As result of water oxygenation, oxidative phenomena are favoured and enhanced, *e.g.* nitrification, phosphorus processing and organic matter oxidation, plants and aerobic microorganisms metabolisms [50]. Finally, resembling a natural marshland where vegetation is partially submerged, surface flow constructed wetlands can provide wildlife habitats, improving the ecological impact mitigation and habitat restoration[51].

1.2.1.3. *Phragmites australis* in Constructed Wetland

The Poaceae family member *Phragmites australis* (Cav.) Trin. ex Steud, commonly referred as reed, is a cosmopolitan perennial plant occurring in a wide range of habitats, including inland and coastal salt-affected wetlands, as well as drought-affected areas and zones subject to flooding [52,53]. Such adaptability to environmental conditions is granted by its ability to employ different protection and degradation mechanisms, such as phytoextraction, phytodegradation and phytostabilisation, as well as microbial boosting, to cope with harsh conditions, as contaminated soil, drought and hypoxia, without an excessive impairment of its functions [53,54]. Thanks to such features, jointly with a high biomass production, *P. australis* has been studied for the application in phytoremediation, and resulted to be particularly suitable for constructed wetland establishment, since capable of absorbing and processing several contaminants from wastewater [55,56]. In the image: *P. australis*, photo of the author.

1.3. Indirect Environmental Status Assessment: Approaches and assays

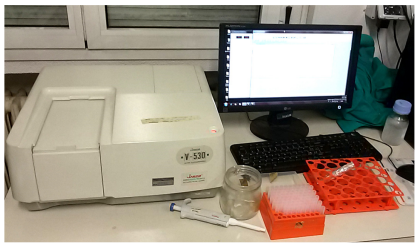

Beside being actively involved in phytoremediation, plants can be indicators of the area pollution levels: some studies demonstrated that some of their biological parameters, as chlorophyll content, and antioxidant molecules and enzymes production, are related to the stress levels that the species experience in contaminated habitats [57,58]. By studying these parameters, the possibility to assess the environment status and to indirectly monitor it during time was surveyed [59,60]. Moreover, also morphological and sonicmostly in leaves tissues and chloroplasts [61]. This is possible as biotic and abiotic stresses are translated within the cells as oxidative stress, characterized by the over- production of highly reactive oxygen species (ROS) represented predominantly by superoxide anion (O^{2-}), hydrogen peroxide (H_2O_2), hydroxyl radical ($^{\cdot}OH$), and singlet oxygen ($^1O_2$). Overproduction of ROS in chloroplasts of plants under stress has been described and is suggested to be the major factor responsible for oxidative damage in leaves [62]. Plants have defensive mechanisms and utilize several biochemical strategies to avoid damage caused by ROS.

A huge variety of natural antioxidants occur in plants, and these comprise of phenolic acid, flavonoids/bioflavonoid, tannic acid (tannins) and commonly less lignans and stilbenes which are collectively referred to as polyphenols (phenolics) [63]. Furthermore, the amino acid proline, an osmosolute and cellular protector largely accumulates in several plant species in response to salt and water stress, acting as direct antioxidant [64].

Plant enzymatic defences also include antioxidant enzymes such as the phenol peroxidase (POX; EC 1.11.1.7), ascorbate peroxidase (APX; EC 1.11.1.1), glutathione peroxidase (GPX; EC 1.11.1.9), superoxide dismutase (SOD; EC 1.15.1.1), and catalase (CAT; EC 1.11.1.6) which, together with other enzymes of the ascorbate-glutatatione cycle, promote the scavenging of ROS. POX is widely distributed in all higher plants and protects cells against the destructive effects of H_20_2 by catalysing its decomposition through oxidation of phenolic and endiolic cosubstrates. SOD catalyses the dismutation of O_2 to H_2O_2 and molecular oxygen. CAT is present in the peroxisomes and is involved in the detoxification from H_20_2 by catalysing its decomposition into O_2 and water [65].

In the image: spectrophotometrical analysis in progress with Jasco V-530 spectrophotometer. Photo of the author.

1.3.1. Structural Analysis: Optical and Scansion Electron Microscopy

Plant growth and anatomy are both directly affected by pollution in general, being ground and water pollution not an exception. Some studies examined the influence of high pollution levels on the plant structures at microscopic levels, and assessed differences between plants growing in unpolluted areas and specimens subjected to pollution [66,67,68]. Changes in photosynthesis, chloroplast morphology and proteomic composition after abiotic stress have been characterised and these microscopic differences can be highlighted by high magnifications, for example by using SEM, which allows the acquisition of more magnified and detailed pictures of the samples, compared to the optical microscope, by applying a high voltage to an electron beam, obtaining as result wavelengths much smaller than the photons' [61,69]. In the image: SEM analysis ongoing with Hitachi S-2400 Scanning Microscope. Photo of the author.

1.3.2. Non-Enzymatic Antioxidants Assays

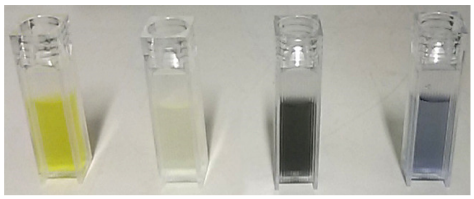

Amongst the NEA assays, ABTS, DPPH, FRAP and Flavonoid-$AlCl_3$ complexation are commonly employed for the quantification of antioxidant. Easy and rapid to performed, these methods are centred on UV-Visible colourimetry. Plants and other natural products contain hundreds of compounds acting as natural non-enzymatic antioxidants. Therefore, several methods have been developed to quantify these compounds individually. The techniques are different in terms of mechanism of reaction, effectiveness and sensitivity. Methods that are widely used to measure the antioxidant activity level in plant extracts can rely on the UV-visible signal decrease of oxidising molecules due to their reduction through the samples antioxidant content, e.g. ABTS and DPPH assays. Alternatively, the generation and dose-dependent increase of a UV-Visible signal might also occur, as in the Flavonoids-$AlCl_3$ complexation and FRAP assays, where such antioxidants form photo-active complexes

[70,71,72,73]. They can, therefore, be readily applied to monitor the health status of plants, and to assess their response to environmental stress. In the image: cuvettes with reacted antioxidant assay mixtures, photo of the author.

1.3.3. Enzymatic Antioxidants Assays

Unitedly with antioxidant molecules, plants express enzymes that concur to the organism detoxification, in particular by processing the excess of reactive oxygen species that are generated within. Amongst the many studies, Elavarthi and Martin (2010) optimised pre-existent spectrophotometric assays for enzymatic antioxidants, which permit to easily measure their activity and, hence, assess the plants response to the environmental stress [74]. In the image: multiwell plate with reacted SOD assay mix, photo of the author.

1.3.4. Elemental Analysis: ICP-OES

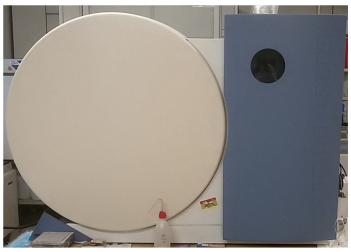

As some plants can absorb nutrients and pollutants from the soil and accumulate them within their structures, the monitoring of their status and their efficiency in depollution, as well as - indirectly - the environmental concentrations of such species, can be performed through elemental analysis [48,55,57]. Based on the matter ionisation and subsequent atomic and ionic signal registration, Inductively Coupled Plasma-Optical Emission Spectroscopy (ICP-OES) is one of the techniques that can be applied to detect and quantify many elements, in particular metals, contained in the samples [75]. In the image: Spectro Arcos-Ametek ICP-OES, photo of the author.

2. Aim of the Study

In the framework of a pre-existing project of Department of Agricultural and Food Sciences (DiSTAl), this work integrates the knowledge and data relative to an Emilia Romagna (IT) constructed wetland plant managed by Consorzio di Bonifica Canale Emiliano Romagnolo, in order to expand the knowledge about this particular facility and of the system in general. By assaying antioxidants, both non- enzymatic and enzymatic, chlorophylls content and by measuring the elemental composition of the specimens, the health status and the elemental uptake of the wetland *P. australis* specimens sampled in different areas were investigated. Results were compared amongst the examined plants with the aim to detect areas where there may be a higher stress due to a different wastewater composition, potentially varying along the constructed route, and to further examine the plant properties.

In addition, the protocols applied to the plant material extraction and the assays for antioxidant assessments were optimised, in order to reduce resource and time waste and to increase their reliability, as well as to integrate missing data such as minimum extraction time and reagent solutions durability.

3. Materials and Methods

3.1. Study Area

The sampling was performed on a surface flow constructed wetland (Figure 2) associated to a 12.5 ha experimental agricultural farm (44°34'22.2" N, 11°31'44.9" E) of the Canale Emiliano Romagnolo Land Reclamation Consortium, in the vicinity of Emilia-Romagna Budrio village, Italy. Characterised by a subtropical humid climate (Cfa) according to the Köppen classification of climate, the area has a mean annual temperature of around 13.7 °C and a mean annual rainfall of 771 mm, with most of precipitations during spring and fall, as specified by Regional Agency for Environmental Protection (ARPAE) from 30-year normal values [48].

The facility was established on an Udifluventic Haplustept soil (Soil Survey Staff, 2010)[76], and consists of a non-waterproofed channel of 470 m with four meanders, with an overall surface of 0.4 ha and a width to length aspect ratio of approximately 1:52. The capacity of the system is 1477 m^3, with an average depth of 0.40 m, and hosts mainly *P. australis*, *Iris* spp. and *Carex* spp. [36].

As reference and for protocols optimisation, a *P. australis* specimen was harvested from the Bologna Botanical Garden (44°30'3.4" N, 11°21'14.4" E). Characterised by a subtropical humid climate (Cfa) according to the Köppen classification of climate, the area has a mean annual temperature of around 14.3 °C and a mean annual rainfall of 825 mm, with most of precipitations during spring and fall, as specified by ARPAE from 30-year normal values [48].

Plant sampling occurred at the end of the vegetative cycle, on November 4th 2020, in order to evaluate the whole extent of the pollutants removal and accumulation potential, and to achieve data uniformity with the colleague research group of Agronomy.

The wetland area was divided in three zones, and the sampling was based on the position on the water route, performed choosing the healthiest plants, *i.e.* adult specimens, photosynthetically active and with lowest chlorosis.

3.1.1. Zones Description and Plants Selection

In the Zone 1 (Z1) the flowing water should arguably present the lowest pollutant concentrations, being towards final section of the wetland channel. The only species present was *P. australis*, whose 4 specimens were collected.

The Zone 2 (Z2) is the middle of the water route, and was detected as host of the highest

vegetal variety along the wetland. Followed by *Iris* spp., *P. australis* resulted the most abundant species of this area, and 2 specimens were collected.

In Zone 3 (Z3) the water is first injected in the treatment plant, and should contain the highest pollutant levels. Being present in almost all of the wetland, *P. australis* were selected as the overall reference, and here collected in 2 samples. Particularly abundant, Carex spp. were also present. To obtain the soil composition profile and to examine potential correlations with the plants, soil samples were extracted as well in cylindrical sections up to 60 cm deep. The collected soil was divided in 4 sections, corresponding to the depth of 0-5 cm, 5-15 cm, 15-30 cm and 30-60 cm.

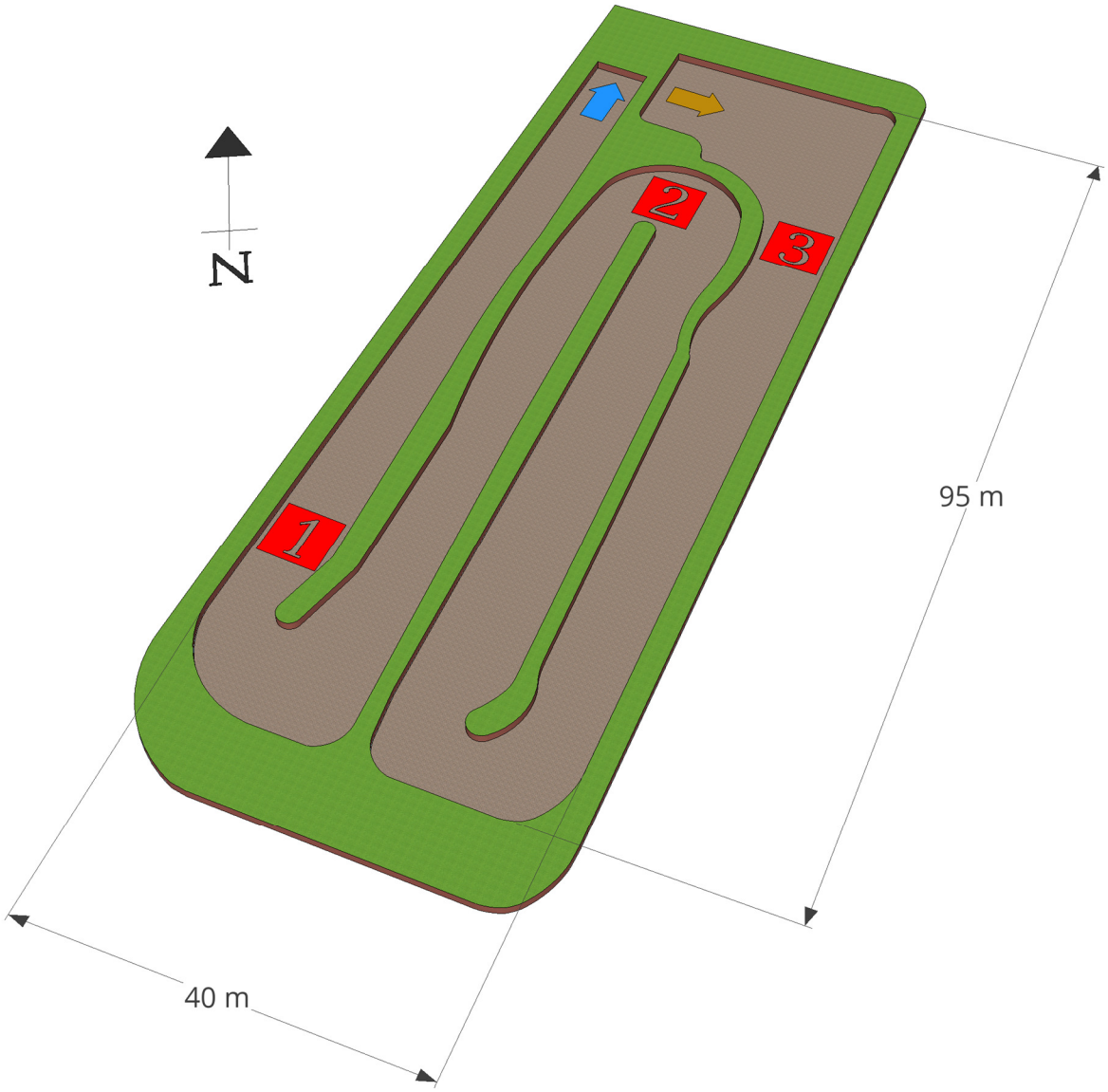

Figure 2: Budrio surface flow constructed wetland 3D model; sampling zones are highlighted in red. The arrows indicate the input (dark orange) and output (blue) of the effluents. Model of the author.

Throughout the year, 14 wastewater samples were gathered at the inlet, with the aim to study its composition and its variation over time; each sample corresponds to a date throughout one year of the facility operation cycle: 23-01-2020, 24-07-2020, 03,04,05-08-2020, 22-09-2020 (x4), 11-12-2020, 14-12-2020, 03,09-12-2020, 07-01-2021.

The reference specimen was sampled in a sunlit area adjacent to a pond.

3.2. Samples storage

Each plant specimen was cleaned from dirt, rinsed and sectioned in the following organs, in order to separately collect the broadest variety of tissues:

- Leaves
- Stem
- Rhizome
- Roots

Figure 3: sampling on November, in Budrio CER wetland. Photo of the author.

During the processing, the sample P1Z3 resulted to have not enough roots to be analysed; therefore, data about such sample part are missing.

For the reference specimen, only the leaves were harvested, since employed for the pigments and antioxidant assays protocols optimisation only.

The healthiest parts, especially green leaves with no or very low chlorosis and deprived of sheath, were then cut into pieces of ≤5 mm and mixed to reduce the potential composition variability.

Four different methods of sample storing were tested to assess which one best preserved the samples for the chosen analysis: each of the part was portioned in 4 aliquots, and prepared as follows:

1. Oven drying at 40 °C until reaching a constant weight;
2. Freezing at -80 °C;
3. Fixation with 2.5 % (v/v) glutaraldehyde in 100 mM phosphate buffer pH 7.4 overnight and subsequent dehydration in increasing concentrations of ethanol (from 30 % to 100 %);
4. Dehydration in 10 % ethanol + 3 % acetic acid.

Figure 4: samples preparation after the harvest. Photo of the author.

Figure 5: some of the samples treated with glutaraldehyde.

Zone	1				2		3	
No. / Part	1	2	3	4	1	2	1	2
Roots	P1Z1R	P2Z1R	P3Z1R	P4Z1R	P1Z2R	P2Z2R		P2Z3R
Rhizome	P1Z1Rh	P2Z1Rh	P3Z1Rh	P4Z1Rh	P1Z2Rh	P2Z2Rh	P1Z3Rh	P2Z3Rh
Stem	P1Z1S	P1Z1S	P1Z1S	P1Z1S	P1Z1S	P1Z1S	P1Z3S	P2Z3S
Leaves	P1Z1L	P1Z1L	P1Z1L	P1Z1L	P1Z1L	P1Z1L	P1Z3L	P2Z3L

Table 1: *P. australis* harvested specimen list, with the respective sampling zone, number and univocal denomination.

The soil samples were cleaned from any plant parts, crushed, sieved and milled.

3.3. Chemicals and Reagents

The following chemicals and reagents were provided by Sigma-Aldrich, Inc.: (+)-Sodium L-ascorbate, A7631, crystalline (≥98 %); 2-mercaptoethanol, M3148, GC/titration grade (99 %); 2,2′-azino-di-(3-ethylbenzthiazoline sulfonic acid) (ABTS), A1888-1G, HPLC grade (≥98 %); Acetic acid, 33209, ACS reagent grade (≥98 %); Acetone, 32201-1L-M, GC grade (≥95.5 %); $C_2H_3NaO_2 \cdot 3H_2O$, S7670-500G, BioXtra grade (≥99.0 %); DL-Methionine, 64340, ≥99.9 %; 2,2-diphenyl-1-picrylhydrazyl (DPPH), D913-2, 99.9%; $FeCl_3 \cdot 6H_2O$, F2877, reagent grade (≥ 98 %); Glutaraldehyde, 340855, 50 % wt. in H_2O; Hydrochloric Acid, 30721, ACS reagent grade (≥37 %); $K_2S_2O_8$, 216224-5G, ACS reagent grade (>99.0 %); NA_2CO_3, S7795, BioXtra grade (≥99.0 %); Nitro Blue Tetrazolium (NBT), N6639, molecular biology grade (≥90.0 %); Riboflavin, R-4500, ≥98 %; Quercetin, Q4951, HPLC Grade (≥98 %); 2,3,5-

triphenyltetrazolium chloride (TPTZ), T1253, Spectrophotometric grade (≥98 %); Triton™ X-100, T8787, molecular biology grade , (≥99 %); Trolox, 238813-1G, (97 %).

$AlCl_3 \cdot 6H_2O$, 416946 reagent grade (≥99 %); K_2HPO_4 anhydrous, 471786, ≥99 %; KH_2PO_4, 471686, ≥99.5 %; H_2O_2, AH/1811/17, electronic grade (≥30 % w/v) were provided by Carlo Erba Reagents.

$C_2H_3KO_2$, 236500, ACS reagent grade (>99 %); Ethylenediaminetetraacetic acid (EDTA), 03610, ≥99.0 %; HNO_3, 17952, PURANAL™ semiconductor grade, (≥69 %) were provided by Honeywell Fluka™. Ethanol was provided by Silcompa, 8937, technical grade (99.9 %). Methanol was provided by Honeywell Chromasolv™, 34860-1L-R, HPLC grade (≥99.9 %).

MilliQ 18.2 MΩ cm^{-1} water was produced with Sartorius Stedim Biotech Arium® pro VF Ultrapure Water System.

Community Bureau of Reference provided the Reference material No. 482: Trace elements in Lichen (*Pseudevernia furfuracea*), Sample identification No. 714, for the IPC-MS analysis.

3.4. Instruments, Equipment, Software & Materials

For the microscopic analyses and imaging, a Leica DM750 microscope equipped with a Leica ICC50 W camera was employed.

For the SEM analyses and imaging, the plant samples were coated with gold with Bio-Rad SC 502 SEM Coating System and subsequently analysed with a Hitachi S-2400 Scanning Microscope at 18 kV, interfaced with DIPS Digital Imaging Processing System 2.6.20.1. The samples were coated with carbon through an Edwards S150B Sputter Coater for the SEM-EDX analysis and imaging performed with a Jeol JSM – 5400 Scanning Microscope at 15 kV, 33 µA equipped with a SGX Sensortech IXRF Systems Model 55i interfaced with the software Semaphor.

The powdered and homogenised samples were solvent-extracted, either with Elma Transsonic TP690 sonicator, 35 kHz, or on an ASAC S.R.L. 711/CT stirrer, used for the assays as well; and subsequently centrifuged with an Eppendorf 5804R Centrifuge. The resulting extracts and the reacted assay mixes were analysed with a Jasco V-530 UV/Vis Spectrometer (quick response mode, 2.0 nm band width, 1.0 data pitch) interfaced with Spectra Manager, version 1.54.03 (build 1), JASCO Corporation with Kortell S.p.a. Semi-micro 1,5mL optical polystyrene cuvettes, n. 1938, 1 cm optical path length.

For the SOD assay, the reaction was carried out by illuminating the plates with the samples with a 21W, 0.17 A, 3000 K fluorescent light of DURA® Lamp, Italy, emanating a light of 120 lux, after having posed them on a stirrer at 100 oscillations min-1 and at 15 cm from the light source. The analyses were then performed with an Infinite 200 PRO - Tecan Austria GmbH (configuration: Infinite M Nano) microplate reader, interfaced with the Tecan i-control, version 3.9.1.0 software; on Costar 3548 - 48 Well Cell Culture Cluster, Flat Bottom and on Falcon 353078 Multiwell 48 wells microplates.

For the elemental analyses, Whatman filters no. 42, CAT no. 1442-125, Sartorius Biolab Products - Sartolon® Polyamid 0.45 µm filters, and a simultaneous and sequential ICP-OES Spectro Arcos-Ametek, 160 nm ~ 780 nm, equipped with ASX-520 AutoSampler, interfaced with the software Smart Analyser Vision 5.01.0926 - Spectro Smart Studio, were employed.

For carbon and nitrogen content, a Flash 2000 Series Organic Elemental Analyser, equipped with a Delta V Advance IRMS was used.

Documents redaction, data elaboration and graph plotting were performed with Microsoft Office 365©. For spectra elaboration, Spectra Manager for Windows, version 1.53.04 (build 1), JASCO Corporation was employed. For the 3D model creation, it was used Google LLC SketchUp© Trimble, Inc.. Adobe® Photoshop® 5.0 was employed for image processing. For multivariate analysis it was utilised RStudio®.

3.5. Structural Analysis

For the structural analysis, the samples treated with glutaraldehyde and the samples in 10% ethanol + 3 % acetic acid were employed.

3.5.1. Optical Microscope

For each sample, a small transversal section of <1 mm was cut and deposited on a glass slide, a drop of water was added, and a glass cover was placed. During the microscope observation, pictures at 4x, 10x and 40x were taken and analysed.

3.5.2. SEM and SEM-EDX Analysis

For each sample, a small transversal section of <1 mm was cut and fixed on a stub coated with conductive carbon tape. The stubs were then either coated in gold and analysed with the

SEM apparatus or in carbon and analysed with the SEM-EDX apparatus. Pictures ad different magnification (20x ~ 15000x) were taken and analysed.

3.6. Sample Preparation and Extraction and Protocols Optimisation

3.6.1. Sample Preparation and Extraction for Pigments and Non-Enzymatic Antioxidants

For the preliminary analyses and the protocols optimisation, it was employed the PRL sample.

3.6.1.1. Chloroplast Extraction

600 mg of leaves were ground in 6 mL of a PBS solution 50 mM, EDTA 2 mM, 2-mercaptoethanol 10 mM, sucrose 300 mM, pH 7.5. The resulting solution was decanted in two 1.5 mL tubes and centrifuged at 3000 g and 4 °C for 7 minutes. The supernatant solution and the pellets were separated, re-suspending the latter with 100 µL of buffer solution and 4900 µL of 80% acetone [77]. The spectra of the two resulting solutions were then registered at the UV-Spectrometer between 400 and 700 nm, being the wavelength range that organisms employ for the photosynthesis, *i.e.* the photosynthetically active radiation [78].

Even if the protocol does not indicate the registration of the spectrum of the supernatant, the analysis was nonetheless performed, in order to evaluate the potential loss of solute in case of disposal.

3.6.1.2. Mix Investigation for Direct Solvent Extraction,

Having found in literature both 70 % and 80 % acetone mix as suggested extraction solvent, these two possibilities were investigated [79,80].

The *P. australis* leaf samples were powdered with a pestle in liquid N_2 in a mortar and homogenised; 300 mg of material were extracted with 15 mL of 70 % acetone and either stirred overnight at 100 oscillations min^{-1} or for 30 min with a sonicator. The extracts were then centrifuged for 5 min at 4500 g and 4 °C, the liquid phase recovered, and the resulting solutions stored at 4 °C until usage. In the image: sample powdering with mortar and liquid N_2. Photo of the author.

The analyses were performed in polystyrene cuvettes with a UV-Vis spectrometer, recording the spectra from 700 nm to 400 nm in quick response mode, 2.0 nm band width and 1.0 data

pitch, 200 nm min^{-1}. Considering this wavelength range, pure samples resulted to be too concentrated for an adequate signal record, since saturating the detector (refer to results, Section 4.2.5, Figure 12). Trials on dilution were therefore performed, and the dilution of 1:10 in either 70 % or 80 % acetone was selected as the standard dilution for the spectra, the chlorophylls and the carotenoids measurements, with the further objective to minimise sample consumption. 70 % acetone extracts showed slightly more intense spectra than the 80 % ones (Section 4.2.5, Figure 13); the first percentage was therefore chosen for the extraction procedures. Since the ultrasound-assisted extraction yielded an extract spectrophotometrically from the direct solvent one, the sonication was hence rejected to avoid inhomogeneity between the samples.

3.6.1.3. Extraction Time Study

Having found contradictory information regarding extraction time, this parameter was also contemplated in the present study [57,81,82].

After the selection of 70 % acetone as extraction mix, the material was extracted at the same parameters as previously described (see section 3.6.1.2), and the spectral analysis was performed at intervals of 1 h up to 8 h (for the spectra, refer to the results, Section 4.2.6, Figure 15). It was assessed that after 7 h of extraction, a plateau was reached; the information was hence integrated, and such time was applied to the extraction protocol.

3.6.1.4. Chloroplast vs. Direct Solvent Extraction

In the procedure of selecting the proper extraction protocol, a comparison between the chloroplast extraction procedure and the direct solvent protocol was conducted. Even if being less time consuming, the chloroplast extraction resulted to yield a less concentrated extract in comparison to the 70 % acetone, 7 h extraction (Figure 16). Moreover, it involves more passages and reagents, whereas the counterpart consists in a straightforward procedure. Therefore, the direct solvent extraction was elected as the standard procedure in this study.

3.6.2. Spectrophotometer Scanning Speed

From preliminary examinations, no difference was observed between the reference spectrum recording at 200, 1000 and 2000 nm min^{-1} (for the spectra, refer to Section 4.3, Figure 17). Hence, the measurements were performed at 2000 nm min^{-1} scanning speed, in order to optimise the analysis times.

3.6.3. Sample Storage Examination

3.6.3.1. Freezing

With the aim to reduce their degradation, it was assessed whether it was possible to store the extracts at -20 °C, by posing an aliquot of PRL extract for 12 h in freezer. The fact that the relative spectrum resulted to differ considerably from the 4 °C-stored sample (refer to section 4.4.1, Figure 18) might indicate that the extract decayed. To avoid inhomogeneity amongst the samples, it was opted for the 4 °C fridge storage.

3.6.3.2. pH Change

To assess whether the extracts storage could benefit of a pH change, as suggested by Setyati *et al.* (2020), in the dilution to 1:10 of the reference extract a fraction of the solvent was substituted with either acetic acid or Na_2CO_3 solutions, in order to reach a concentration of 2 % [83]. Nonetheless, it was opted to maintain the extracts in their native form, in order to avoid potential alterations of the non-enzymatic antioxidants assays, which might have experienced kinetic and thermodynamic modifications.

3.6.3.3. Sample Photolysis

In order to investigate the susceptibility of the extracts to light exposure, a sample aliquot was exposed to a fluorescent lamp for 20 min, and its spectrum was recorded before and after the exposure. Considering the results obtained (refer to section 4.4.3, Figure 20), it was decided to perform the extractions and to store the samples shielded from light.

3.6.4. Sample Preparation and Extraction for Pigments and Non-Enzymatic Antioxidants Assays: Assessed Extraction Protocol

After the preliminary analyses (Sections 3.6.1 and 3.6.2), it was opted for a solvent extraction of 300 mg of the samples in 15 mL of 70 % acetone - milliQ water mix, on a stirrer set at 100 oscillations min^{-1}, for 7 h and in the dark, and for a 4 °C fridge storage, shielding the samples from light in both phases. For the spectra recording, a 2000 nm min^{-1} scanning speed was chosen.

3.6.5. Sample Preparation and Extraction for Enzymatic Antioxidants Assays

Ground samples were lysated as indicated by Aloisi *et al.* with minor modifications [84]: 20 mg

of powdered leaves were suspended in 2 mL PBS 150 mM, pH 7.5 with 0.1 mM, sonicated twice on ice for 15 s and centrifuged for 25 min at 5000 g and 4°C. Freshly prepared crude extracts were used to determine CAT, SOD and APX antioxidant enzymes activities according to the protocols written by Elavarthi and Martin (2010) [74].

3.7. Sample Spectra Measurement: Chlorophylls and Carotenoids Content Calculation

Once obtained the spectra, the formulae which follow were applied to calculate the concentration of such molecules, deriving from the formulae proposed by Lichtenthaler (1987), corrected for the here-employed acetone concentration by linear regression extrapolation [85]:

$$\text{Chlorophyll a } (Chl_a, \text{ mg g}^{-1}) = \frac{(12.755 \cdot ABS_{663} - 3.165 \cdot ABS_{647}) \cdot \text{extracted material (mg)} \cdot \text{dilution factor}}{\text{extraction volume (mL)}}$$

$$\text{Chlorophyll b } (Chl_b, \text{ mg g}^{-1}) = \frac{(22.185 \cdot ABS_{647} - 5.555 \cdot ABS_{663}) \cdot \text{extracted material (mg)} \cdot \text{dilution factor}}{\text{extraction volume (mL)}}$$

$$\text{Chlorophyll a + b (mg g}^{-1}) = \frac{(7.2 \cdot Chl_a + 19.02 \cdot Chl_b) \cdot \text{extracted material (mg)} \cdot \text{dilution factor}}{\text{extraction volume (mL)}}$$

$$\text{Carotenoids (mg g}^{-1}) = \frac{(1000 \cdot ABS_{470} - 1.82 \cdot Chl_a - 85.02 \cdot Chl_b) \cdot \text{extracted material (mg)} \cdot \text{dilution factor}}{198 \cdot \text{extraction volume (mL)}}$$

3.7.1. Calibration Curves for Antioxidant Analyses

Considering the wavelengths studied in the non-enzymatic antioxidant assays (see section 3.9), it was assessed that sample spectra may increase the signal, and thus interfere with the readings and, consequentially, alter the quantifications. To prevent such issue, calibration curves were obtained by a progressive dilution of 150 µL of the reference sample with cumulative additions of 750 µL of 70% acetone, ranging from a factor of 1:10 to a factor of 1:43, and by registering the relative spectra (Figure 23), noting the signal at each wavelength examined in the NEA assays, *i.e.* 734 nm (ABTS), 693 nm (FRAP), 517 nm (DPPH), 415 nm (Flavonoids). For the spectra, refer to Section 4.5.1, Figure 23. The ABS value relative to each wavelength was then subtracted from the values obtained in the assays, in order to obtain their true values.

3.8. Non-Enzymatic Antioxidants assays

As for the chlorophylls and carotenoids assessment (section 3.7), pure samples turned out to be too concentrated for non-enzymatic antioxidants assays, and caused the signal to be either too low or too high, depending on the assay. A dilution of 1:2 was identified as the most suitable, and applied for all the extracts to be assayed for non-enzymatic antioxidants assays.

3.8.1. ABTS

As indicated by Miller *et al.* (1993) [71], 50 mL of 2 mM ABTS methanol stock solution was prepared and radicalised in the dark for 12 h by adding 500 µL of a 70 mM Potassium persulfate aqueous solution. The resulting solution was diluted to 1:25 (0.08 mM) with methanol prior to the assay, giving an absorbance (ABS) of 0.6 units at 734 nm.

A stock solution of 25 mM of Trolox was prepared by dissolving 312.9 mg of the chemical in 50 mL of methanol. Points of the calibration curve were prepared by diluting the Trolox solution to 3, 2, 1, 0.5 and 0.25 mM.

14 tubes of 1.5 mL volume were prepared: 5 for the standard curve, one for the blank, and one for each *P. australis* sample. 990 µL of the ABTS diluted solution, and 10 µL of (I) the standard (Trolox) at different dilutions for the calibration curve, (II) methanol or for the blank, and (III) the plant extract for the sample were added to each tube. The tubes were then shaken at 150 oscillations min^{-1} in the dark at room temperature for 5 minutes, and the ABS was read at 734 nm, employing methanol or ethanol as reference. Each set was performed in triplicate.

After some trials, it was assessed that the concentration of 2 mM was insufficient to give a good response, since the reactant got excessively decolourised by the samples, and the resulting signals resulted to be too similar to be distinguished. Therefore, it was employed 1:12.5 methanolic dilution (0.15 mM) of the radicalised ABTS stock solution, corresponding to an ABS of 1.10-1.12 units at 734 nm, at the same conditions.

With the aim to integrate the information about the radicalised ABTS stock solution storability, found as vague in the bibliography, a 4-month-old stock solution at the same dilution, previously stored at 4 °C, was simultaneously employed for the assay.

Additionally, in order to survey the possibility to reduce the hazardousness of the procedure, a set of analysis was prepared substituting methanol with ethanol, applying a dilution of 1:12.6

(0.16 mM), corresponding to an ABS of 1.10-1.12 units at 734 nm.

3.8.2. DPPH

A DPPH stock solution was prepared dissolving 200 mg L^{-1} (0.5 mM) DPPH in methanol, as shown by Thaipong *et al.* (2006)[72] and Chua *et al.* (2013) [73] and stored in the dark at -20 °C. For the assay, a dilution to 20 mg L^{-1} (0.05 mM, ABS_{517nm} = 0.52) was applied.

The calibration curve was prepared by diluting the Trolox solution to 500, 400, 300, 200 and 100 µM.

14 tubes of 1.5 mL volume were prepared: 5 for the calibration curve, one for the blank, and one for each *P. australis* sample. 840 µL of the DPPH diluted solution and 60 µL of (I) the standard (Trolox) at the different dilutions for the calibration curve, (II) methanol for the blank, and (III) the plant extract for the sample were added to each tube. Such volumes derive from the ones indicated in the original protocol, and were reduced keeping the proportions, in order to diminish reagents and sample consumption. The tubes were then shaken at 150 oscillations min^{-1} for 20 minutes in the dark at room temperature, and the ABS was read at 517 nm, employing the methanol or ethanol as reference. Each set was performed in triplicate.

Similarly to the ABTS assay, it was assessed that such concentration was insufficient to give a good response since the reactant was highly decolourised and the signals of the samples resulted to be too similar to be distinguished. Hence, 40 mg L^{-1} methanolic solution (0.1 mM, ABS_{517nm} = 1.19) was employed at the same conditions.

Since the relative information found in the bibliography resulted contradictory, to assess the storability of the DPPH stock solution a 4-month-old stock solution, previously stored at - 20 °C, was employed for the assay, at the same dilution.

Furthermore, in order to survey the possibility to reduce the hazardousness of the procedure, a set of analysis was prepared substituting methanol with ethanol for the other solution dilution.

3.8.3. FRAP

For each measurement set, a reaction solution was prepared mixing 30.6 mL of 0.3 M Sodium acetate buffer (pH = 3.6), with 3.0 mL of a 10 mM TPTZ in 40 mM HCl solution, and a 20 mM Ferric chloride aqueous solution, following the protocols of Ebner *et al.* (1967)[86] Thaipong et *al.*(2006)[72] and Chua *et al.*(2013)[73], with minor modifications: differently from

the original protocols, the volumes were hereby reduced in order to minimise reagents and sample consumption, using 1.5 mL instead of 15 mL tubes.

The points of the calibration curve were prepared by diluting the 25 mM Trolox stock solution to 3, 2, 1, 0.5 and 0.25 mM. If performing the FRAP assay during the same day of the ABTS assay, the employment of the same Trolox solutions for both the assays may reduce resource and time consumption.

15 tubes of 1.5 mL volume were prepared: 6 for the standard curve, one for the blank, and one for each plant sample. 1220 µL of the working solution, and 10 µL of (I) the standard (Trolox) at different dilutions for the calibration curve, (II) milliQ water for the blank, and (III) the plant extract for the sample were added to each tube were added.

To assess the reactants storability, a set was prepared employing a mix of 3-month-old stock solutions.

The tubes were shaken at 150 oscillations min^{-1} for 1 h at 37 °C, and the ABS was read at 593 nm, employing water as reference. Each set was performed in triplicate.

3.8.4. Flavonoid-$AlCl_3$ Complexation

For each measurement set, a reaction solution was prepared mixing 9 mL of methanol, 600 µL of $AlCl_3$, 600 µL of $C_2H_3KO_2$ and 16.8 mL of milliQ water, as previosly demonstrated by Bag *et al.*(2015)[87] and Setyati *et al.*(2020)[88], with minor modifications. In fact, differently from the original protocols, the volumes were hereby reduced in order to minimise reagents and sample consumption, using 1.5 mL instead of 15 mL tubes.

The points of the calibration curve were prepared starting from an ethanolic Quercetin stock solution of 1000 mg L^{-1} (3.3 mM), and diluting it with ethanol to 250, 125, 62.5 and 31.25, 15.625 and 7.8125 (sequential 1:2 dilutions) mg L^{-1}.

15 tubes of 1.5 mL volume were prepared: 6 for the calibration curve, one for the blank, and one for each plant sample. 900 µL of the working solution, and 100 µL of (I) the standard (Quercetin) at different dilutions for the standard curve, (II) milliQ water for the blank, and (III) the plant extract for the sample were added to each tube.

To assess the reactants storability, a measurement set was prepared employing a mix of 3-month-old stock solution, and a 3-month-old quercetin solution as standard for the calibration curve.

In order to survey the possibility to reduce the hazardousness of the procedure, a set of analysis was prepared substituting methanol with ethanol.

The tubes were then shaken at 150 oscillations min^{-1} in the dark at room temperature for 30 minutes, and the ABS was read at 415 nm, employing water as reference. Each set was performed in triplicate.

3.9. Enzymatic Antioxidants Assays

The following assays were performed applying the protocols proposed by Elavarthi and Martins (2010)[74], with some variations for the SOD analysis.

3.9.1. Superoxide Dismutase Activity as Function of Absorbance Difference

A buffer solution of 50 mM PBS buffer, pH = 7.8, 2 mM EDTA, 9.9 mM L-methionine, 55 µL NBT was prepared.

Regarding the riboflavin stock solution, the proposed concentration of 3.8 mg in 10 mL of water resulted to be too high for the compound to be fully solubilised. Hence, a higher solvent volume was employed, dissolving 3.8 mg of the compound in 50 mL of water; the assay volumes were corrected accordingly.

1.5 mL, instead of 2 mL, of buffer were poured into the wells of a microplate. To each well were added 15 µL of (I) the reaction mix as blank and (II) the sample, and 75 µL of riboflavin stock solution, instead of 15 µL. Each series was prepared in triplicate in order to obtain statistical significance and data. The plate was then fixed to a stirrer, set at 100 oscillations min^{-1}, and the reaction was started by illuminating the wells with a fluorescence lamp posed at 15 cm from the samples. The ABS readings at 560 nm were performed on a microplate reader, set for a 5 s, 1 mm amplitude shaking, with 25 flashes and 9 nm of bandwidth, and the values were subtracted to the blank, taken as negative reference

3.9.1.1. Time evolution

To examine the variation over time and to ensure the completion of the reaction, the measurements were performed every 10 min, until reaching 100 min, obtaining calibration curves relative to the exposure time. Between each illumination session, the samples were kept at dark, in order to avoid the undesired reaction progression.

The resulting ABS values were then subtracted to the blank signal.

3.9.2. Catalase Activity as Function of Time

A buffer solution of 50 mM PBS, pH = 7.0, was prepared and employed to dilute the samples to 1:200, whose 2 mL were poured in a cuvette; 1 mL of H_2O_2 30 % (w/w) was added to start the reaction. Each measurement was performed in triplicates. The change in ABS was monitored for 3 min at 240 nm; in the obtained ABS vs. time data, only the ranges which presented a significant slope were selected. Linear regression was then applied, in order to obtain the mean slope of the associated line, representative of the H_2O_2 decomposition rate of each sample. Such values were employed for comparing the different plant samples.

3.9.3. Ascorbate Peroxidase Activity as Function of Time

A buffer solution of 50 mM PBS, pH 7.0 and an aqueous stock solution of sodium ascorbate 100 mM were prepared; they were combined in order to obtain a 0final ascorbate concentration of 5 mM.

For each sample, 820 µL of the solution were poured into a cuvette, 10 µL of the extracts and, lastly, 170 µL of H_2O_2 10 % were then added to start the reaction.

The change in ABS at 290 nm, related to the ascorbate peroxidation, was recorded for 3 min. in the obtained ABS vs. time data, only the ranges which presented a significant slope were selected. Linear regression was then applied, in order to obtain the mean slope of the associated line, indicating of the ascorbate to dehydroascorbate oxidation rate of each sample. Such values were employed for comparing the different plant samples.

3.10. Elemental Analysis

To obtain the material for total suspended solids, variable volumes of each wastewater sample (from 100 to 200 mL, depending on the turbidity and ease of filtration) were vacuum-assisted filtered onto pre-weighted, oven-dried Sartolon® filters. The resulting material was oven-dried and its weight normalised to the employed volume. The solids were then recovered and prepared for the elemental analysis.

3.10.1. C, N Analysis

250 mg of each oven dried sample part was transferred into a tin vessel and analysed with the

Flash 2000 Series Organic Elemental Analyser.

3.10.2. ICP-OES Analysis

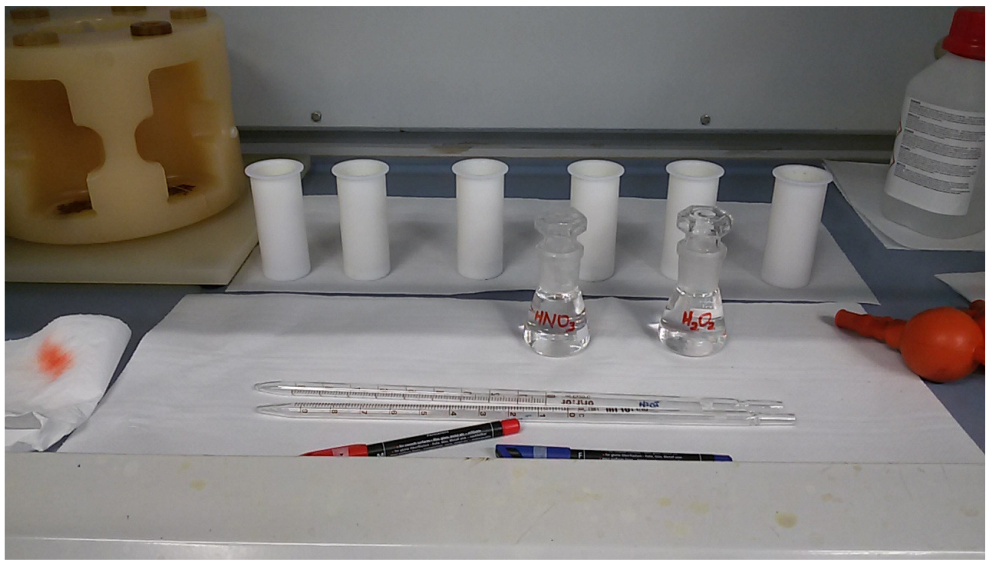

Figure 6: sample preparation for mineralisation.

For the plant and soil samples mineralisation, 200 mg of the each oven-dried sample were transferred in TFM™ cartridges (Figure 6); 0.5 mL of electronic grade H_2O_2 30 %, and 6 mL HNO_3 65 % were then added.

For the wastewater samples mineralisation, 19.8 mL of each were poured in TFM™ cartridges, and 0.2 mL of HNO_3 65 % were added.

The vessels were sealed and inserted in the microwave, set with the following working programme for the samples oxidative digestion: 250 W, 2 min; 400 W, 2 min; no power, 1 min; 750 W, 2 min.

The resulting solutions were transferred in 10 mL graduated flasks, brought to volume with water, filtered with paper filters and analysed with the ICP-OES (Figure 7), following the procedure indicated by EPA [89].

3.10.2.1. Translocation Factors

The translocation factors, *i.e.* the ratio of elements found in the different plants organs, were calculated according to Bonanno *et al.* (2018)[90], by dividing the concentrations of the elements measured in leaves by the content found in the stem (L/S) and in the rhizome, (L/Rh), and by dividing the same elemental concentrations found in the stem by the rhizome content (S/Rh).

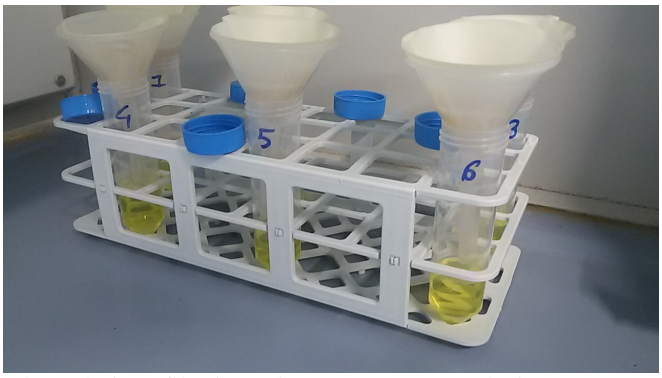

Figure 7: mineralised samples solutions filtering prior to ICP-OES analysis.

3.11. Multivariate Analysis - PCA

After having obtained and elaborated the output of all the quantitative analyses, the data were combined and analysed with RStudio®, in order to examine whether the specimens were affected by zonal differentiation and, if positive, to detect particular trends and factors which induced such differentiation.

4. Results and Discussion

4.1. Conservation Protocol

At a macroscopic analysis, glutaraldehyde-treated (Figure 8a) samples resulted to better maintain their pigmentation compared to the samples conserved in ethanol (Figure 8b), that appeared bleached instead. It is probable that glutaraldehyde causes the pigments to bind to the plant structures, preventing the solvent to extract them, and that may exert a general preservative activity.

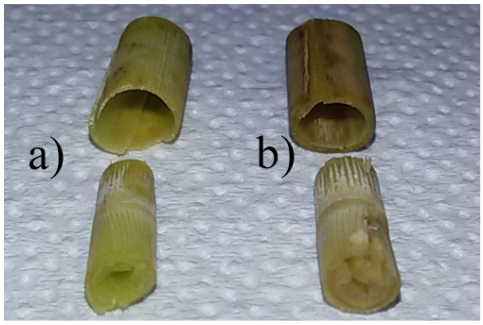

Figure 8: stem treated with glutaraldehyde (a) and 10 % ethanol + 3 % acetic acid (b).

4.2. Sample Preparation and Extraction

4.2.1. Structural Analysis

Even though glutaraldehyde allowed the samples to better retain their pigments (refer to section 4.1), this is probably due to a stiffening of the tissues: glutaraldehyde-treated samples, in fact, presented a considerable hardiness, and resulted to be particularly difficult to cut. Conversely, ethanol-conserved samples resulted soft, elastic, and easy to section.

4.2.2. Optical Microscope

Through optical microscopy, no difference was noted neither between the two different storage strategies (beside pigment stabilisation in glutaraldehyde) nor amongst the samples.

4.2.3. SEM-EDX

Visualised at SEM, samples treated with glutaraldehyde appeared brittle, with a collapse of the tissues structure that impeded a detailed structural analysis (Figure 10a).

Conversely, the ethanol and acetic acid mixture proved to preserve the plant structures in a soft, elastic and resistant form, which experienced much less disintegration upon cut (Figure 10b).

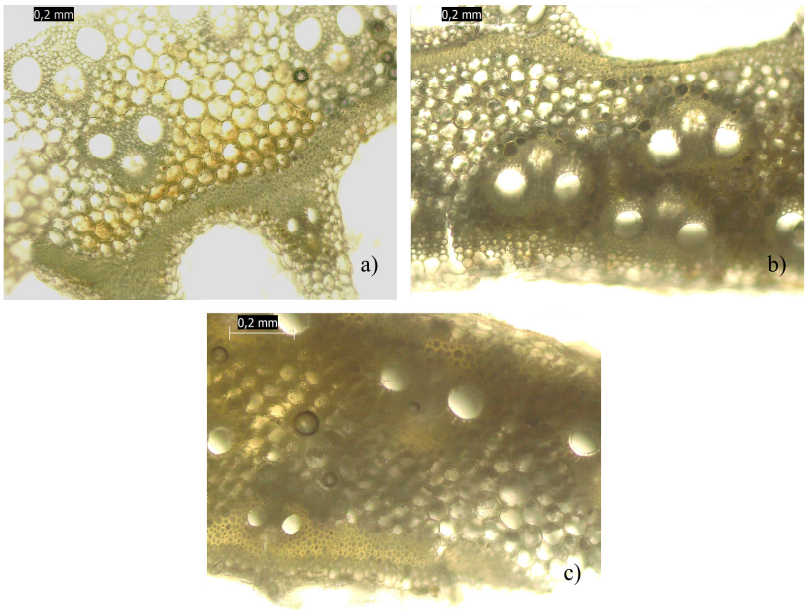

Figure 9: P1 rhizome sections treated with 10 % ethanol from: Zone 1 (a), Zone 2 (b) and zone 3 (c). Magnification: 100x.

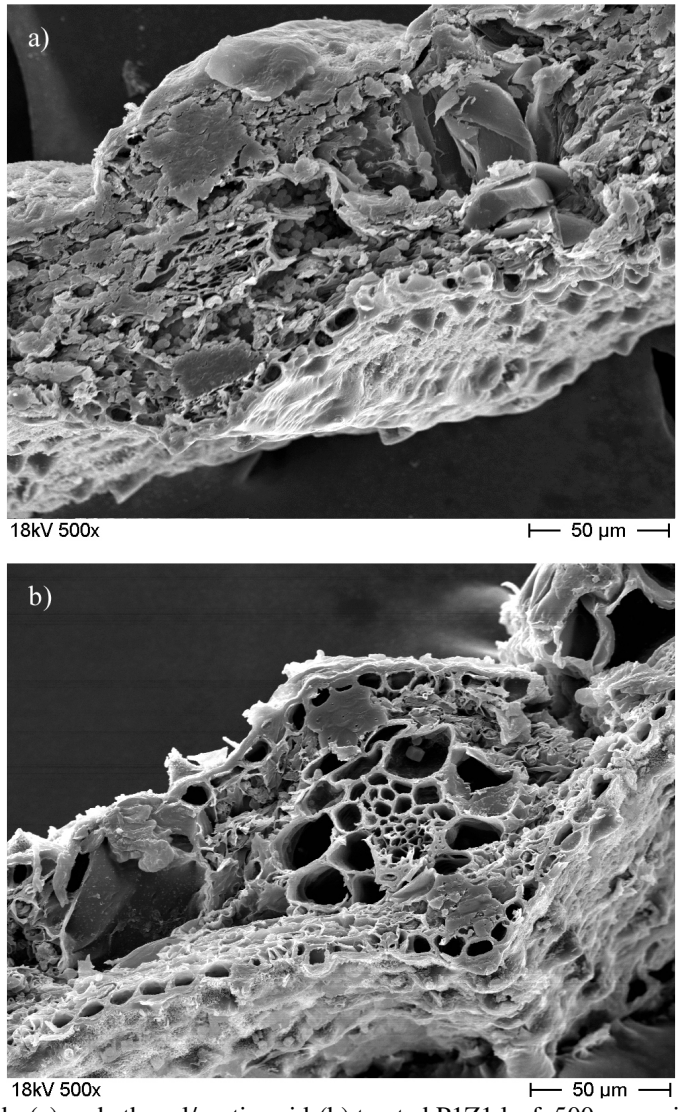

Figure 10: glutaraldehyde-(a) and ethanol/acetic acid-(b) treated P1Z1 leaf, 500x magnification, 18 kV.

Due to the complexity of the matrix, it was not possible to measure the elements content through EDX, since it was impossible to locate where they were stored, and also because the signals of the most abundant elements masked the signals of the elements in traces.

4.2.4. Chloroplasts Extraction

In Figure 11, the spectrum obtained from the supernatant and from the debris solutions are reported.

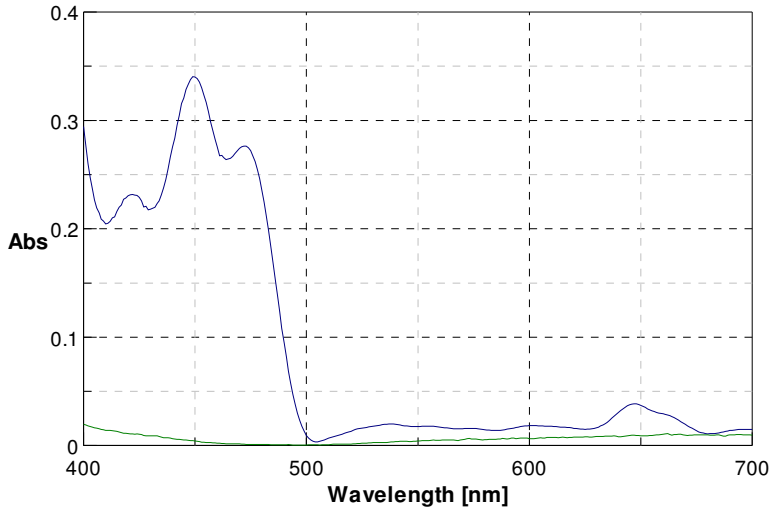

Figure 11: pellets (blue) and supernatant (green) solutions spectra, deriving from the PRL chloroplast extraction procedure.

Since the signal obtained for the supernatant was particularly weak, especially in comparison to the pellet - less than 0.02 ABS units at the highest peak - it was ascertained that such loss is minimal and negligible.

4.2.5. Direct Solvent Extracted Samples Dilution

Considering the studied wavelength range between 400 nm and 700 nm, the pure extractes of the PRL samples directly with the acetone mixes resulted to be too concentrated for an adequate signal record, since saturating the detector (Figure 12). A dilution of 1:10 was therefore applied.

Figure 13 reports the spectra deriving from the PRL extraction with 70 % and 80 % acetone - water mix. The spectra differ slightly in profile and intensity.

In Figure 14 the spectra of the PRL 70 % acetone stirred and sonicated 1:10 extracts are reported. The ultrasound-assisted extraction yielded an extract with a spectrum considerably different in profile and intensity in comparison to the stirred extract.

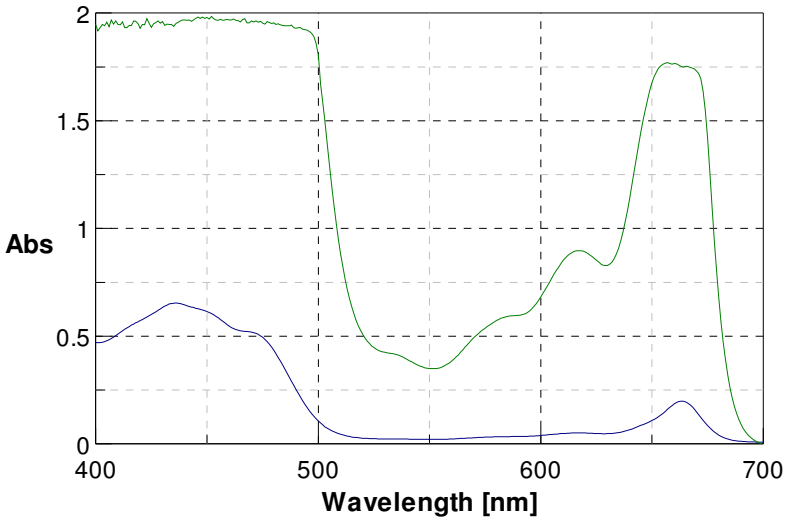

Figure 12: undiluted (green) vs. 1:10 (blue) overnight PRL 80 % acetone extract spectrum.

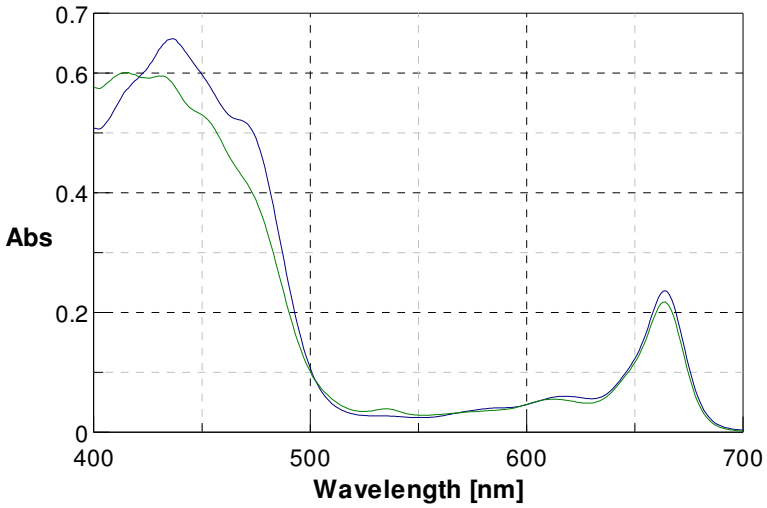

Figure 13: 70% acetone (blue) and 80 % acetone (green) overnight PRL 1:10 extracts spectra.

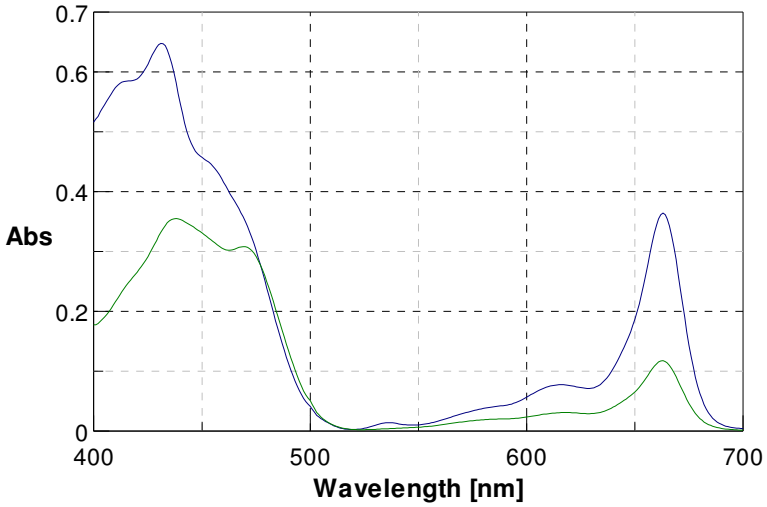

Figure 14: PRL 70 % acetone stirring (blue) and sonication (green) 1:10 extracts spectra.

4.2.6. Extraction Time Study

In Figure 15 are reported the spectra of the PRL 1:10 extract during the extraction procedure, sampled every 1 h, and between 1 h and 8 h.

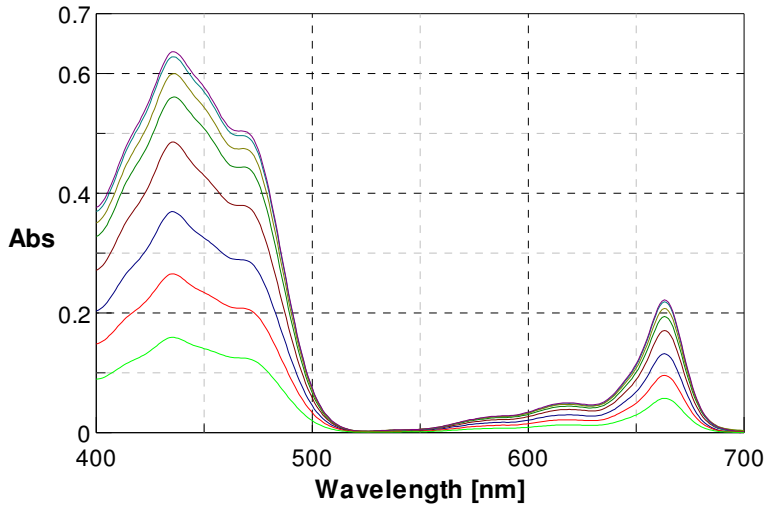

Figure 15: 70 % acetone PRL 1:10 extract spectra at 1 h (bright green), 2 h (red), 3 h (dark blue), 4 h (dark red), 5 h (dark green), 6 h (beige), 7 h (turquoise) and 8 h (purple).

It was assessed that after 7 h of extraction, a plateau was reached; the information was hence integrated, and such time was applied to the extraction protocol.

4.2.7. Chloroplasts vs. Direct Solvent Extraction

In Figure 16, the spectra of 70% acetone, 7 h PRL 1:10 extract and of the chloroplast extract are reported.

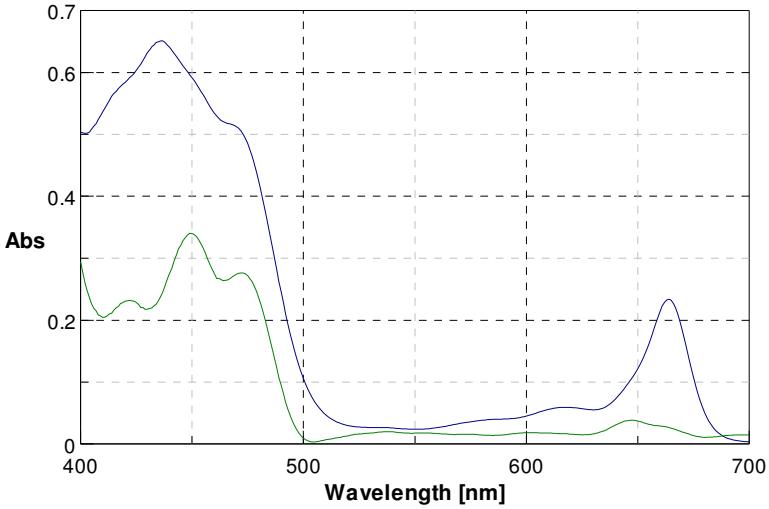

Figure 16: 70 % acetone, 7 h PRL 1:10 (blue) and chloroplasts (green) extracts spectra.

Considering a material-to-solvent ratio of 0.02 mg L-1 for the chloroplasts extract vs. 0.1 g mL-1 of the direct solvent extract, the signal intensity for the chloroplasts extract is

considerably lower than the counterpart, which implies a much less efficient extraction.

4.3. Spectrometer Scanning Speeds

No difference was observed between the reference spectrum recording at 200, 1000 and 2000 nm min^{-1} (Figure 17).

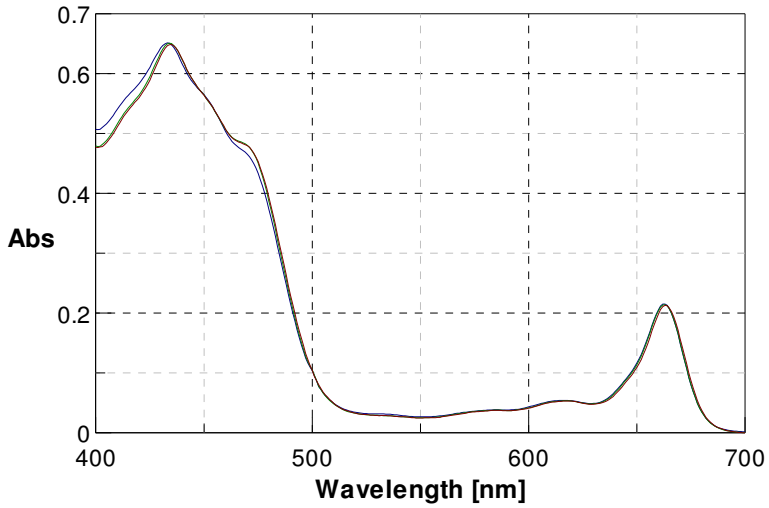

Figure 17: 70 % acetone, 7 h PRL 1:10 extract spectrum recorded at 200 nm min^{-1} (green), 1000 nm min^{-1} (blue) and 2000 nm min^{-1} (red).

4.4. Sample Storage Examination

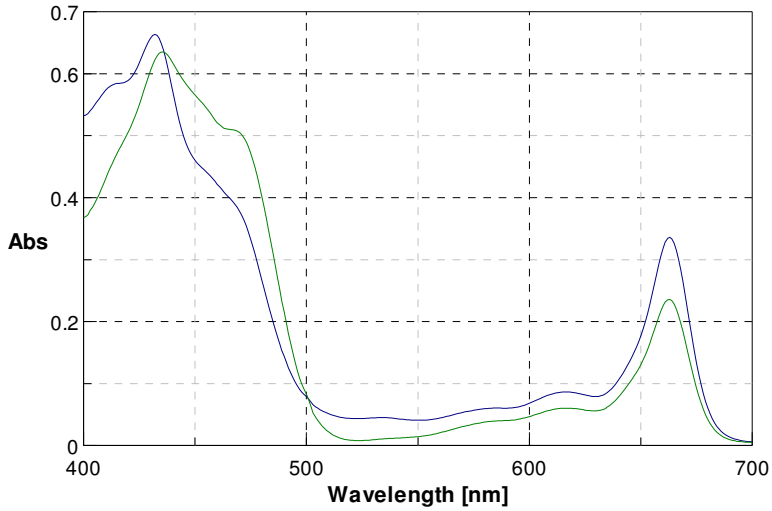

Figure 18: Spectra of the 70% acetone PRL 1:10 extract stored at 4 °C (blue) and at -20 °C (green).

4.4.1. Freezing

The spectrum resulted to differ considerably between the 4 °C-stored and the -20 °C-stored samples (Figure 18); this might indicate that the second extract decayed.

4.4.2. pH Change

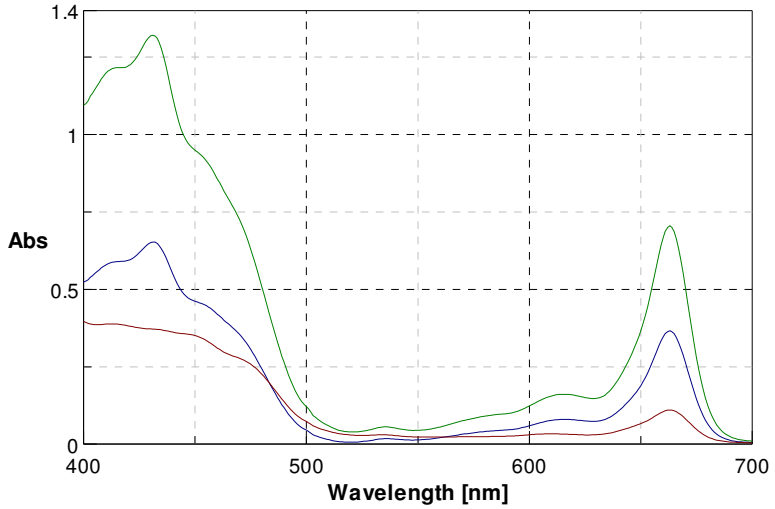

Figure 19: 70% acetone, 7 h PRL 1:10 extracts spectra with unvaried pH (blue), 2 % Na_2CO_3 (green) and 2 % acetic acid (red).

The solution acidification resulted to destabilise its content, causing a reduction of the main peaks intensity and a change in profile (Figure 19), especially for the carotenoid area, around 470 nm. This is consistent with the pigment destabilisation hypothesis reported in literature, assuming a yellow shift due to the protonation and the consequent isomeric change from trans to cis conformations for carotenoids, and the loss of the Mg^{++} ion from the chlorophylls chlorin group. Contrariwise, a pH rise caused the increase of the main peaks, arguably due to a stabilisation of the carotenoids in their blue-absorbing conformation and to a decrease of degradation rate [83].

4.4.3. Sample Photolysis

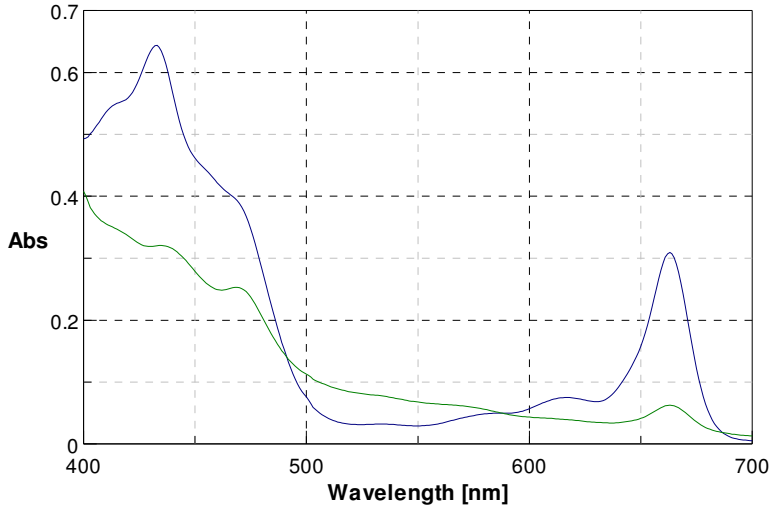

Figure 20: 70 % acetone, 7 h PRL 1:10 sample fresh extract (blue) and after an exposure of 20 min to a fluorescence lamp (green).

Figure 20 reports the spectrum of the PRL 70% acetone, 7 h, 1:10, extract before and after 20 min exposure to a fluorescent light.

The ABS profile varied considerably after the exposition, and the peaks decreased in intensity. It is possible that the pigments, particularly sensitive to light especially when removed from the live tissues, decomposed.

4.5. Pigments Quantification

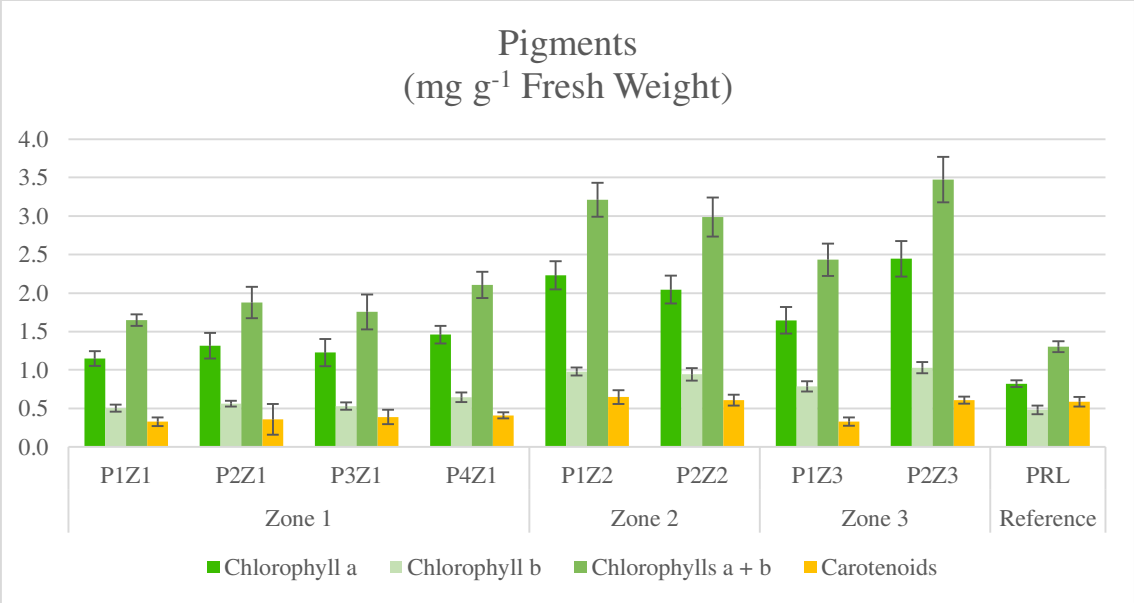

Figure 21: *P. australis* leaf samples chlorophyll a (dark green), chlorophyll b (pale green) chlorophyll a + b (bright green) and carotenoids (orange) content, expressed in mg of pigment per g of fresh leaf sample. Error bars correspond to the standard deviations related to the assay replicates.

The samples analysed show important differences in pigments content, that are in agreement with the area of the wetland the plants were collected in. The specimens richest in pigments belonged either to Zone 2 (mean chlorophyll a + b 3.1 ± 0.2 mg g^{-1}, carotenoids 0.6 ± 0.2 mg g^{-1}) or Zone 3 (mean chlorophyll a + b 3.0 ± 0.7 mg g^{-1}, carotenoids 0.5 ± 0.7 mg g^{-1}). Zone 1 resulted to host the specimens with less pigments (mean chlorophyll a + b 1.8 ± 0.2 mg g^{-1}, carotenoids 0.37 ± 0.04 mg g^{-1}), that had a pigment content similar to the reference plant (chlorophyll a + b 1.3 ± 0.07 mg g^{-1}, carotenoids 0.60 ± 0.06 mg g^{-1}). This is consistent with the fact that Zone 1 is downstream and the plants it harbours are expected to be exposed to lower amounts of contaminants, which should be progressively reduced by the vegetation throughout the water route.

Hence, plants in the Zone 1 should experience lower levels of stress. Meanwhile, Zone 3 is upstream and the plants therein should be exposed to higher levels of water pollutants and consequently more stressed, thus expressing higher chlorophylls and carotenoids levels [60,91].

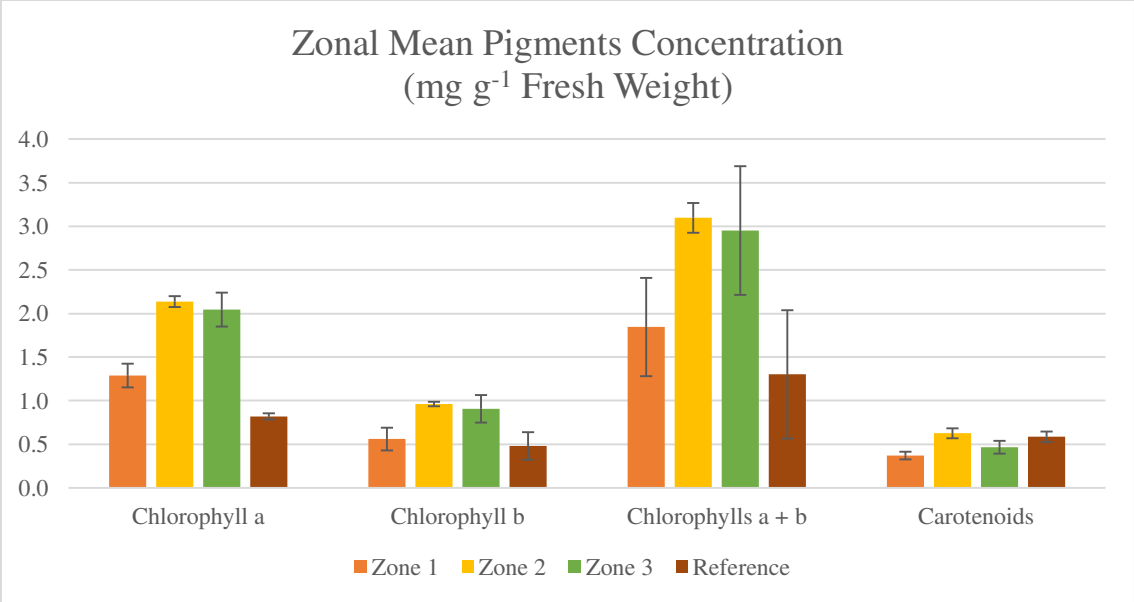

Figure 22: mean zonal pigments concentrations of *P. australis* leaves grouped by type and expressed in mg g-1 of fresh material. Error bars correspond to the standard deviation between samples.

Considering the standard deviation of its samples, Zone 2 may be in an intermediate situation, which would be coherent to its position along the water route, and that could lead to a stimulation of the plants that does not damage their physiology.

4.5.1. Calibration Curves for Antioxidant Analyses

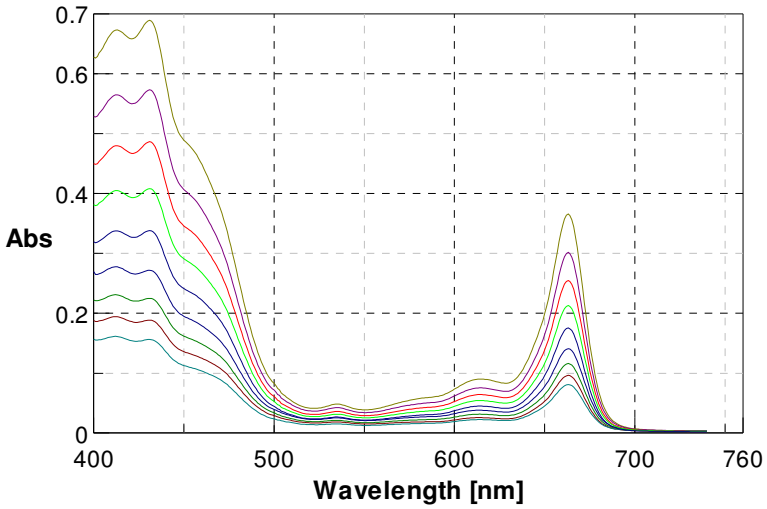

Figure 23: 70 % acetone PRL extract spectra at progressive dilutions: 1:10 (beige), 1:12 (purple), 1:14 (red), 1:17 (bright green), 1:21 (dark blue), 1:25 blue), 1:30 (pine green), 1:36 (dark red) and 1:43 (green-blue).

Figure 23 depicts the spectra relative to the progressive dilution of the PRL solvent extracts,

employed for the signal correction of the non-enzymatic antioxidants assays.

4.6. Non-Enzymatic Antioxidants Assays

4.6.1. ABTS

The results of the assay with the methanolic 0.08 mM ABTS working solution are reported in Figure 24. The calibration curve showed a linearity loss for Trolox concentrations superior to 1 mM. This was probably due to the excessive concentration of the standard compared to the ABTS, which converted all the spectrophotometrically active form, attenuating its signal. Nonetheless, calibration curves for Trolox concentrations up to 1 mM showed a good fitting, with a mean R^2 of 0.91 ± 0.03. The reed sample signal resulted to fall within the linear range, with a mean ABS value of 0.48 ± 0.02, corresponding to a Trolox equivalent concentration of 0.45 ± 0.03 mM.

4.6.1.1. Concentration Increase

The results related to the 0.15 mM ABTS assay are reported in Figure 24. A better linearity for the signals of all the Trolox dilutions was reached, with a mean R^2 of 0.993 ± 0.001. For the reed sample, a mean ABS value of 0.92 ± 0.03 was recorded, corresponding to a mean Trolox equivalent concentration of 0.46 ± 0.06 mM, consistently with the 0.08 mM methanolic ABTS assay set results.

The increase of the ABTS concentration resulted in an extension of the linearity of the calibration curve to the whole Trolox concentration span, and grated a better repeatability compared to the standard protocol.

4.6.1.2. Wetland Samples

The ABTS assay results revealed a discrete zonation, with the samples of the same zone having similar antioxidants concentrations. The specimens with higher levels of antioxidants were those collected in the Zone 2 (mean Trolox equivalent concentration 1.3 ± 0.2 mM), followed by Zone 1 (1.1 ± 0.3 mM). Zone 3 presented values similar to the Reference (1.0 ± 0.2 mM vs. 1.0 ±0.1 mM), both falling in the range of the samples from Zone 1, considering the standard deviation.

4.6.1.3. Storability Examination

The results obtained using 0.15 mM methanolic ABTS working solution prepared from a 4-month-old MS are reported in Figure 24. The calibration curves for the signals of the standard dilutions were characterised by a good linearity, with a mean R^2 of 0.995 ± 0.001. For the reed sample, a mean ABS value of 0.96 ± 0.01 was recorded, corresponding to a Trolox equivalent concentration of 0.45 ± 0.02 mM, in coherence with the 0.08 and 0.15 mM methanolic ABTS assay sets results (sections 4.6.1 and 4.6.1.1).

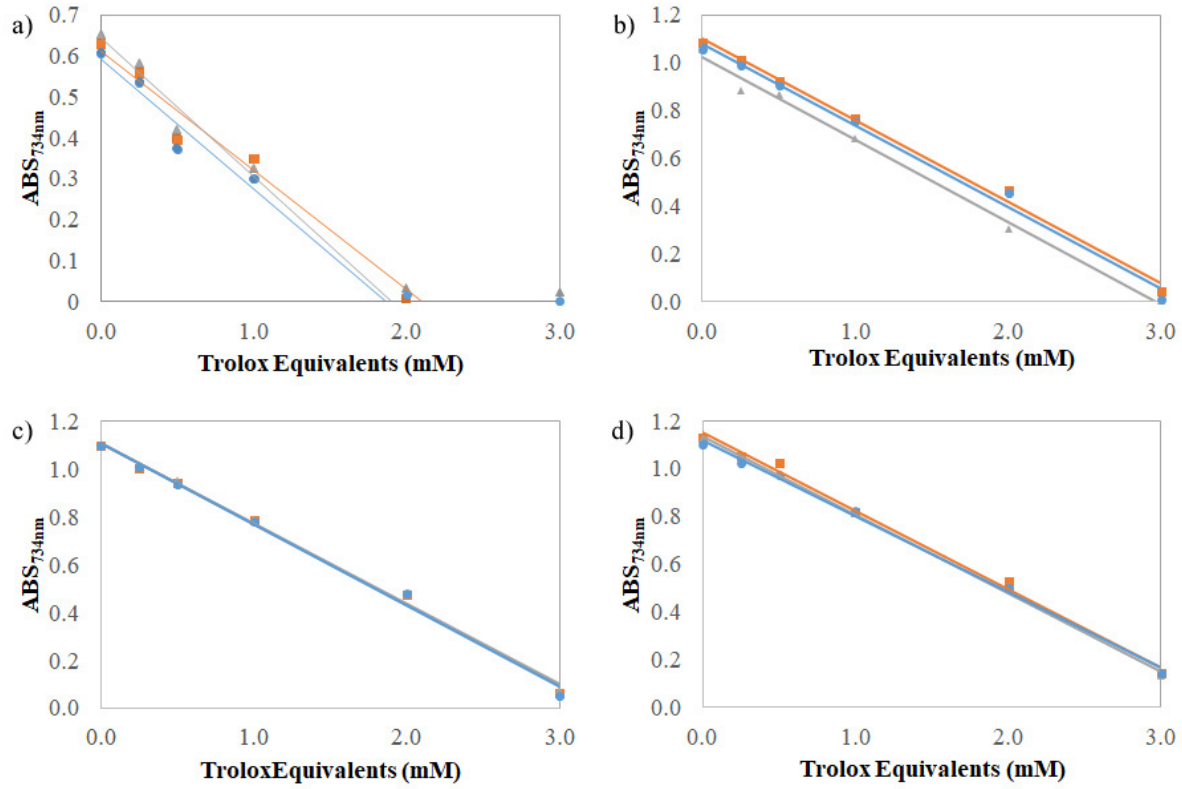

Figure 24: ABS_{734nm} data plot and calibration curves of a) the 0.08 mM methanolic ABTS reaction solution assay set, b) the 0.15 mM methanolic ABTS reaction solution assay set, c) the 0.15 mM methanolic ABTS, old stock solution, d) the 0.16 mM ethanolic ABTS reaction solution assay set. Replicate A: orange squares and line; replicate B: grey triangles and line; replicate C: blue circles and line.

If stored in the dark and at 4 °C, the radicalised ABTS MS proved to be stable for at least 4 months.

4.6.1.4. Solvent Substitution

The results deriving from the assay with the ethanolic 0.16 mM ABTS solution are reported in Figure 24. In all three replicates, the ABS values recorded for all the calibration points showed an optimal linearity, with a mean R^2 of 0.997 ± 0.002. For the plant sample, a mean ABS value of 0.97 ± 0.01 was recorded, corresponding to a Trolox equivalent concentration

of 0.50 ± 0.02 mM, which is consistent with most of the previous ABTS working solution sets (sections 4.6.1, 4.6.1.1 and 4.6.1.3).

Substituting methanol with the less toxic ethanol is therefore possible.

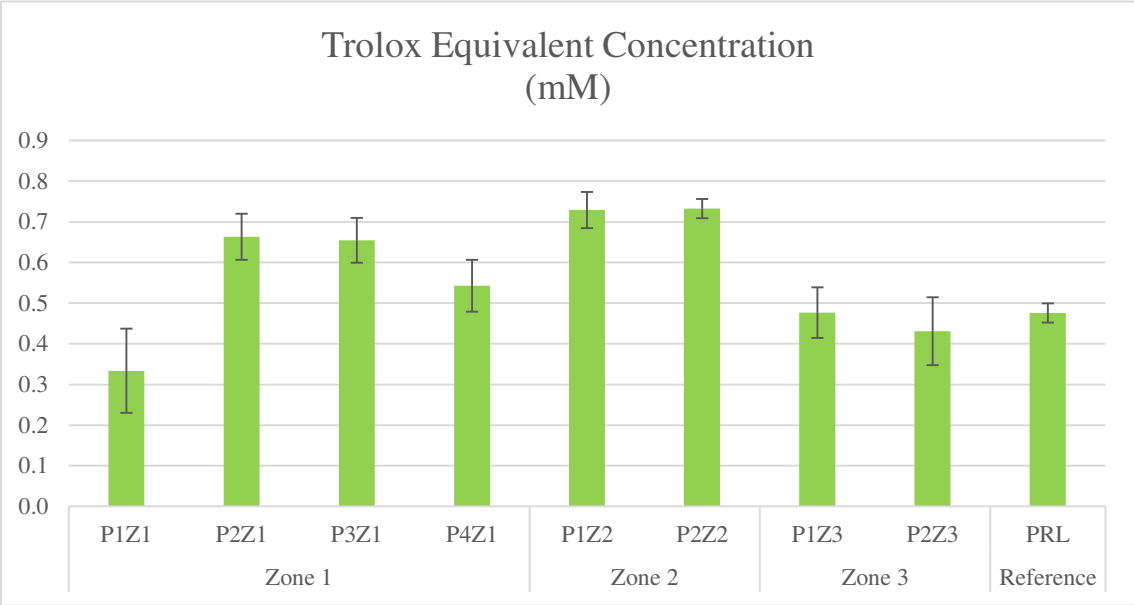

Figure 25: ABTS assay results of the wetland and reference samples, expressed in mM Trolox equivalent concentration. Error bars correspond to the standard deviations of the replicated measurements.

4.6.2. DPPH

The results regarding the use of methanolic 20 mg L^{-1} DPPH working solution (standard protocol) are reported in Figure 26. Similarly to the ABTS assay, for Trolox concentrations higher than 300 µM, the standard titration curve lost linearity. This was probably due to the excessive standard concentration, compared to the DPPH one, which converted all the spectrophotometrically active form, attenuating its signal. However, for concentrations of Trolox up to 300 µM, the calibration curve showed an optimal linearity, with a R^2 mean value of 0.99 ± 0.01. The reference sample gave a mean ABS signal of 0.06 ± 0.01, which corresponds to a Trolox equivalent concentration of 285 ± 10 µM.

4.6.2.1. Solvent Substitution

The results of the assay using ethanolic 20 mg L^{-1} DPPH working solution are reported in Figure 26. As for the methanolic working solution, a linearity loss was observed in the calibration curve for Trolox concentrations superior to 300 µM. Nonetheless, the points up to that concentration were characterised by a good linearity, with a R^2 mean value of 0.933 ± 0.001.

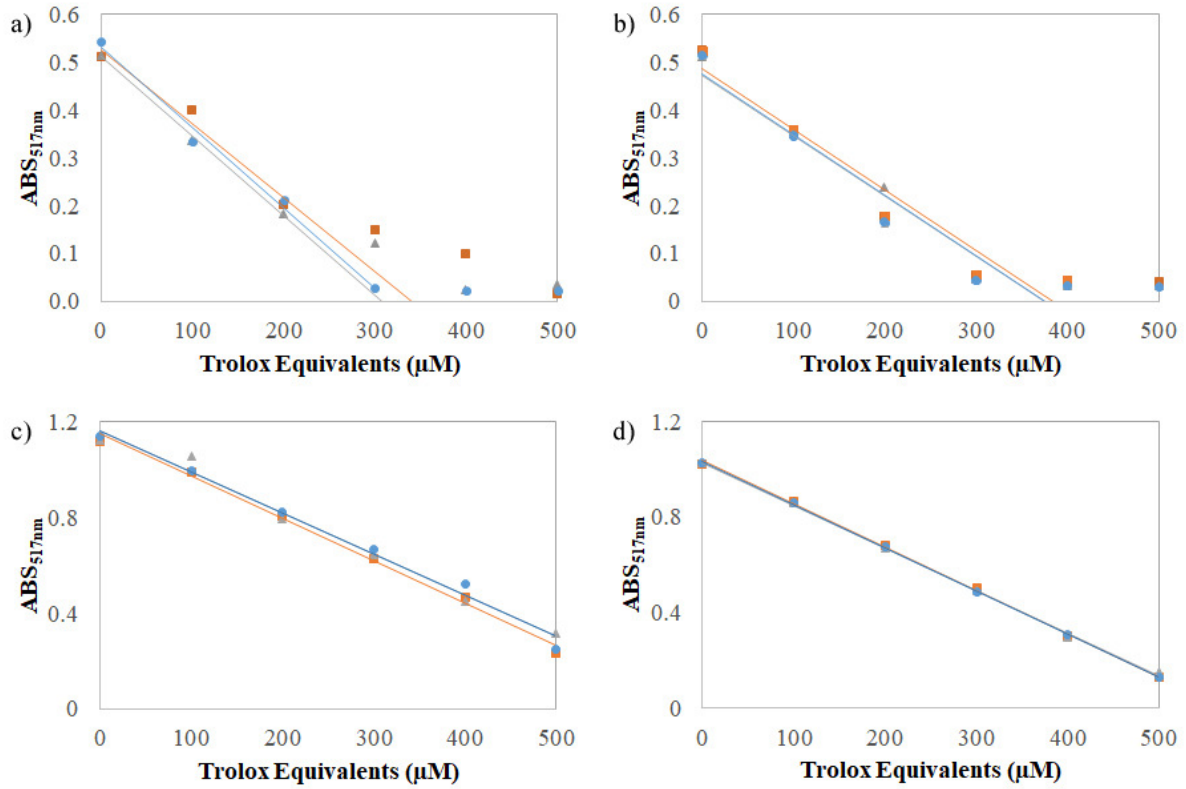

Figure 26: ABS_{517nm} data plot and calibration curves of: a) the 20 mg L^{-1} methanolic DPPH reaction solution assay set, b) the 20 mg L^{-1} ethanolic DPPH reaction solution assay set, c) the 40 mg L^{-1} ethanolic DPPH reaction solution assay set, d) the 40 mg L^{-1} ethanolic DPPH, old stock solution, reaction solution assay set. Replicate A: orange squares and line; replicate B: grey triangles and line; replicate C: blue circles and line.

The reference sample gave a mean ABS signal of 0.119 ± 0.008, which corresponds to a Trolox equivalent concentration of 278 ± 8 µM, a result consistent with the value obtained from the methanolic DPPH solution set (section 4.6.2).

It is therefore possible to substitute methanol with ethanol without altering the results, and such choice was selected for the assays.

4.6.2.2. Concentration Increase

Figure 26 reports the results of the assay using an ethanolic 40 mg L^{-1} DPPH working solution.

The ABS values recorded for all the calibration points showed an optimal linear correlation, with a mean R^2 value of 0.990 ± 0.004. The reed sample gave a mean ABS signal of 0.665 ± 0.002, corresponding to a Trolox equivalent concentration of 284 ± 8 µM, consistent with the precedent sets results (sections 4.6.2 and 0). The increase of the DPPH concentration resulted in an extension of the linearity to the whole Trolox concentration span, and granted a higher linearity degree of the standard curve compared to the standard protocol.

4.6.2.3. Wetland samples

Consistently with the ABTS results (Section 4.6.1.2), plants collected in the Zone 3 presented the lowest mean Trolox equivalent concentration (478 ± 43 µM), arguably due to a higher level of water contamination. Considering the standard deviations, Zone 1 (650 ± 173 µM) and Zone 2 (851 ± 22 µM) fell in the same range, with Zone 2 presenting the highest mean value. The Reference Zone (637 ± 20 µM) showed an antioxidant activity slightly superior to the Zone 3 specimens. Statistically, only Zone 3 resulted to differ significantly from the other zones, while Zone 1 and 2 resulted to be comparable.

4.6.2.4. Storability examination

The results of the assay performed employing the ethanolic 40 mg L^{-1} DPPH working solution obtained from a 4-month-old MS are represented in Figure 26. The ABS values recorded for all the calibration points showed an optimal linear correlation, with a mean R^2 value of 0.9992 ± 0.0006.

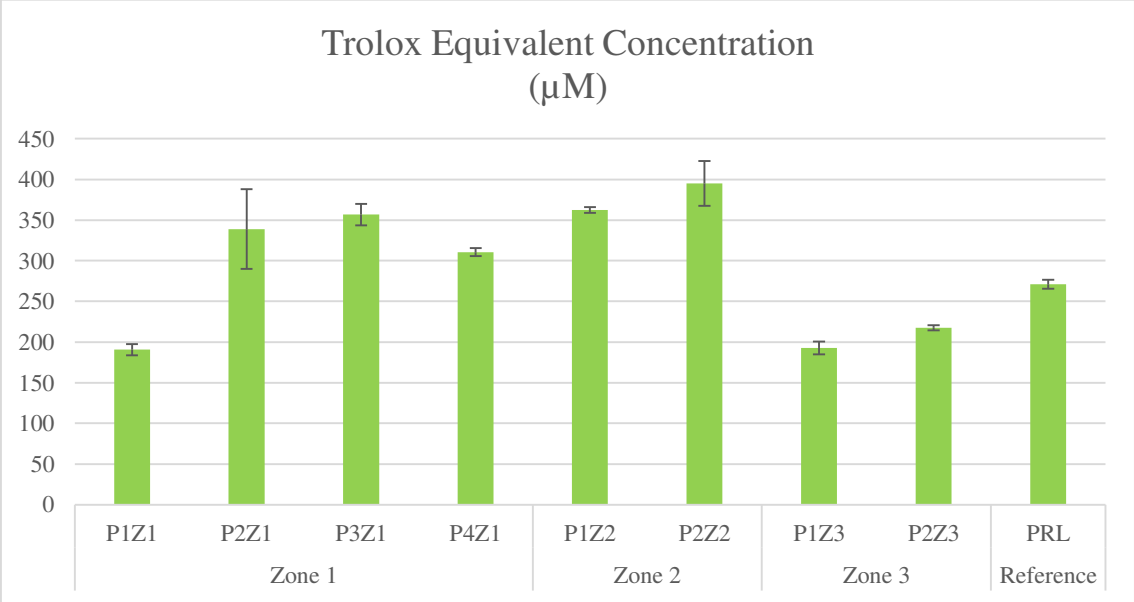

Figure 27: DPPH assay results of the wetland and reference samples, expressed in µM Trolox equivalent concentration. Error bars correspond to the standard deviations of the replicated measurements.

The ABS signal relative to the sample was recorded to be as high as 0.47 ± 0.02; the corresponding Trolox equivalent concentration resulted to be higher than the precedent sets (sections 4.6.2, 0 and 4.6.2.2), reaching a mean value of 313 ± 9 µM. This might imply that the DPPH MS had decayed by the experiment date.

Further trials however are required, in order to further investigate this aspect and to assess whether it would be possible to calculate a correction factor for results obtained using old

DPPH stock solutions.

4.6.3. FRAP

Figure 29 represents the results obtained using fresh stock solutions for each reactant. ABS values of the calibration points showed an optimal linear correlation with their concentrations (Figure 29), with a mean R^2 value of 0.992 ± 0.004. The plant sample gave a mean ABS signal of 0.665 ± 0.002, corresponding to a Trolox equivalent concentration of 0.64 ± 0.03 mM.

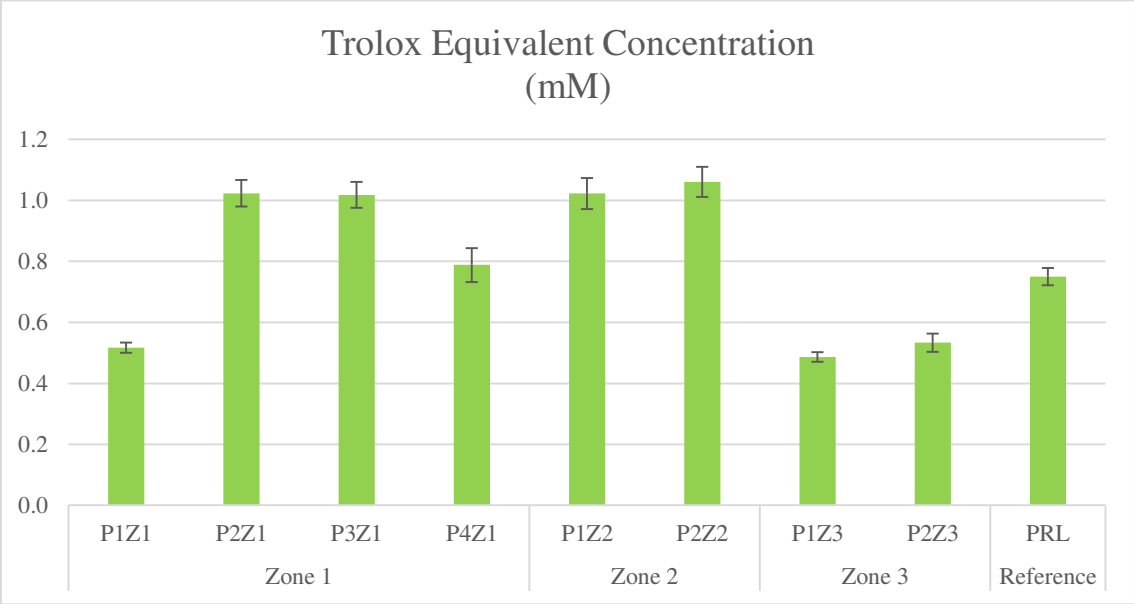

Figure 28: FRAP assay results of the wetland and reference samples, expressed in mM Trolox equivalent concentration. Error bars correspond to the standard deviations of the replicated measurements.

4.6.3.1. Wetland Samples

Consistently with the ABTS and DPPH analyses (Sections 4.6.1.2 and 4.6.2.3), Zone 3 resulted to host the less active specimens in terms of non-enzymatic antioxidant power (mean Trolox equivalent concentration of 0.51 ± 0.01 mM), while Zone 2 (1.042 ± 0.001 mM) was characterised by the most active plants. Zone 1 resulted to be the less active (0.8 ± 0.2 mM)

The reference sample once again showed intermediate activity (1.4 ± 0.1 mM).

4.6.3.2. Storability Examination

The results regarding the use of 3-months-old stock solutions to prepare FRAP working solution are represented in Figure 29. ABS values of the calibration points showed an optimal linear correlation with the Trolox concentrations, with a mean R^2 value of 0.994 ± 0.005. The

plant sample gave a mean ABS signal of 0.39 ± 0.06, corresponding to a mean Trolox equivalent concentration of 0.612 ± 0.04 mM, that is consistent with the results of the FRAP working solution prepared from a fresh stock solution (section 4.6.3).

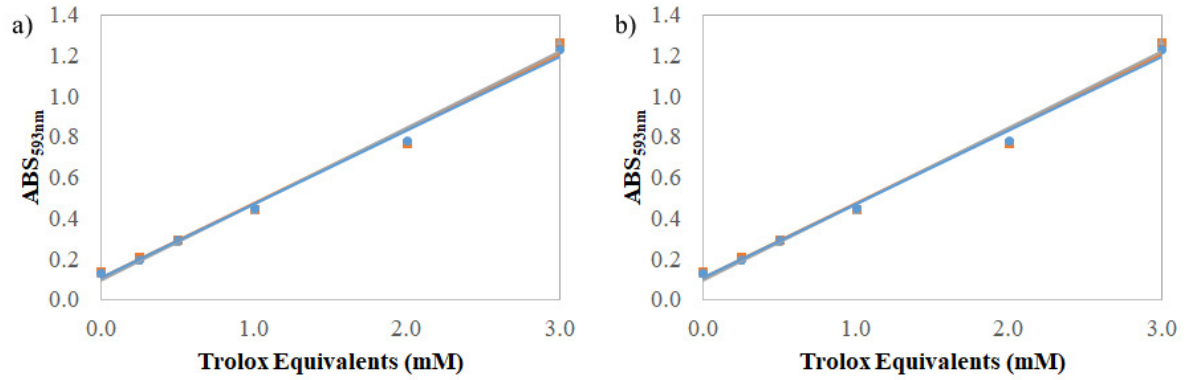

Figure 29: ABS_{593nm} standards data plot and calibration curves of the FRAP a) fresh stock solutions assay set, b) 3-months-old stock solutions assay set. Replicate A: orange squares and line; replicate B: grey triangles and line; replicate C: blue circles and line.

If stored at 4°C, $C_2H_3NaO_2$ buffer, TPTZ and $FeCl_3$ solutions were thus proved to be usable for at least 3 months.

4.6.4. Flavonoids

4.6.4.1. Wetland Samples

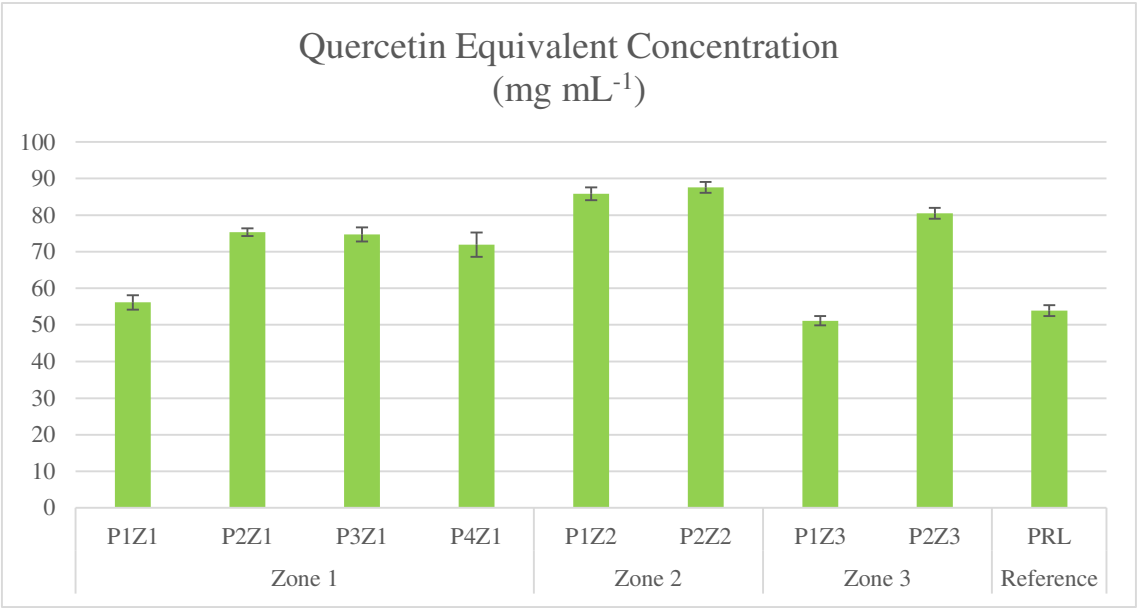

Figure 30: Flavonoids-$AlCl_3$ complexation assay results of the wetland and reference samples, expressed in mg mL^{-1} Quercetin equivalents. Error bars correspond to the standard deviations of the replicated measurements.

The results obtained by employing fresh stock solutions of the reactants in the Flavonoids-$AlCl_3$ complexation are presented in Figure 29. ABS values of the calibration points showed

a perfect linearity with the standard concentrations, with a mean R^2 of 0.9998 ± 0.0002. The plant sample gave a mean signal of 0.395 ± 0.06 ABS units, corresponding to a quercetin equivalent concentration of 54 ± 1 mg L^{-1}.

According to the mean values obtained with the Flavonoids-$AlCl_3$ complexation assay, Zone 2 (167 ± 4 mg mL^{-1}) resulted to host the most active specimens in terms of quercetin equivalent concentration. Zone 1 specimens (147 ± 9 mg mL^{-1}) resulted to cluster at a slightly lower activity, which is consistent with the previous non-enzymatic assays results (Sections 4.6.1.2, 4.6.2.3 and 4.6.3.1).

However, considering the standard deviations, Zone 3 (132 ± 38 mL^{-1}) presents values that are comparable to the others, and that do not contribute to the zonation: since its specimens gave two different results, in facts, it is not possible to state if one of them consists in an outlier result, and to distinguish the zone from the others. In order to better investigate this aspect, it will be necessary to repeat the sampling including more specimens per area, so that the individual variability can be mediated.

In this case, the reference sample showed the lowest mean antioxidant activity (110 ± 4 mg mL^{-1}), comparable, however, with the Zone 3 samples.

4.6.4.2. Storability examination

Figure 31 reports the results of the assay performed using 3-months-old stock solutions to prepare the reactants of the working solution. ABS values of the calibration points showed a perfect linear correlation, with a mean R^2 of 0.998 ± 0.003. The plant sample returned a mean signal of 0.431 ± 0.005 ABS units, corresponding to a quercetin equivalent concentration of 56 ± 2 mg L^{-1}, in accordance with the previous results (section 4.6.4).

If stored at 4°C, $AlCl_3$, $C_2H_3KO_2$ and quercetin solutions were therefore proved stable for at least 3 months.

4.6.4.3. Solvent Substitution

The results deriving from the substitution of methanol with ethanol in the working solution are depicted in Figure 31. ABS values of the calibration points showed a perfect linear correlation with quercetin concentrations, with a mean R^2 of 0.9996 ± 0.0001. The plant sample gave a signal of 0.35 ± 0.01 ABS units, corresponding to an equivalent quercetin mean concentration of 51 ± 3 mg L^{-1}, which is consistent with the other Flavonoids-$AlCl_3$ complexation sets results (sections 4.6.4 and 0).

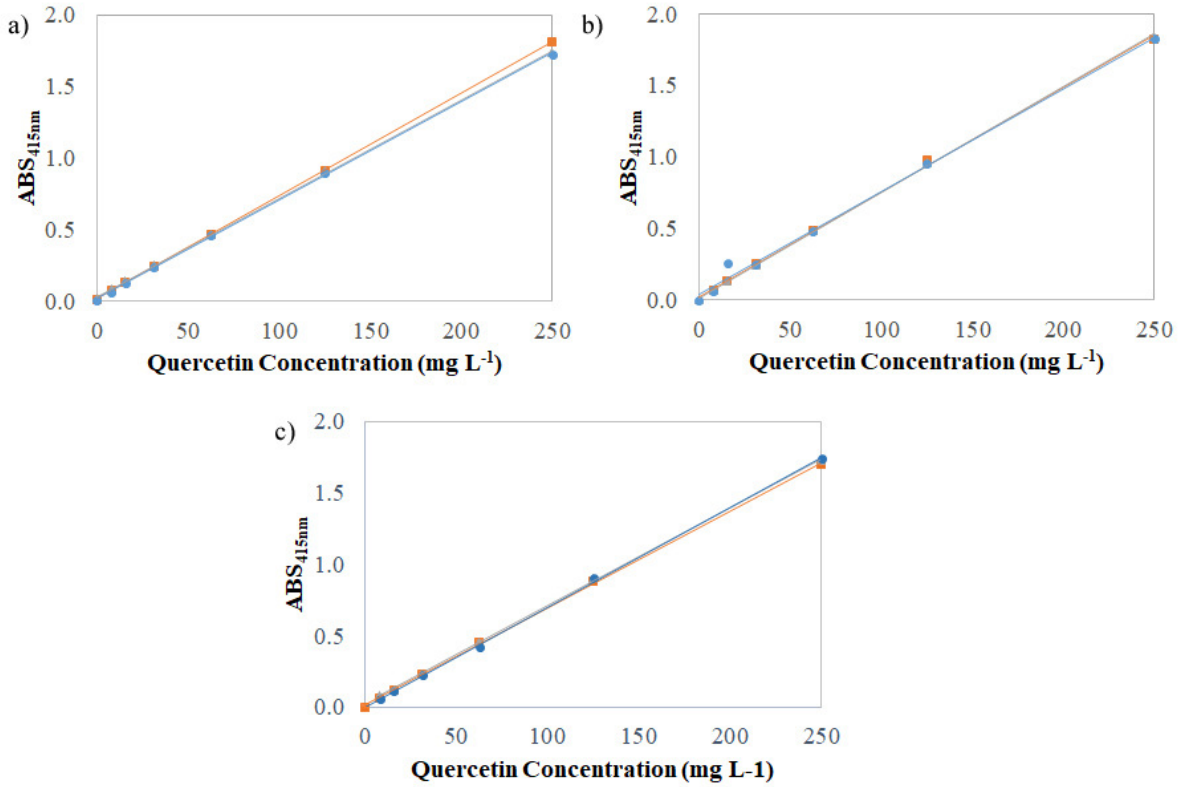

Figure 31: ABS_{415nm} data plot and calibration curves of a) the flavonoids, fresh stock solutions, assay set, b) the flavonoids, 3-months-old stock solutions, assay set and c) the flavonoids, ethanolic working solution, assay set. Replicate A: orange squares and line; replicate B: grey triangles and line; replicate C: blue circles and line.

It is therefore possible to substitute methanol with ethanol in the Flavonoids-$AlCl_3$ complexation assay without altering its results.

4.6.5. Summary

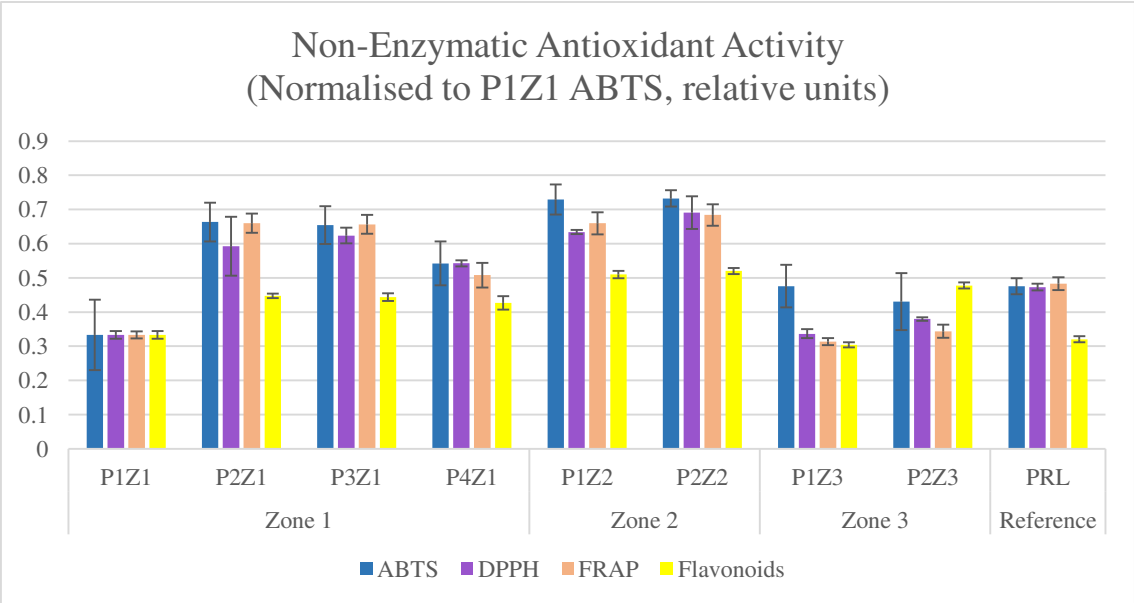

Figure 32: summary of the non-enzymatic antioxidant activity resulted from the relative assays, normalised to P1Z1 ABTS mean value. ABTS (blue), DPPH (purple), FRAP (pink) and Flavonoids-$AlCl_3$ complexation (yellow) outcomes are reported. Error bars correspond to the standard deviation.

In all of the antioxidants assays, Zone 2 resulted to host the specimens exerting the highest non-enzymatic antioxidant activity; Zone 3 plants, conversely, were proved to be the least active, while Zone 1 presented intermediate characteristics.

As hypothesised for the pigments (Section 4.5), this trend might be explained assuming the plant response to water pollution not to be linear: the plants may present weak responses with low levels of water contaminants (Zone 1); they might experience a balance between the stressing factors and their response system in intermediate conditions, reaching a peak of the oxidative activity (Zone 2); and their stress response might weaken at high concentrations of pollutants, possibly because they damage the defence mechanisms of the plant, or they impair their metabolism not allowing a proper response (Zone 3).

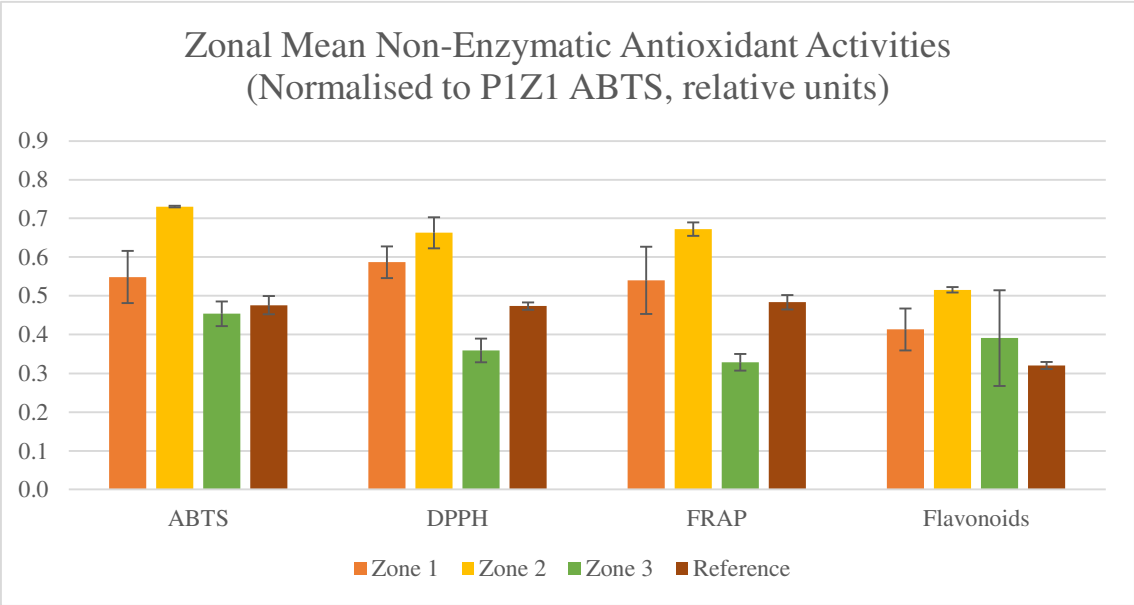

Figure 33: zonal mean values summary of the non-enzymatic antioxidant activity resulted from the relative assays, normalised to the Zone 1 ABTS mean value. Error bars correspond to the standard deviation.

4.7. Multivariate Analysis - PCA

Datasets of pigments and non-enzymatic antioxidants concentrations for the different plant samples were analysed in PCA multivariate analysis. The first two components collected the 76.29546% of all the variance. The graphs (Figure 34 and Figure 35) show a marked clustering by their sampling zones, with a clear separation of the samples belonging to Zone 2, which was mainly influenced by the pigments concentrations. The two specimens of Zone 3 are clearly separated, confirming their marked difference and prompting the necessity of a more conspicuous sampling of reed individuals per zone in the future. One specimen collected in Zone 1 (P1Z1) influenced the overlapping of values for Zone 1 and Zone 3, which are otherwise clustered separately along the PC2, differentiation driven mainly by the

antioxidants content. The reference group (Ref) is not clearly separated from the samples of Zone 1 and 3.

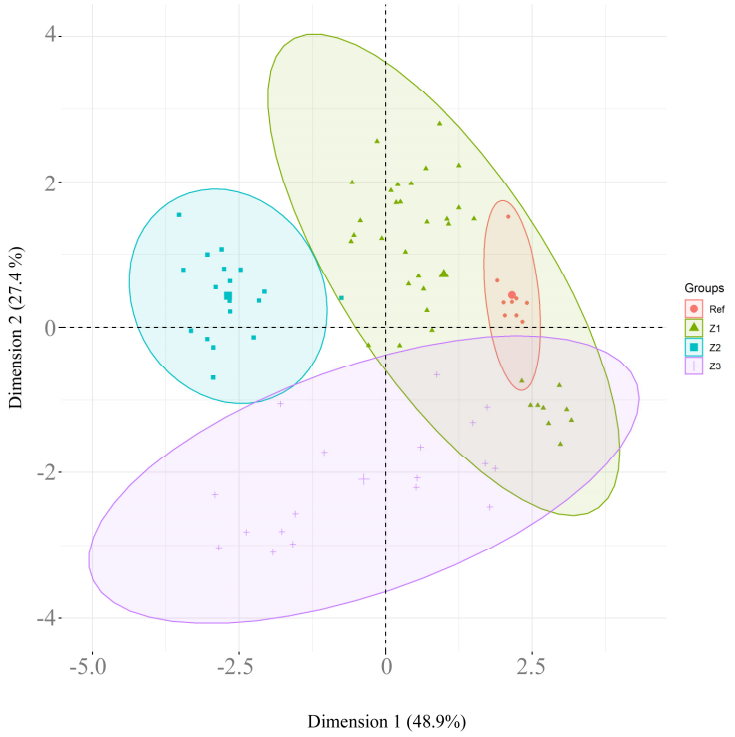

Figure 34: Principal components 1 and 2 of the PCA Multivariate analysis on the pigment contents and NEAs for reel leaves. Samples collected in the same zone (Z1, Z2, Z3, Ref) are represented with the same symbol and colour. Ellipses represent the point distribution in the bidimensional space. The geometric mean is represented by a larger symbol.

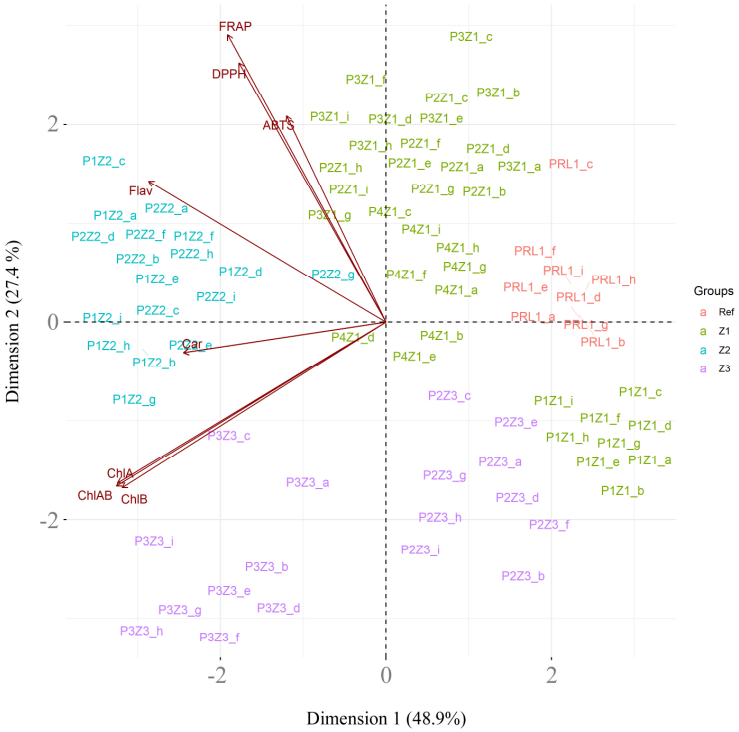

Figure 35: Biplot of the principal components 1 and 2 of the PCA Multivariate analysis performed on the pigment contents and NEAs for reel leaves. Samples collected in the same zone (Z1, Z2, Z3, Ref) are represented with the same colour. Original variables are plotted in red.

4.8. Enzymatic Antioxidants Assays

4.8.1. Differential SOD Activity Measurement

Zone 1 presented the plants with the highest mean SOD activity (0.45 ± 0.06 ABS units min^{-1}), followed by Zone 3 (0.43 ± 0.03 ABS units min^{-1}), while Zone 2 resulted to host the specimens with the lowest mean values (0.37 ± 0.05 ABS units min^{-1}). The highest SOD activity was recorded for 3 out of 4 specimens. The reference sample gave an intermediate value (0.39 ± 0.03 ABS units min^{-1}). However, samples from different zones did not show significant statistical differences. The results are reported in Figure 37.

A linear growth of the absorbance units was observed for all the samples with the increasing of the exposure time; a calibration curve was therefore obtained, as shown in Figure 36. Contrarily to what indicated in the protocol of Elavarthi and Martin (2010), the debris formation due to an excessive time of reaction was observed only after 60 min of cumulative illumination [74].

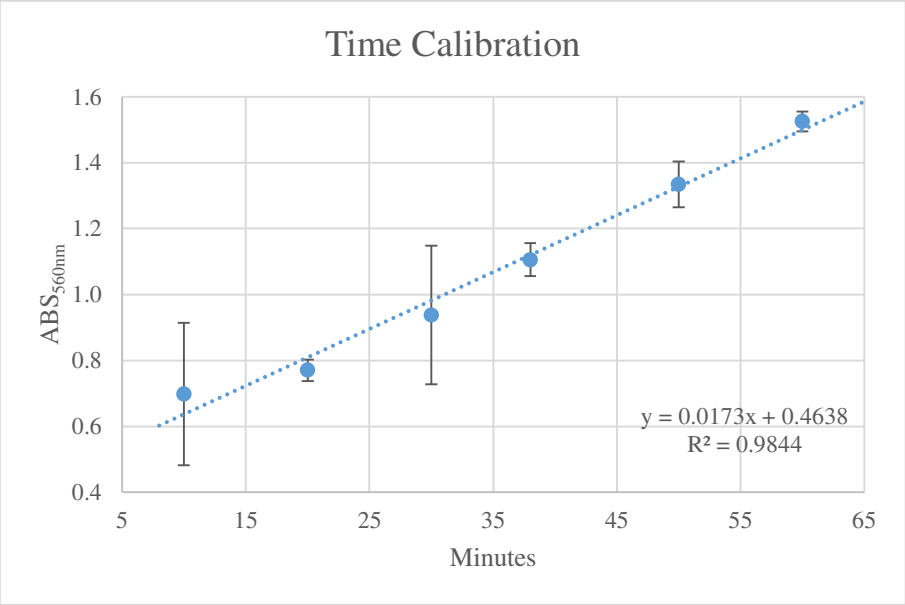

Figure 36: ABS_{560nm} vs. min time calibration curve for the SOD assay; the errors consist in the standard deviations of the analysis results.

4.8.2. CAT Activity Measurement: ABS Variation over Time

The highest mean activity was recorded for the specimens collected in Zone 3 (0.20 ± 0.04 ABS units min^{-1}), consistently with most of the non-enzymatic antioxidants assays (Sections 4.6.1.2, 4.6.2.3 and 4.6.3.1). With the exception of P4Z1, samples from Zone 1 had the lowest CAT expression (0.08 ± 0.01 ABS units min^{-1}), coherently with the fact that plants in this area should experience the lowest pollutants concentrations and, thus, the lesser stress.

Zone 2 resulted to host specimens exhibiting an intermediate CAT activity (0.10 ± 0.03 ABS units min^{-1}). Differently than the previous analyses, the reference sample presented the lowest activity (0.07 ± 0.03 ABS units min^{-1}). However, considering the standard deviations affecting the mean values, there is no net statistical difference between the specimens of the various zones, which might imply that they responded in analogous ways. The results are reported in Figure 37.

4.8.3. APX Activity Measurement: ABS Variation over Time

Zone 2 presented the specimens with the highest mean APX activity, with a mean ABS variation per minute of 0.16 ± 0.02. Besides, considering the standard deviations, the other zones resulted to host plants with similar APX activity, with a mean ABS variation per minute of 0.12 ± 0.05 (Zone 1), 0.14 ± 0.05 (Zone 3) and 0.14 ± 0.02 (Zone 2). The results are reported in Figure 37.

4.8.4. Summary

By combining the results of the enzymatic antioxidant assays (Figure 38), it emerged that there is no net zonal differentiation: even though the mean values differ amongst zones, considering the standard deviation values the samples are statistically homogeneous.

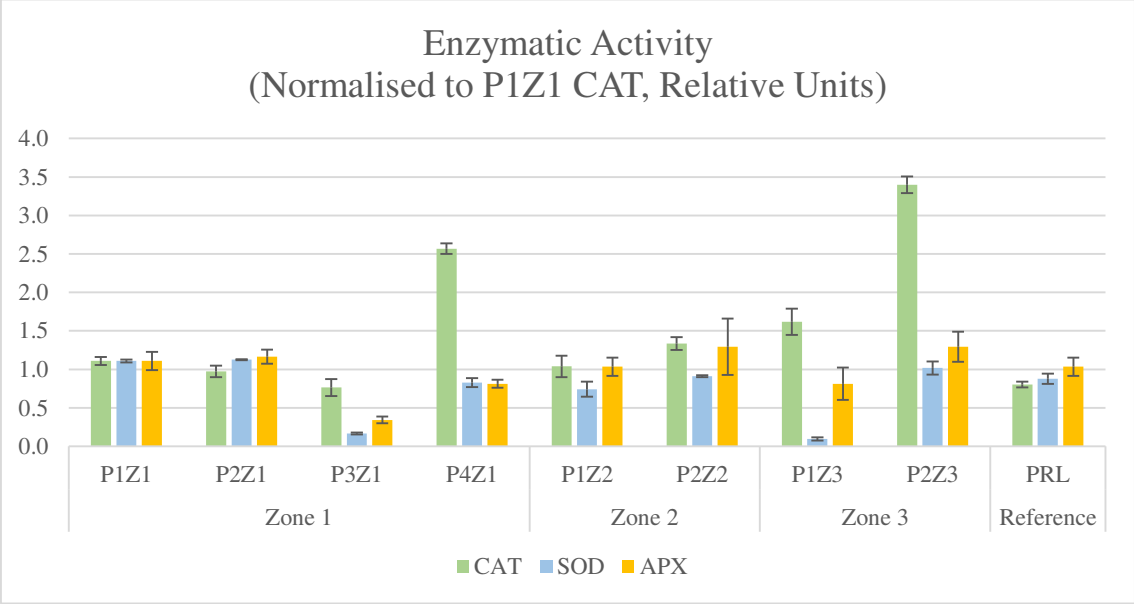

Figure 37: results of the enzymatic antioxidant assays grouped by specimens and zones, normalised to P1Z1 CAT mean value and expressed in relative units; the error bar is the standard deviation.

Such results are in contrast to the non-enzymatic antioxidants assays data, where a marked difference between the zones was detected. This may be due to the fact that the expression of

enzymes is much more energy-intensive in respect to the production of antioxidant simple molecules, and would be an ideal quick response towards a sudden stress, but not advantageous for long times, as during adaptation. Therefore, it might be that the specimens relied mostly on their non-enzymatic antioxidant machinery to cope with the wastewater contaminants, while expressing only the strictly necessary enzymes amount, in order to maintain their metabolic efficiency.

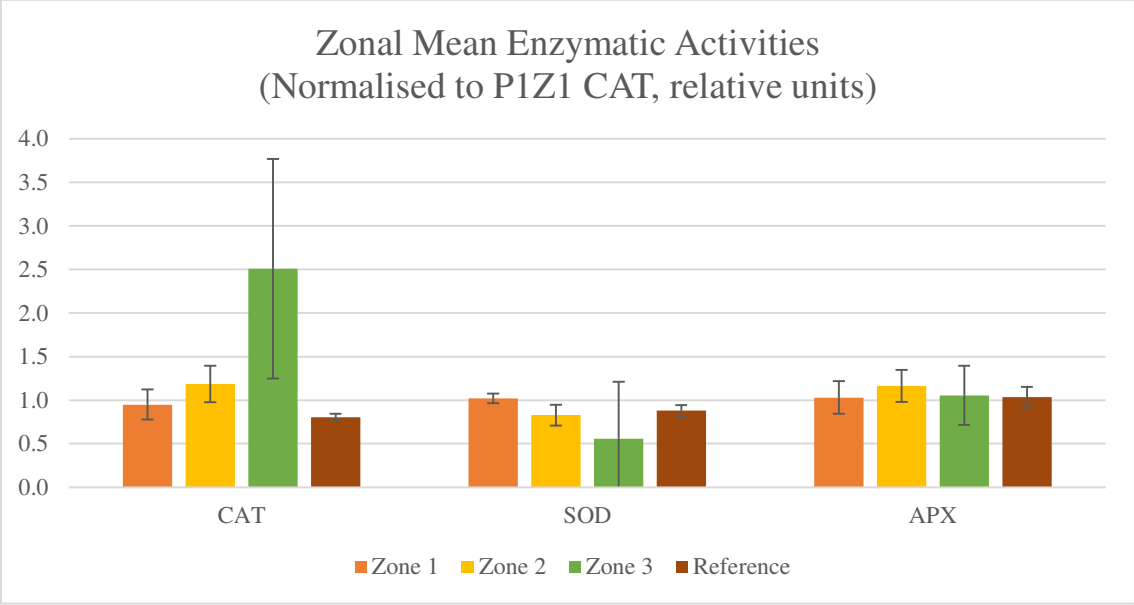

Figure 38: zonal mean values of the enzymatic antioxidant assays grouped by assay, normalised to P1Z1 CAT mean value and expressed in relative units; the error bar is the standard deviation.

4.9. Elemental Analysis

4.9.1. C, N Analysis

In the total organic carbon analysis, no significant difference between the samples nor between their parts was observed. The mean content of C resulted 377 ± 22 g per kg of dry material.

Conversely, it was assessed a marked clustering for specimens from Zone 3 (Figure 39) in terms of N content. In fact, they presented the highest N concentration, in particular in the leaf (33 ± 3 g kg^{-1}) and in the rhizome (10 ± 3 g kg^{-1}).

As hypothesised in Section 4.5 and Section 4.6, this might be attributable to the harsher conditions that Zone 3 plants may suffer due to the highest wastewater contaminants concentrations, and might be correlated to the higher chlorophylls expression reported in Section 4.5, in comparison to the other zones specimens.

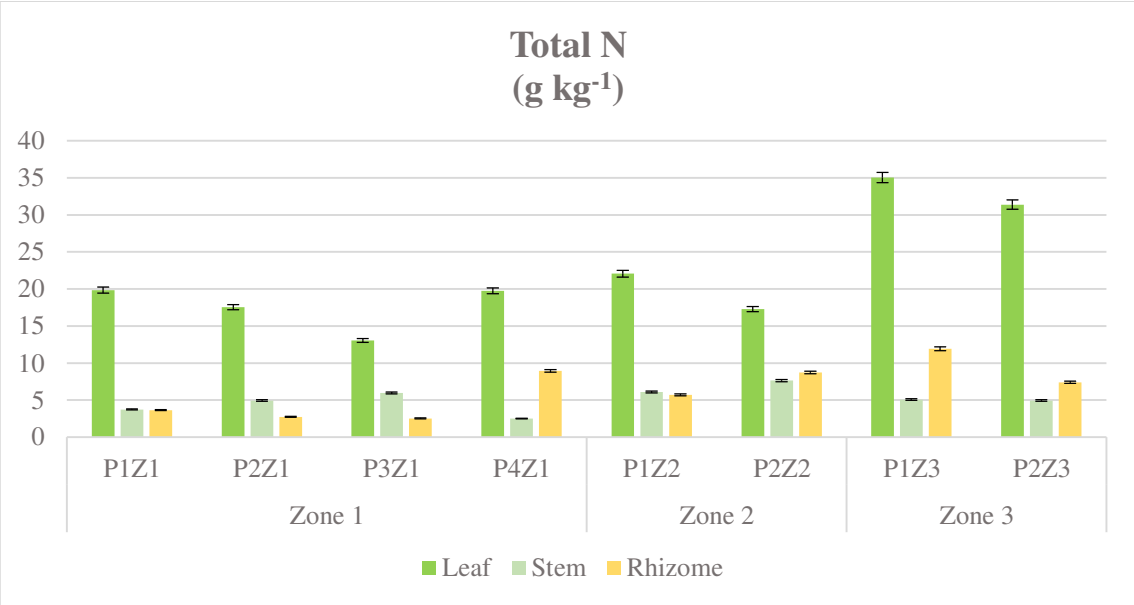

Figure 39: N percentages measured in samples of three organs of specimens of *P. australis* collected in different zones of the wetland, expressed in g kg^{-1} of dry matter. The error is based on the instrument sensitivity.

4.9.2. ICP-OES Analysis

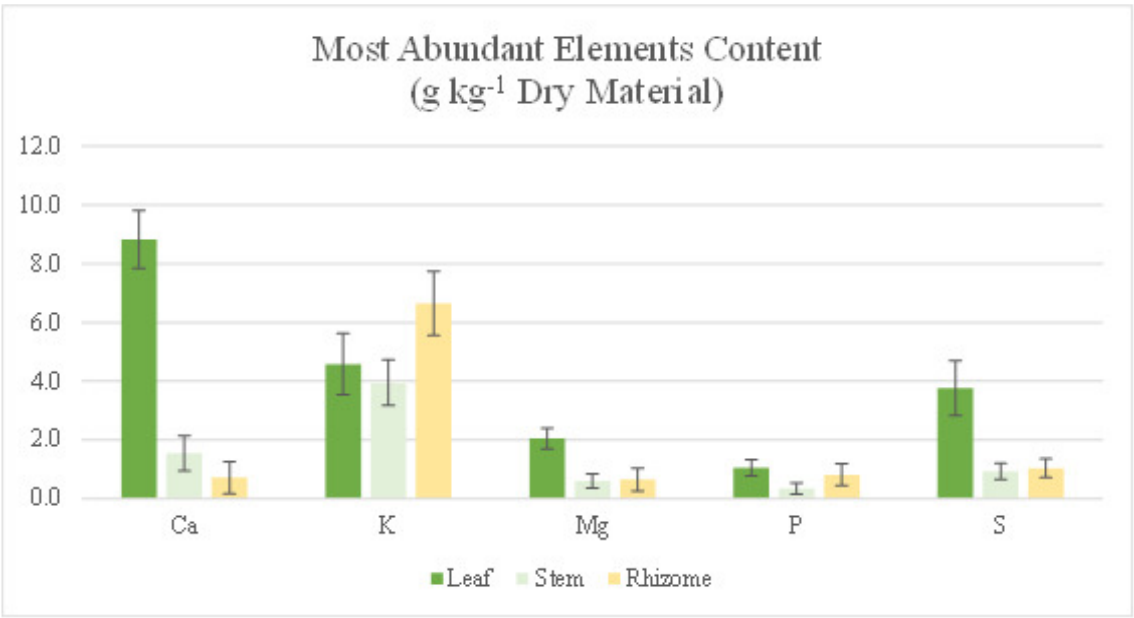

Figure 40: most abundant (≥ 1 g kg^{-1} dry material) elements measured in samples of three organs of *P. australis*, expressed as mean concentration values of all the Zone 3 specimens, in g kg^{-1} of dry matter. Error bars correspond to the standard deviations.

It was assessed that the leaf presented the highest concentration of Ca (9 ± 1 g kg^{-1} of dry matter), Mg (2 ± 0.2 g kg^{-1}) and S (3.8 ± 0.9 g kg^{-1}) amongst all the parts. The stem and the rhizome resulted to contain similar amounts of such elements, around 0.1 g kg^{-1}.

Conversely, the rhizome resulted to concentrate K to the highest extent (7 ± 1 g kg^{-1}), followed by the leaf (5 ± 1 g kg^{-1}) and the stem (3.9 ± 0.8 g kg^{-1}); considering the standard deviation values, however, there is no significant statistical difference between the different

organs. The same applies to P, present at a concentration of 1.1 ± 0.3 g kg^{-1} in the leaf, 0.3 ± 0.2 g kg^{-1} in the stem and 0.8 ± 0.4 g kg^{-1} in the rhizome.

Regarding the minor elements, present between 1 and 0.001 g kg^{-1} of dry material, there was no significant statistical difference between the parts. Two elements in particular stood out: Na resulted to be the most abundant, with concentrations of 0.8 ± 0.5 g kg^{-1} in the rhizome, 0.6 ± 0.2 g kg^{-1} in the stem, and 0.2 ± 0.2 g kg^{-1} in the leaf. Sr resulted to be the second in concentration, with 0.12 ± 0.05 g kg^{-1} in the leaf, 0.03 ± 0.02 g kg^{-1} in the stem and 0.01 ± 0.02 g kg^{-1} in the rhizome.

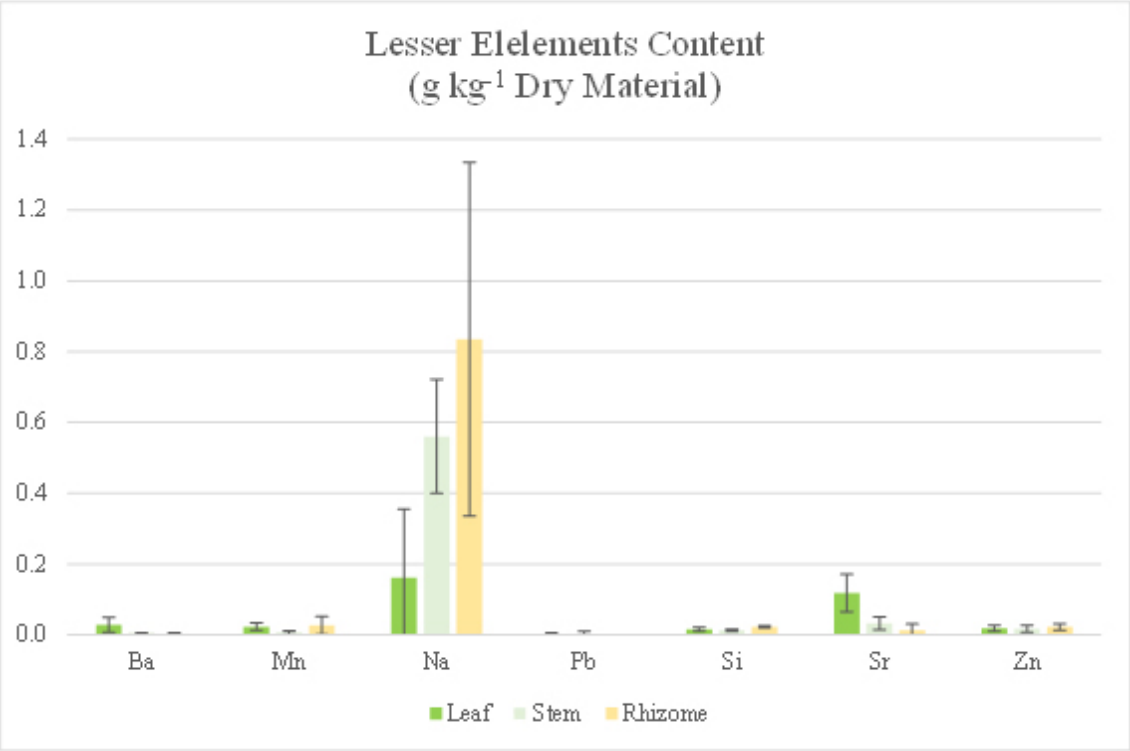

Figure 41: mean concentration values of lesser (between 0.001 and 1 g kg^{-1} dry material) elements, measured in three different organs of all the *P. australis* specimens sampled, expressed in g kg^{-1} of dry matter. Error bars correspond to the standard deviations.

Ba, Mn, Pb, Si and Zn resulted to be present in concentrations of around 0.01 g kg^{-1}.

4.9.2.1. Translocation factors for Zone 3

It was assessed that the Zone 3 plants, hypothesised as the most stressed specimens, presented a particular active translocation (translocation factor ≥ 7 g g^{-1}) of Ba, Ca, Pb, and Sr towards their leaves from the rhizomes and the stem, in particular from the rhizome, exception made for Pb. A high mean value of Pb translocation factor was achieved by the stem as well, but the associated standard deviation is too high for these data to be reliable.

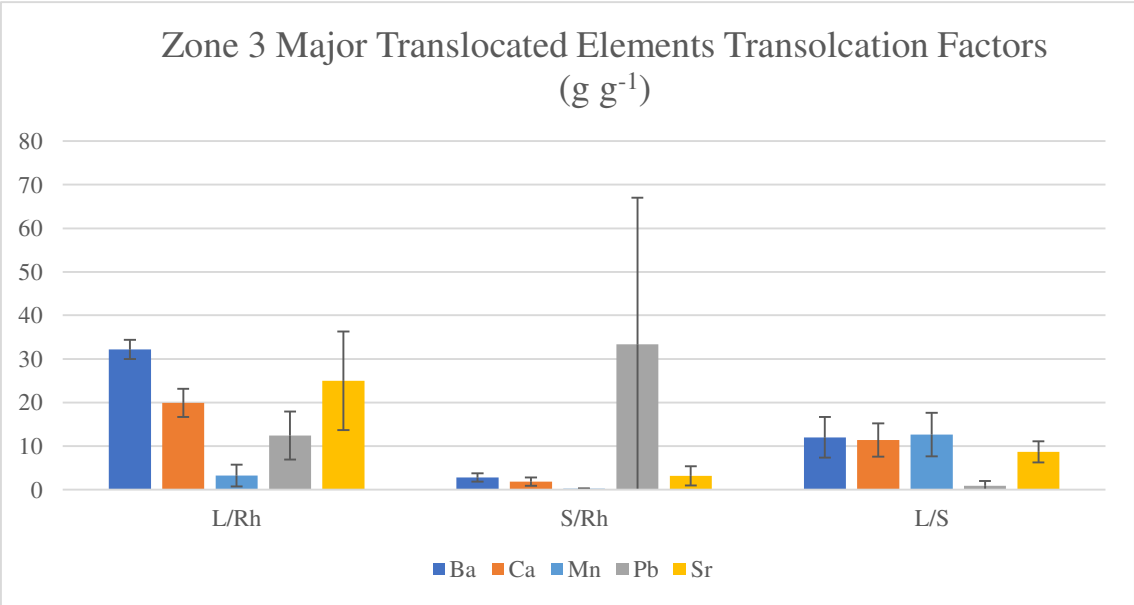

Figure 42 Major translocated elements (≥ 7 g g^{-1}) for the specimens of Zone 3. The translocation factors are averaged between plants and expressed in g g^{-1} of dry matter. Error bars correspond to standard deviations.

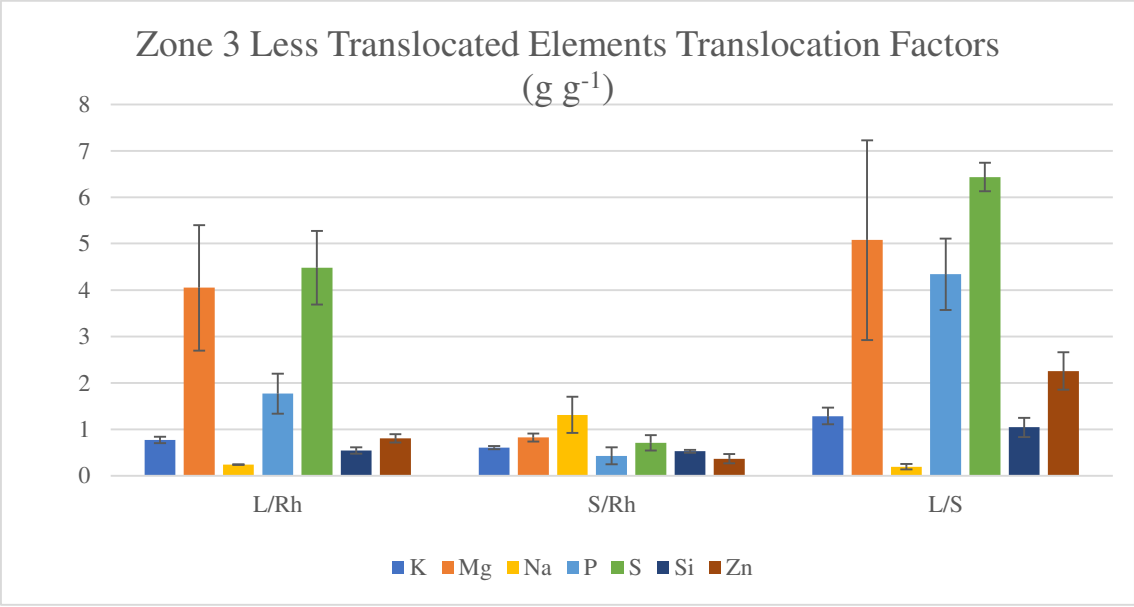

Figure 43: Zone 3 specimens less translocated elements (< 7 g g^{-1}) translocation factors, means between plants and standard deviation as error, expressed in g g^{-1} of dry matter.

With regard to the elements with a translocation factor < 7 g g^{-1}, the leaves proved anew to promote translocation more than the stem, except for Na. In particular, P and S resulted to be moderately translocated from, respectively, the stem and the rhizome, as Mg, in both cases.

4.9.2.2. Wastewater Analysis

The results of the elemental analysis on the wastewater are presented in Figure 44, Figure 45 and Figure 46.

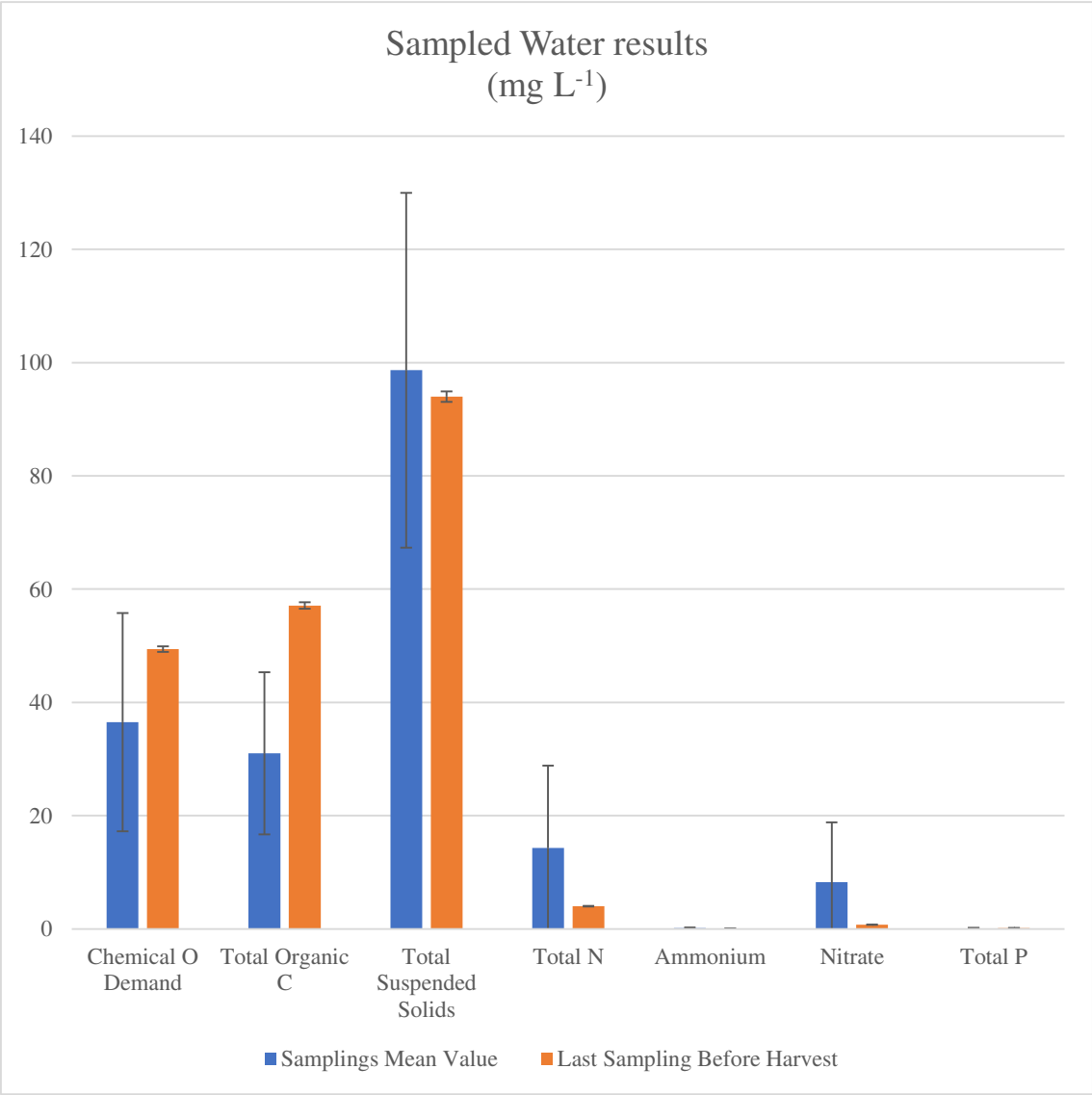

Figure 44: chemical oxygen demand, total organic carbon, total suspended solids, total N, ammonium, nitrate and total P mean values in one year (blue) and last values before plants sampling (orange), expressed in mg L^{-1} of solution. In the mean values, the error represents the variability throughout the 14 samplings performed in one year. For the last wastewater sampling (orange), the error represents the standard deviation.

The chemical oxygen demand characterising the water samples resulted to vary throughout the year between 13.4 and 75.1 ± 0.4 mg L^{-1}, with a mean value of 37 ± 19 mg L^{-1}. The last value registered before the *P. australis* sampling was 49.4 ± 0.4 mg L^{-1}.

The total organic carbon varied between 31 and 57 ± 0.4 mg L^{-1}, with a mean value of 31 ± 14 mg L^{-1}. The highest value coincided with the last sampling before the harvest.

The total N content spaced between 2.0 and 49.3 ± 0.3 mg L^{-1} , meanly 14 ± 14 mg L^{-1}, with the last sample obtained before the harvest characterised by a nitrogen content of 4.0 ± 03 mg L^{-1}. Only a small part (0.1 ± 0.1 mg L^{-1}) was constituted by $NH4^{+}$, while NO_3^{-} composed approximately the half, ranging between 0.4 and 32.5 ± 0.5 mg L^{-1}, with the last sample gathered before the harvest presenting a value of 0.7 ± 0.5 mg L^{-1}.

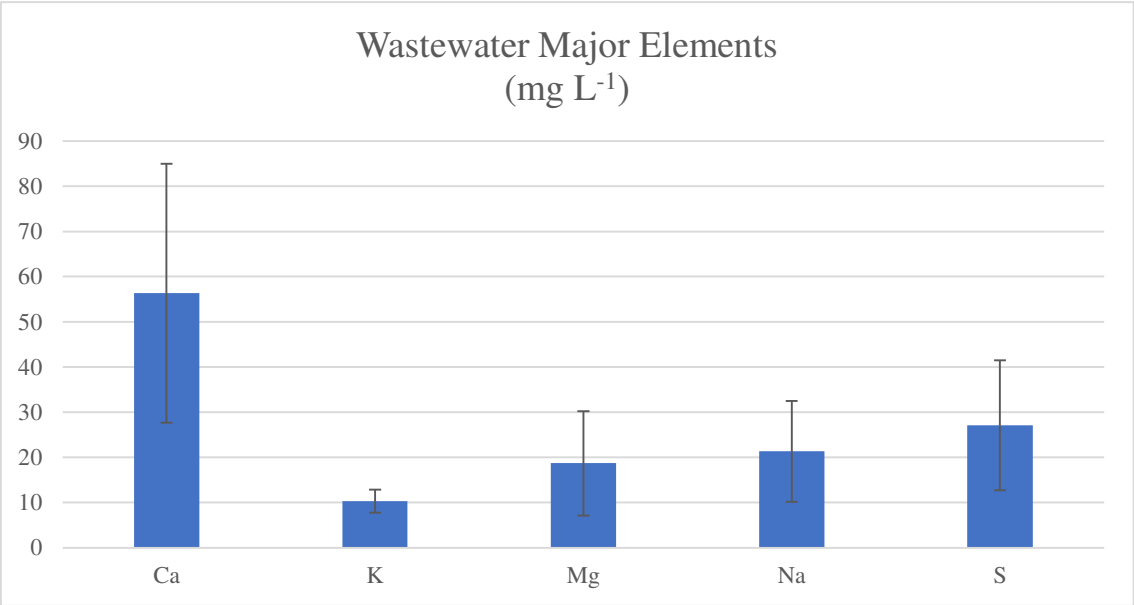

Figure 45: major elements (≥10 mg L^{-1}) detected in the wastewater samples, expressed in mg L^{-1} of solution. The error bar represents the variability throughout the 14 samplings performed in one year.

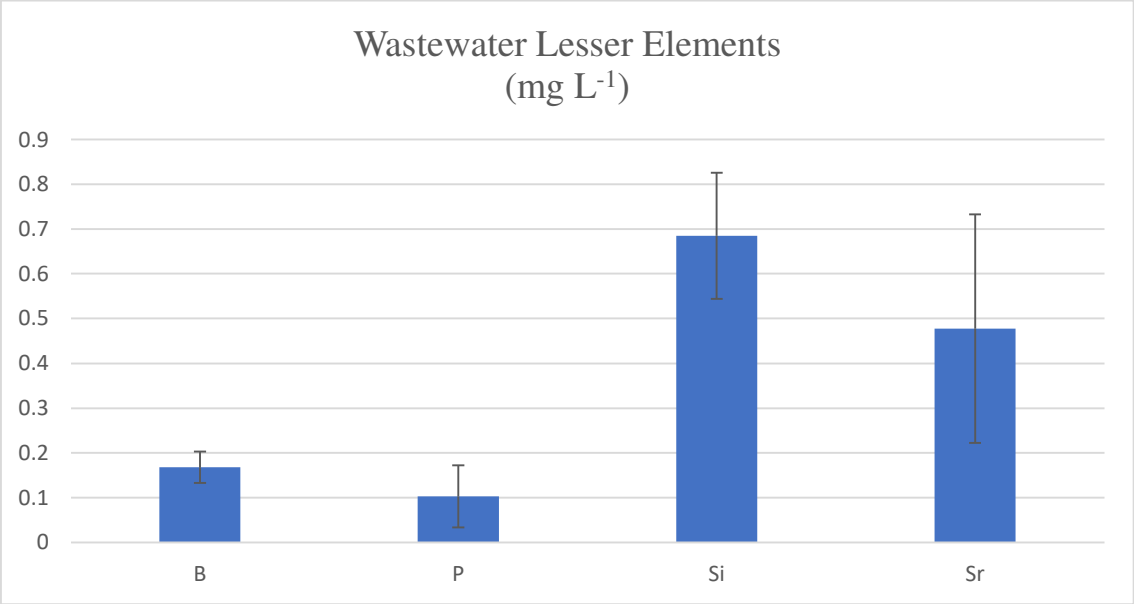

Figure 46: lesser elements (between 0.1 and 10 mg L^{-1}) detected in the wastewater samples, expressed in mg L^{-1} of solution. The error bar represents the variability throughout the 14 samplings performed in one year.

Very little total P amount was detected, ranging from 0.02 to 0.23 ± 0.02 mg L^{-1}, with the last sample before the harvest containing 0.14 ± 0.02 mg L^{-1}.

The solid residue recovered from the wastewater exhibited a value of total suspended solids fluctuating between 36 and 153 ± 1 mg L^{-1}, with a mean value of 98 ± 31 mg L^{-1}. ICP-OES analysis of the solids was also performed, and the mean values of the results of all the samples are reported in Figure 45 and Figure 46.

For the elements with concentrations higher than 10 mg L^{-1} (Figure 45), the highest level was recorded for Ca (56 ± 29 mg L^{-1}), followed by S (27 ± 14 mg L^{-1}), Na (21 ± 11 mg L^{-1}), Mg

(19 ± 12 mg L^{-1}), and K (10 ± 3 mg L^{-1}). Meanwhile, for the elements present in concentrations between 0.1 and 10 mg L^{-1} (Figure 46), the most abundant resulted to be Si (0.7 ± 0.1 mg L^{-1}), followed by Sr (0.5 ± 0.3 mg L^{-1}), B (0.17 ± 0.04 mg L^{-1}), and P (0.10 ± 0.7 mg L^{-1}).

The elemental composition of the examined wastewater is likely to derive from the use of fertilisers in the experimental crop. This is possible in particular for the major elements, *e.g.* $CaCO_3$.

Compared to the concentrations measured in *P. australis*, the wastewater values resulted to be lower: the most abundant element found in the water samples, Ca (56 ± 29 mg L^{-1}), was found almost 3 orders of magnitude lower than the mean leaf concentration (9 ± 1 g kg^{-1}).

4.9.2.3. Soil Analysis

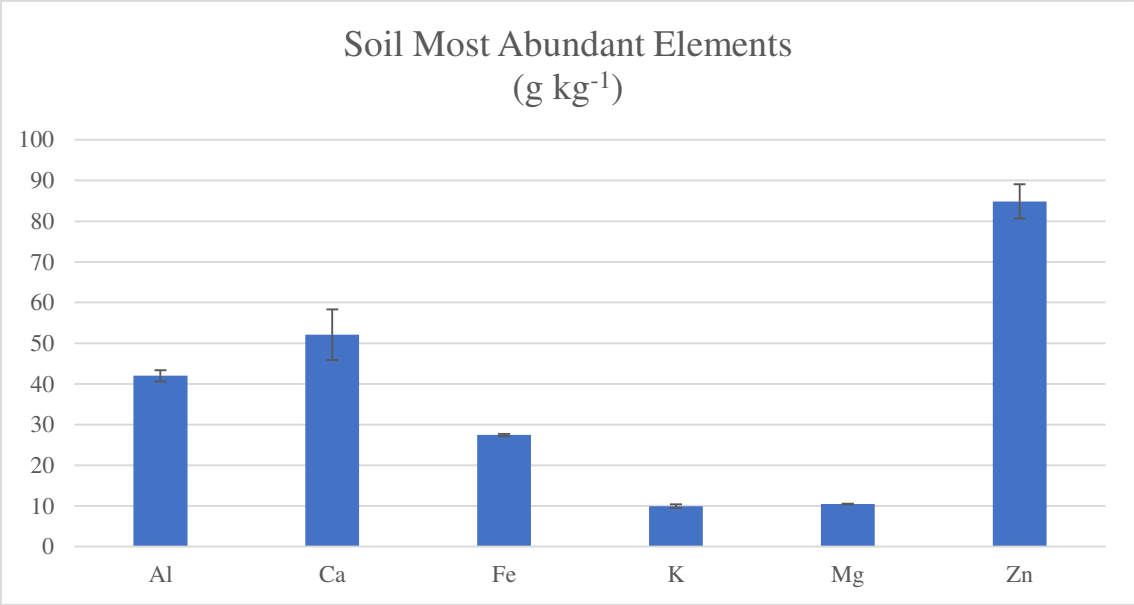

Figure 47: major elements (>1 g kg^{-1}) measured in the soil samples, expressed in g kg^{-1} of dry matter. The error is given by the variability throughout the sampling depths (0-5 cm, 5-15 cm, 15-30 cm, 30-60 cm).

The most abundant element (> 1 g kg^{-1} of dry soil sample) detected in the soil samples (Figure 47) resulted Zn (85 ± 4 g kg^{-1}), followed by Ca (52 ± 6 g kg^{-1}), Al (42 ± 1 g kg^{-1}), Fe (27.5 ± 0.3 g kg^{-1}), Mg (10.43 ± 0.05 g kg^{-1}) and K (9.9 ± 0.4 g kg^{-1}). The reported data are the mean values of the four sampling depths (0-5 cm, 5-10 cm, 15-30 cm, 30-60 cm).

The descending order elements found with concentrations ranging between 1 and 0.1 g kg^{-1} is Mn (0.70 ± 0.04 g kg^{-1}), Na (0.64 ± 0.05 g kg^{-1}), P (0.62 ± 0.09 g kg^{-1}), Ti (0.53 ± 0.02 g kg^{-1}), S (0.30 ± 0.08 g kg^{-1}), Sr (0.23 ± 0.02 g kg^{-1}), Ba (0.19 ± 0.01 g kg^{-1}), and Si (0.12 ± 0.02) g kg^{-1}).

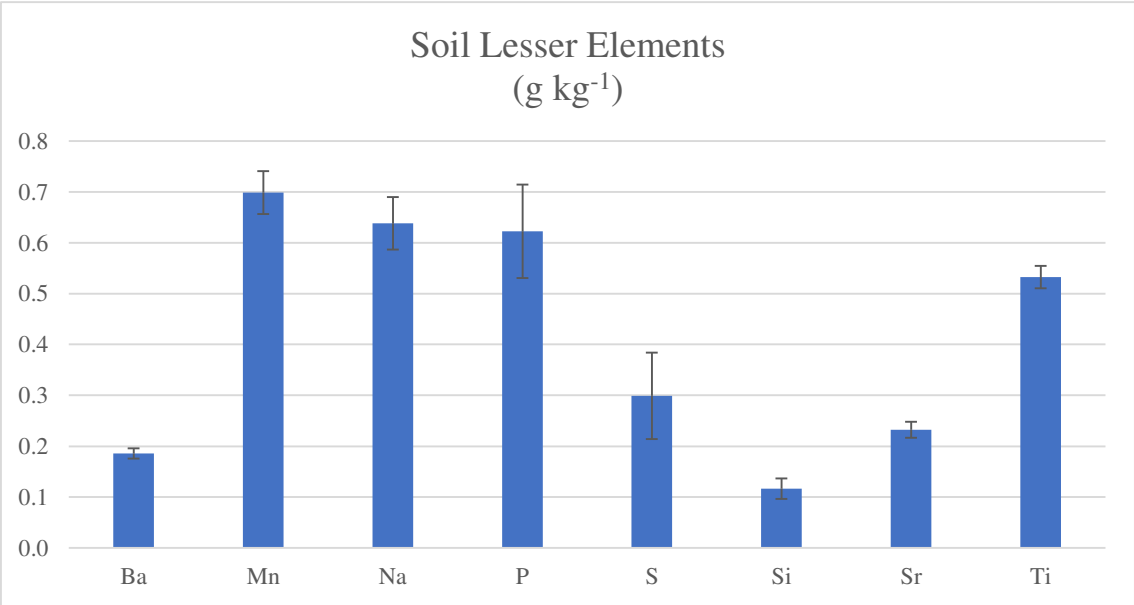

Figure 48: lesser elements (between 1 and 0.1 g kg^{-1}) measured in the soil samples, expressed in g kg^{-1} of dry matter. The error is given by the variability throughout the sampling depths (0-5 cm, 5-15 cm, 15-30 cm, 30-60 cm).

The high levels of metals such as Al, Fe, Mg and Zn is arguably ascribable to the natural soil composition, in particular to oxides and clays presence, which would contain such elements. The same may apply to minor elements as Mn, Na, Ti, and Sr.

The small concentration of P and S may be due to an efficient uptake by the plants, which would consume such elements during their metabolism.

4.9.3. Comparison between Plants, Water and Soil

By comparing the examined parts of the *P. australis* collected in Zone 3 with the soil sampled in the same area, it is possible to notice that the most abundant metals (**>**1 g kg^{-1} of dry material, Figure 49) as Al, Fe, Mg, and Zn tend to be significantly more abundant in the soil than in the plants organs, with a ratio up to 8500:1 (soil to leaves) for Zn and 221:1 (soil to leaves) for Al.

This is consistent with the hypothesis that such elements constitute the soil matrix, and are thus not bioavailable if present in the mineral form. Metallic ions could also have been present in the soil samples, and they may have been bound to the soil particles through electrostatic interactions. For example, even if they are fundamental for the plant metabolic functions, Fe ions bioavailability strongly depends on soil pH, and is usually low; Ca^{++} ion is also useful to plants, but its high charge density may imply a strong binding to the soil, decreasing its availability; the same could apply to Mg^{++}.

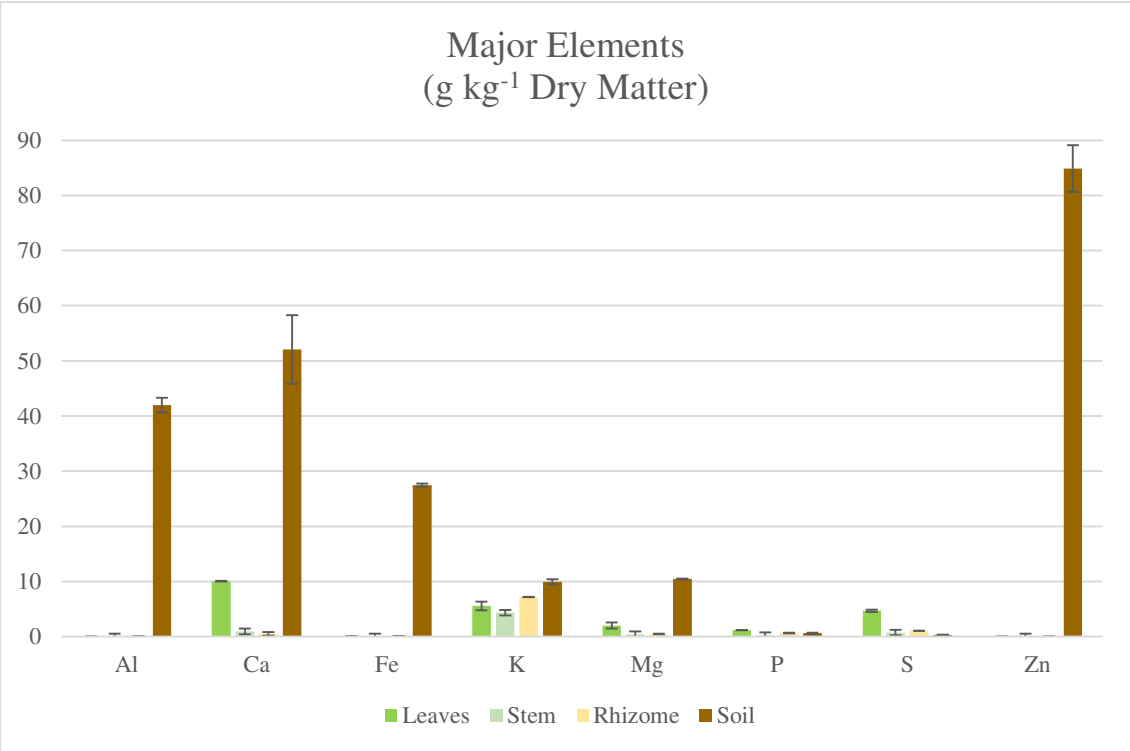

Figure 49: Mean concentrations of the major elements (≥1 g kg^{-1} of dry material) measured in the *P. australis* specimens and soil samples collected in Zone 3, expressed in g kg^{-1} of dry matter. The error bar for the plant concentrations is given by the standard deviation between the samples, while for the soil values is given by the variability throughout the sampling depths (0-5 cm, 5-15 cm, 15-30 cm, 30-60 cm).

In addition, when bioavailable, toxic metals as Al and Zn are probably kept outside the plants through exclusion mechanisms and external chelation through exudates production, in order to avoid metabolic disturbance.

K and P resulted to distribute quite evenly amongst the different plant parts and the soil.

S was mostly absorbed by the plants and particularly relocated into their leaves, arguably due to the fact that plants metabolise accumulated sulphur in this organ.

Elements with concentrations between 0.1 and 1 g kg^{-1} of dry material (Figure 50) were found as Mn (0.70 ± 0.04 g kg^{-1}), Na (0.63 ± 0.05 g kg^{-1}), and Sr (0.53 ± 0.02 g kg^{-1}). Na was the only element found in similar concentration in the plants stem (0.46 ± 0.003 g kg^{-1}) and rhizome (0.4 ± 0.1 g kg^{-1}), but not in the leaf; this might be due to a protection mechanisms which would prevent damages to the sensitive photosynthetic system by relocating Na^+ ions from the leaves to the other plants organs.

Sr was also present in the plants, particularly in the leaf (0.11 ± 0.02 g kg^{-1}), but at a fivefold lower concentration than in soil. As hypothesised for the major metals, this aspect, comprising Ba, Mn and Si, might be ascribable to the soil matrix constitution. Pb presence might be related to the use of pesticides or fungicides in the experimental farm, and could

have been excluded by the plant to avoid toxic effects.

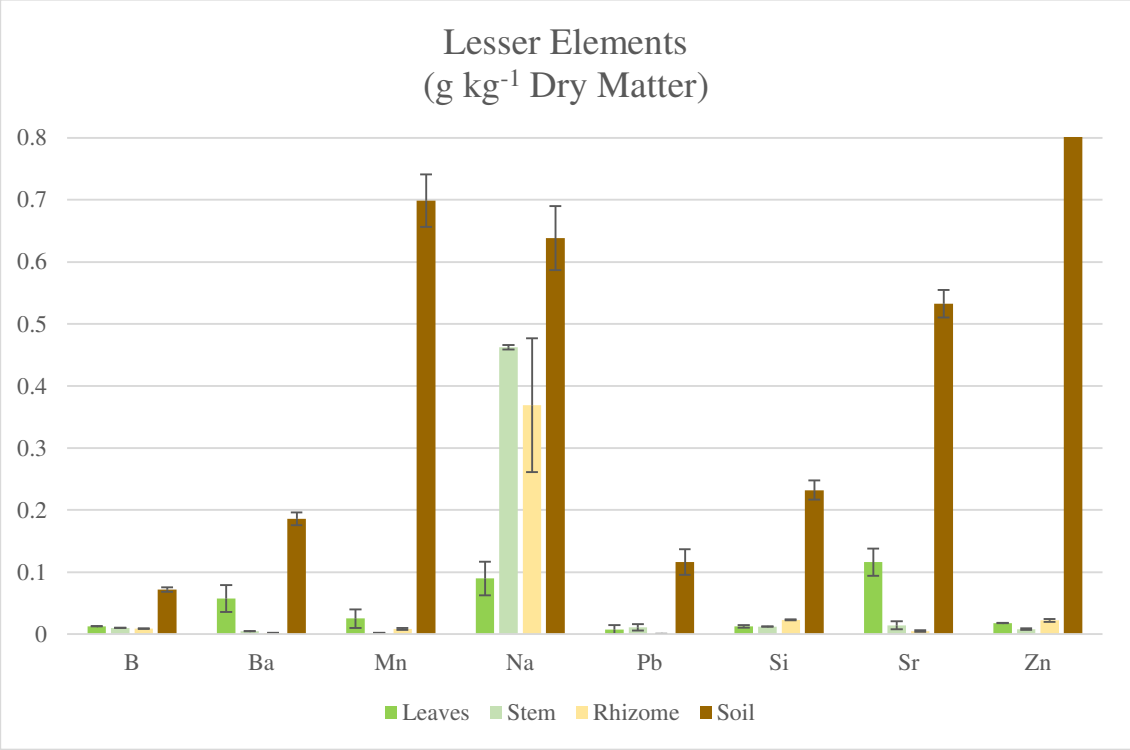

Figure 50: Mean concentrations of the lesser elements (<1 g kg^{-1}) measured for *P. australis* and in soil samples in Zone 3, expressed in g kg^{-1}. Zn value is cropped for convenience, since it is out of scale. The error for the plant concentrations is given by the standard deviation between the samples, while the error relative to soil values is given by the variability throughout the sampling depths (0-5 cm, 5-15 cm, 15-30 cm, 30-60 cm).

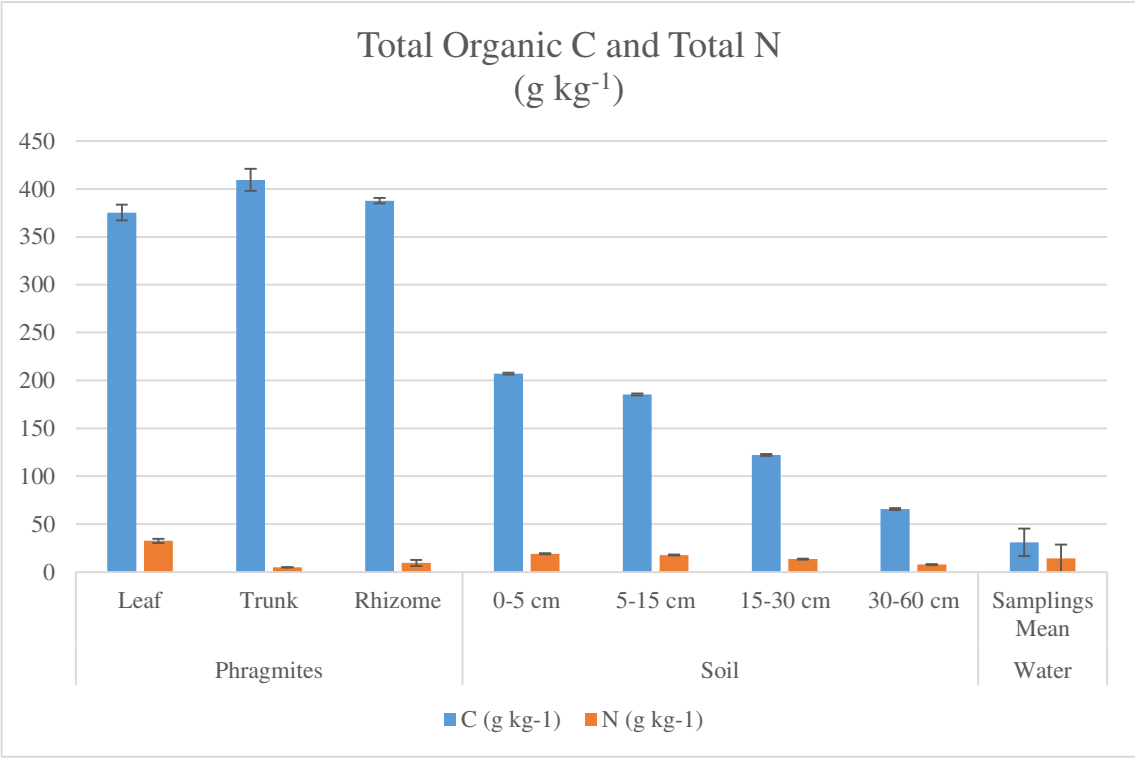

Figure 51: total organic carbon (blue) and total nitrogen (orange) measured in *P. australis*, soil and water samples of Zone 3, expressed in g kg^{-1} of dry matter (plant and soil) or solution (water, approximating a density of 1 kg L^{-1}). The errors are related to the standard deviation amongst samples.

In neither of the two graphs values relative to the water samples were comprised, since they are too small to be compared to the plants and soil data.

Regarding the C content (Figure 51), there was no substantial difference between the plants parts; stem presented the greatest concentration (409 ± 12 g kg^{-1}), which might be related to a higher presence of mechanical tissues, compared to the other organs. For the soil, it was assessed that the C content decreased whit the increasing of the sampling depth, which may be due to the progressive reduction of organic matter content. Wastewater samples plausibly presented the lowest C content (31 ± 14 g kg^{-1}, approximating the solution density to 1 kg L^{-1}), which might be due to the presence of dissolved organic matter.

Amongst all the values, N content resulted to be the highest for the leaves (32 ± 2 g kg^{-1}), in particular in respect to the stem (5.1 ± 0.1g kg^{-1}), which is consistent with their tissue composition. Beside this difference, N content was approximately the same between plants, soil depths and wastewater, with a mean value of (15 ± 9 g kg^{-1}).

.

5. Conclusions

Through this work, it was possible to confirm a variation in the physiology and elemental content amongst specimens of *P. australis* collected in different areas of a constructed wetland. The initial hypothesis of a stronger impact of the effluents in the upstream section of the wetland was verified with different levels of detail and from diverse perspectives.

Before analysing the wetland samples, the protocols for sample storage, pigments and antioxidants isolation and quantfication, and non-enzymatic antioxidant assays were optimised in different aspects, with the additional purpose to perfect the knowledge and to integrate missing or contradictory data and indications. A reference plant was harvested in the Botanical Garden of Bologna and employed to (I) assess the optimal solvent, procedure and time for the material extraction; (II) render the protocols for the assays more efficient, by increasing ABTS and DPPH reagent concentrations; (III) make the protocols safer by substituting toxic solvents, and in particular by substituting methanol with ethanol in ABTS, DPPH and flavonoids assays; (IV) reduce the employed volumes of the reactants and study their storability. If stored at 4°C, $AlCl_3$, $C_2H_3KO_2$ and quercetin solutions proved to be stable for at least 3 months, and radicalised ABTS for at least 4 months. Concentrated DPPH solution resulted to last at least 4 months if kept at – 20 °C.

Afterwards, plants, soil and wastewater samples collected in the wetland were processed and analysed.

The optical and electronic microscopic analysis revealed no difference amongst the examined specimens. SEM, however, allowed to notice that samples treated with glutaraldehyde undergo a tissue degradation, resulting in a fragility of the tissues that tend to collapse upon cut, conversely to the samples treated with ethanol and acetic acid.

The content of photosynthectic pigments in the leaves positively correlates with the hypothetical gradient of contaminant concentrations along the wastewater route. In fact, contaminants are supposed to be progressively removed by plants along the route, causing the wastewater inlet area (Zone 3) to record the highest levels of contaminants, and the outlet area (Zone 1) the lowest ones. This positive correlation might appear inconsistent with the fact that stressed plants usually display signs of chlorosis, *i.e.* the depigmentation of the photosynthetic tissues. In this case, chlorophylls and carotenoids content tends to increase with the increase of pollutants in the water. This might be explained by the fact that the wastewater treated in this wetland are in fact a source of nutrients for the plant, containing high levels of C and N. Hence, as shown in other studies, *P. australis* could actually benefit

from these type of water pollutants [92]. Moreover, carotenoids are involved in the signalling of the antioxidant response, hence they are expected to increase with higher levels of chemical stressors.

The non-enzymatic antioxidant assays (ABTS, DPPH, FRAP and Flavonoids-$AlCl_3$ complexation) indicated that the upstream Zone 3 hosts the specimens with the lowest antioxidant activity, followed by the downstream area, Zone 1, and by the intermediate area, Zone 2, that hosts the plants with the highest antioxidant values. This trend may be related to an excessive concentration of wastewater contaminants at the beginning of the wetland route, which could heavily impact on the plants metabolism, not allowing them to express enough antioxidant molecules before experiencing a metabolic hindrance. In contrast with the results of the pigments analysis, plants from Zone 2 resulted to exert the highest non-enzymatic antioxidant activity, probably in consistence with the abovementioned hypothesis of the ideal balance between stimulating stress factors and growth and development. Another possible explanation is that plants of Zone 3, that are receiving more fertilisers, tend to produce more biomass, thus compensating the impact of high pollutants levels with more cells and tissues able to process them. According to this hypothesis, antioxidants levels of *P. australis* specimens would be similar between Zone 1 and Zone 3, because the ratio of plant biomass and water pollutants concentration is comparable between the two areas. Conversely, in Zone 2 this ratio could be lower, promoting a higher antioxidant activity to compensate.

SOD, CAT and APX enzymatic assays results did not concur to any relevant differentiation amongst the zones, possibly in consistence with the higher metabolic expense required by the enzyme expression, compared to the simple antioxidant molecules production. In a perspective of adaptation, plants would rather invest on the synthesis of non-enzymatic antioxidants, maintaining more energy for their growth and development, than producing expensive macromolecules, which could be effective on sudden, acute stress but are too energetically demanding for a long-term strategy.

Through the elemental analysis, the inlet zone was again confirmed as significantly differing from the others, with a higher N concentration in plant tissues, and particularly in their leaves, coherently with the higher chlorophyll expression. The analyses focused on the plants of this area, and aimed to detect correlations between their elemental composition and the soil and water. However, no significant difference was noticed in the N content between the plants, soil and water samples. Nonetheless, the environmental N concentrations might have

been too low to induce hyperaccumulation phenomena in the plants, and further experiments might be required to examine this hypothesis.

Regarding C content, plants obviously displayed a higher C content of both soil and water, being carbon-based lifeforms. C content of the stem was slightly higher in respect to the leaf, consistently with the abundance of mechanical tissues and fibres in general in this organ, which is coherent to the higher N content in the leaf, where the support structures are fewer. The upper 5 cm of soil resulted to contain a C amount intermediate between the plant and the water, that was decreasing with depth. This is most likely due to the littering and decaying of organic matter on the soil surface.

The analysis of the other elements allowed to hypothesise that *P. australis* adopted an exclusion mechanism towards toxic metals present in soil: in fact, metals such as Al and Zn were found as particularly present in the soil, while did not have significant concentrations in the plants. The soil content is probably linked to its matrix composition, but it is not unlikely that at least a fraction of its elements was bioavailable, and that could have affected the plant metabolism.

Some elements, in particular Ca, S, Na, Mg and K, were found in the analysed wastewater as well, but at concentrations of orders of magnitude smaller than those of the plants and the soil.

In summary, some correlations were found between the water pollutants levels and the plants physiology, but further experiments are required in order to deepen and broaden the knowledge of the examined system and on phytoremediation in general.

It may be of interest the application of spiking, to study whether the plants in the examined system could develop different responses in relation to varying contaminants concentrations. Analogously, by varying water parameters, *e.g.* hydraulic retention time and loading rate, it could be possible to inspect whether the plant would adapt to different conditions, with the aim to detect the best operational parameters.

The sampling of the treated water at the end of its course and at the route midpoint, as well as periodical samplings of the plants, the soil and the water, and of different plants species could be useful to keep track of a possible route and seasonal variability, contributing to study in a more complete way the system, and to evaluate its performance.

Considering the broad availability of analytical techniques, it may be of interest to perform additional analysis, such as photosynthetic activity, and further enzymatic and non-enzymatic antioxidant assays, *e.g.* CUPRAC, ORAC, TRAP, GSH and MAD, cyclic voltammetry, amperometry, fluorimetry, GC and HPLC.

6. Acknowledgments

I, the author, would like to thank my Supervisor Chiar.mo Prof. Stefano Del Duca, who gave me the opportunity to explore such a beautiful field, encouraging me with his gentle presence, giving me new ideas and for having permitted me to grow in his Department.

My special gratitude goes to Dr. Iris Aloisi who rendered possible all of this, with her kindness and enthusiasm, her inventiveness, her capacity to involve everyone and for having contributed to create this amazing experience and the majestic team, the family, I have had the joy to work and joke with.

I would like to thank Dr. Luigi Parrotta, for his professional contribution and the reciprocal esteem, as well as for his jokes which cheered up many a days, and whose niceness has been indispensable in creating this group.

Special thanks to Ph.D. Chiara Suanno for having helped me in the revision of my works, both thesis and article, and for the statistical elaboration during the PCA multivariate analysis.

Thanks to Dr. Simona Corneti for her kind-heartedness, for her help in the communication with the other Departments and for sharing her knowledge in some of the many fields she masters.

My thanks go to Prof. Attilio Toscano and Dr. Stevo Lavrnić, for letting me cooperate with their research group, sharing data and knowledge, making this experience so broad, as well as for permitting me to participate in their laboratory activities related to this work.

Particular thanks to Prof. Fabiana Antognoni for her kind support and esteem, and for the interesting talks we have had.

I would like to thank Dr. Maria Roberta Randi for having shared her knowledge on the SEM functioning, while introducing me to the new instruments, and rendering possible to admire reality under a new, unique perspective.

A thank to Dr. Andrea Simoni for having followed me in the preparation of the samples and for the analysis at the ICP-OES.

I thank Prof. Giovanni Valdrè and Dr. Gianfranco Ulian for having granted me the access to the SEM-EDX.

I thank Ph.D.s Grazia Federica Bencresciuto and Agnese Bonifazi for having helped me during the laboratory sessions held in their Department.

My thanks go to Stefano Anconelli and Domenico Solimando of the Consorzio di Bonifica Canale Emiliano Romagnolo for the precious assistance in the field during sample collection;

Thank to my friend and fellow Filippo, with whom I worked and joked side by side, and my other friends of the Department Giuseppe, Flavia, Luca, Stefania, Maria Grazia, Aida, and Davide.

I want to profoundly thank my great family, my Mother, my Father, my Sister Serena and her companion Luca, who gave me the opportunity and means to study such beautiful field, in this marvellous city, and who supported me with their love, their kindness and their generosity.

I thank the wonderful city I have had the enormous luck to study in, Bologna, which gave me countless opportunities and joys; and the Department of Biological Sciences, Geological and Environmental (BiGeA), which warmly welcomed me with a lot of gentleness.

Dulcis in fundo, I want to thank from my heart Celestina, who tirelessly supported me in all my life, with a lot of love and care, with her sympathy, her intelligence, her culture, and her enormous heart.

Without these special people, without this special place, their fundamental presence and their esteem, all of my experience would probably have been different, elsewhere, and I doubt I would have had all the opportunities and joy I have had in this Department, and in life. In this brief but incredibly intense experience, I have grown as I would have never imagined, both personally and professionally. I thank you all, may your lives be bright and full of satisfaction.

7. References

1. Novotny, V. - Water quality : diffuse pollution and watershed management. 864 (2003).

2. Anandhi, A. & Kannan, N. - Vulnerability assessment of water resources – Translating a theoretical concept to an operational framework using systems thinking approach in a changing climate: Case study in Ogallala Aquifer. *Journal of Hydrology* **557**, 460–474 (2018).

3. Castellari, S. & Kurnik, B. *Climate change, impacts and vulnerability in Europe 2016*. (2017).

4. Anandhi, A. & Kannan, N. - Vulnerability assessment of water resources – Translating a theoretical concept to an operational framework using systems thinking approach in a changing climate: Case study in Ogallala Aquifer. *Journal of Hydrology* **557**, 460–474 (2018).

5. Giri, S. *et al.* - Water security assessment of current and future scenarios through an integrated modeling framework in the Neshanic River Watershed. *Journal of Hydrology* **563**, 1025–1041 (2018).

6. Cui, N. *et al.* - Roles of vegetation in nutrient removal and structuring microbial communities in different types of agricultural drainage ditches for treating farmland runoff. *Ecological Engineering* **155**, 105941 (2020).

7. Chislock, M. F., Doster, E., Zitomer, R. A. & Wilson, A. E. - Eutrophication: Causes, Consequences, and Controls in Aquatic Ecosystems. *Nature Education Knowledge* **4**, 10 (2013).

8. EPA. - Basic Information about Nonpoint Source (NPS) Pollution. https://www.epa.gov/nps/basic-information-about-nonpoint-source-nps-pollution.

9. McPherson, K. A. - The united states. *Central Organizations of Defense* 200–222 (2019) doi:10.4324/9780429044717-11.

10. Kobayashi, Y. *et al.* - Life cycle assessment of decentralized greywater treatment systems with reuse at different scales in cold regions. *Environment International* **134**, 105215 (2020).

11. Spångberg, J. *et al.* - Environmental impact of recycling nutrients in human excreta to agriculture compared with enhanced wastewater treatment. *Science of the Total Environment* **493**, 209–219 (2014).

12. Dominguez, S. *et al.* - LCA of greywater management within a water circular economy restorative thinking framework. *Science of the Total Environment* **621**, 1047–1056 (2018).

13. Li, F. *et al.* - Review of the technological approaches for grey water treatment and reuses. *Science of the Total Environment* **407**, 3439–3449 (2009).

14. Mehta, C. M. *et al.* - Technologies to Recover Nutrients from Waste Streams: A Critical Review. *Critical Reviews in Environmental Science and Technology* **45**, 385–427 (2015).

15. Jensen, S. M. *et al.* - Phosphorus Recovery from Wastewater: Bioavailability of P Bound to Calcareous Material for Maize (Zea Mays L.) Growth. *Recycling* **6**, 25 (2021).

16. Masi, F. - Water reuse and resources recovery: the role of constructed wetlands in the Ecosan approach. *Desalination* **246**, 27–34 (2009).

17. Lam, K. L. *et al.* - Life cycle assessment of nutrient recycling from wastewater: A critical review. *Water Research* **173**, (2020).

18. Melián, J. A. H. - Sustainable waste water treatment systems (2018-2019). *Sustainability (Switzerland)* **12**, 7–11 (2020).

19. Ahmed, S. F. *et al.* - Recent developments in physical , biological , chemical , and hybrid treatment techniques for removing emerging contaminants from wastewater. *Journal of Hazardous Materials* **416**, 125912 (2021).

20. Nedjimi, B. - Phytoremediation: a sustainable environmental technology for heavy metals decontamination. *SN Applied Sciences* **3**, 1–19 (2021).

21. Pandey, V. C. & Bajpai, O. *Phytoremediation: From Theory Toward Practice*. *Phytomanagement of Polluted Sites: Market Opportunities in Sustainable Phytoremediation* (Elsevier Inc., 2018). doi:10.1016/B978-0-12-813912-7.00001-6.

22. Tiwari, J. *et al. Ecorestoration of Polluted Aquatic Ecosystems Through Rhizofiltration*. *Phytomanagement of Polluted Sites: Market Opportunities in Sustainable Phytoremediation* (Elsevier Inc., 2018). doi:10.1016/B978-0-12-813912-7.00005-3.

23. Richard B Meagher. - Phytoremediation of toxic elemental and organic pollutants. *Current Opinion in Plant Biology* **3:153–162**, 153–162 (2000).

24. Heineke, D. & Scheibe, R. - Photosynthesis: The Calvin Cycle. in *Encyclopedia of Life Sciences* (American Cancer Society, 2009). doi:10.1002/9780470015902.a0001291.pub2.

25. Pirrera, G. & Pluchino, A. - Phytoremediation for ecological restauration and industrial ecology. *Procedia Environmental Science, Engineering and Management* **4**, 273–282 (2017).

26. EUROSTAT. - Agricultural land prices by region. *Land prices and rents (online data code: APRI_LPRC)* https://ec.europa.eu/eurostat/databrowser/view/apri_lprc/default/map?lang=en (2018).

27. Pandey, V. C. *et al.* - Sustainable phytoremediation based on naturally colonizing and economically valuable plants. *Journal of Cleaner Production* **86**, 37–39 (2015).

28. Weir, E. & Doty, S. - Social acceptability of phytoremediation: The role of risk and values. *International Journal of Phytoremediation* **18**, 1029–1036 (2016).

29. Koelmel, J. *et al.* - Bibliometric Analysis of Phytotechnologies for Remediation: Global Scenario of Research and Applications. *International Journal of Phytoremediation* **17**, 145–153 (2015).

30. Shah, V. & Daverey, A. - Phytoremediation: A multidisciplinary approach to clean up heavy metal contaminated soil. *Environmental Technology and Innovation* **18**, 100774 (2020).

31. Pandey, V. C. & Souza-Alonso, P. *Market Opportunities: In Sustainable Phytoremediation*. *Phytomanagement of Polluted Sites: Market Opportunities in Sustainable Phytoremediation* (Elsevier Inc., 2018). doi:10.1016/B978-0-12-813912-7.00002-8.

32. Petroselli, A. *et al.* - Integrated System of Phytodepuration for Agroindustrial Wastewater: Three Different Case Studies. *International Journal of Phytoremediation* **17**, 1227–1236 (2015).

33. Sharma, P. *et al.* - Integrating phytoremediation into treatment of pulp and paper industry wastewater: field observations of native plants for the detoxification of metals and their potential as part of a multidisciplinary strategy. *Journal of Environmental Chemical Engineering* 105547 (2021) doi:10.1016/j.jece.2021.105547.

34. Jenssen, P. D. *et al.* - High performance constructed wetlands for cold climates. *Journal of Environmental Science and Health - Part A Toxic/Hazardous Substances and Environmental Engineering* **40**, 1343–1353 (2005).

35. Adhikari, U. *et al.* - Use of duckweed-based constructed wetlands for nutrient recovery and pollutant reduction from dairy wastewater. *Ecological Engineering* **78**, 6–14 (2015).

36. Lavrnić, S. *et al.* - Performance of a full scale constructed wetland as ecological practice for agricultural drainage water treatment in Northern Italy. *Ecological Engineering* **154**, 105927 (2020).

37. Wu, H. *et al.* - A review on the sustainability of constructed wetlands for wastewater treatment: Design and operation. *Bioresource Technology* **175**, 594–601 (2015).

38. Gupta, P. *et al.* - Use of biochar to enhance constructed wetland performance in wastewater reclamation. *Environmental Engineering Research* **21**, 36–44 (2016).

39. Davis, M. L. *Secondary Treatment By Suspended Growth Biological Processes, Chapter (McGraw-Hill Professional, 2010), Access Engineering*. *Water and Wastewater Engineering: Design Principles and Practice.* (2010).

40. Hua, C. - The use of CWs for Wastewater Treatment. 24 (2003).

41. Anawar, H. M. *et al. Long-term performance and feasibility of using constructed wetlands for*

treatment of emerging and nanomaterial contaminants in municipal and industrial wastewater. Emerging and Nanomaterial Contaminants in Wastewater: Advanced Treatment Technologies (Elsevier Inc., 2019). doi:10.1016/B978-0-12-814673-6.00003-6.

42. Luo, P. *et al.* - Nitrogen removal and recovery from lagoon-pretreated swine wastewater by constructed wetlands under sustainable plant harvesting management. *Bioresource Technology* **258**, 247–254 (2018).

43. Plaines, D. & Watersheds, R. - Final Report Region 5 Wetland Management Opportunities and Marketing Plan :

44. Stefanakis, A. I. - The Role of ConstructedWetlands as Green Infrastructure for Sustainable Urban Water Management. *Sustainability (Switzerland)* **11**, (2019).

45. Ghermandi, A. - Evaluating functions and benefits of constructed wetlands. 1–15 (2005).

46. Sun, G. J. *et al.* - Generating 'tide' in pilot-scale constructed wetlands to enhance agricultural wastewater treatment. *Engineering in Life Sciences* **6**, 560–565 (2006).

47. Elsaesser, D. *et al.* - Assessing the influence of vegetation on reduction of pesticide concentration in experimental surface flow constructed wetlands: Application of the toxic units approach. *Ecological Engineering* **37**, 955–962 (2011).

48. Lavrnić, S. *et al.* - Long-term monitoring of a surface flow constructed wetland treating agricultural drainagewater in Northern Italy. *Water (Switzerland)* **10**, (2018).

49. Bodin, H. *et al.* - Tracer behaviour and analysis of hydraulics in experimental free water surface wetlands. *Ecological Engineering* **49**, 201–211 (2012).

50. Kadlec, R. H. & Wallace, S. *Treatment Wetlands*. *Treatment Wetlands* (2008). doi:10.1201/9781420012514.

51. DuPoldt, C. *et al.* - A Handbook of Constructed Wetlands: General Considerations. *Ecological Engineering* **1**, 53 (1996).

52. J0rgen Lissner, H.-H. S. - Effects of salinity on the growth of Phragmites australis. *Aquatic Botany* **55**, 247–260 (1997).

53. Nada, R. M. *et al.* - Growth, photosynthesis and stress-inducible genes of Phragmites australis (Cav.) Trin. ex Steudel from different habitats. *Aquatic Botany* **124**, 54–62 (2015).

54. Rezania, S. *et al.* - Phytoremediation potential and control of Phragmites australis as a green phytomass: an overview. *Environmental Science and Pollution Research* **26**, 7428–7441 (2019).

55. Vymazal, J. & Březinová, T. - Accumulation of heavy metals in aboveground biomass of Phragmites australis in horizontal flow constructed wetlands for wastewater treatment: A review. *Chemical Engineering Journal* **290**, 232–242 (2016).

56. Srivastava, J. *et al.* - Environmental perspectives of Phragmites australis (Cav.) Trin. Ex. Steudel. *Applied Water Science* **4**, 193–202 (2014).

57. Ayeni, O. *et al.* - Assessment of Metal Concentrations, Chlorophyll Content and Photosynthesis in Phragmites australis along the Lower Diep River, CapeTown, South Africa. *Energy and Environment Research* **2**, (2012).

58. Eller, F. *et al.* - Cosmopolitan species as models for ecophysiological responses to global change: The common reed phragmites australis. *Frontiers in Plant Science* **8**, (2017).

59. Bonanno, G. & Lo Giudice, R. - Heavy metal bioaccumulation by the organs of Phragmites australis (common reed) and their potential use as contamination indicators. *Ecological Indicators* **10**, 639–645 (2010).

60. Kalaji, H. M. *et al.* - Chlorophyll a fluorescence as a tool to monitor physiological status of plants under abiotic stress conditions. *Acta Physiologiae Plantarum* **38**, (2016).

61. Paul, P. *et al.* - Structural and functional heat stress responses of chloroplasts of Arabidopsis thaliana. *Genes* **11**, 1–20 (2020).

62. Foyer, C. H. & Noctor, G. - Redox sensing and signalling associated with reactive oxygen in chloroplasts, peroxisomes and mitochondria. *Physiologia Plantarum* **119**, 355–364 (2003).

63. Sulaiman, M. - An Overview of Natural Plant Antioxidants: Analysis and Evaluation. *Advances in Biochemistry* **1**, 64 (2013).

64. Gomes Silveira, J. A. *et al.* - Proline accumulation and glutamine synthetase activity are increased by salt-induced proteolysis in cashew leaves. *Journal of Plant Physiology* **160**, 115–123 (2003).

65. Cavalcanti, F. R. *et al.* - Superoxide dismutase, catalase and peroxidase activities do not confer protection against oxidative damage in salt-stressed cowpea leaves. *New Phytologist* **163**, 563–571 (2004).

66. Minkina, T. *et al.* - Morphological and anatomical changes of Phragmites australis Cav. due to the uptake and accumulation of heavy metals from polluted soils. *Science of the Total Environment* **636**, 392–401 (2018).

67. Nawrot, N. *et al.* - Heavy metal accumulation and distribution in Phragmites australis seedlings tissues originating from natural and urban catchment. *Environmental Science and*

Pollution Research **28**, 14299–14309 (2021).

68. Kleche, M. *et al.* - Phytoremediation using Phragmites australis roots of polluted water with metallic trace elements (MTE). *Scholars Research Library Annals of Biological Research* **4**, 130–133 (2013).

69. Haus, J. W. - Nanocharacterization. *Fundamentals and Applications of Nanophotonics* 185–210 (2016) doi:10.1016/B978-1-78242-464-2.00006-3.

70. Sadeer, N. B. *et al.* - The versatility of antioxidant assays in food science and safety—chemistry, applications, strengths, and limitations. *Antioxidants* **9**, 1–39 (2020).

71. Miller, N. J. *et al.* - A novel method for measuring antioxidant capacity and its application to monitoring the antioxidant status in premature neonates. *Clinical Science* **84**, 407–412 (1993).

72. Thaipong, K. *et al.* - Comparison of ABTS, DPPH, FRAP, and ORAC assays for estimating antioxidant activity from guava fruit extracts. *Journal of Food Composition and Analysis* **19**, 669–675 (2006).

73. Chua, L. S. *et al.* - Antioxidant activity of three honey samples in relation with their biochemical components. *Journal of Analytical Methods in Chemistry* **2013**, (2013).

74. Elavarthi, S. & Martin, B. - Spectrophotometric assays for antioxidant enzymes in plants. *Methods in molecular biology (Clifton, N.J.)* **639**, 273–281 (2010).

75. Wilschefski, S. C. & Baxter, M. R. - Inductively Coupled Plasma Mass Spectrometry: Introduction to Analytical Aspects. *Clinical Biochemist Reviews* **40**, 115–133 (2019).

76. Soil Survey Staff. - Keys to Soil Taxonomy. *Soil Conservation Service* **12**, 410 (2010).

77. Mason, C. B. *et al.* - A rapid method for chloroplast isolation from the green alga Chlamydomonas reinhardtii. *Nature Protocols* **1**, 2227–2230 (2006).

78. I., A. & L., A. A. - Direct and diffuse photosynthetically active radiation: Measurements and modelling. *Agricultural and Forest Meteorology* **93**, 27–38 (1999).

79. Hu, X. *et al.* - Simple extraction methods that prevent the artifactual conversion of chlorophyll to chlorophyllide during pigment isolation from leaf samples. *Plant Methods* **9**, 1 (2013).

80. Porra, R. J. - Spectrometric Assays for Plant, Algal and Bacterial Chlorophylls. *Chlorophylls and Bacteriochlorophylls* 95–107 (2007) doi:10.1007/1-4020-4516-6_7.

81. Arnon, D. I. - Copper Enzymes in Isolated Chloroplasts. Polyphenoloxidase in Beta Vulgaris . *Plant Physiology* **24**, 1–15 (1949).

82. Ishida, A. & Donnell, D. O. - Quantification of Chlorophyll A Using UV-Vis Absorbance

Spectroscopy. 55104 (2013).

83. Alizadeh-Sani, M. *et al.* - pH-sensitive (halochromic) smart packaging films based on natural food colorants for the monitoring of food quality and safety. *Trends in Food Science and Technology* **105**, 93–144 (2020).

84. Aloisi, I. *et al.* - Natural polyamines and synthetic analogs modify the growth and the morphology of Pyrus communis pollen tubes affecting ROS levels and causing cell death. *Plant Science* **239**, 92–105 (2015).

85. Lichtenthaler, H. K. - [34] Chlorophylls and carotenoids: Pigments of photosynthetic biomembranes. in *Plant Cell Membranes* vol. 148 350–382 (Academic Press, 1987).

86. Ebner, H. *et al.* - Hormonelle Beeinflussung des experimentellen Portiocarcinoms. *Verhandlungen der Deutschen Gesellschaft fur Innere Medizin* **73**, 366–369 (1967).

87. Bhaigyaba, T. *et al.* - Assessment of total flavonoid content and antioxidant activity of methanolic rhizome extract of three Hedychium species of Manipur valley. *International Journal of Pharmaceutical Sciences Review and Research* **30**, 154–159 (2015).

88. Setyati, D. *et al.* - The Flavonoid and Alkaloid Content of Cyclosorus Parasiticus (Linn.) Farwell Ferns At the Plantation Areas of Jember Regency. *BIOLINK (Jurnal Biologi Lingkungan Industri Kesehatan)* **7**, 23–37 (2020).

89. US EPA. - Selected Analytical Methods for Environmental Remediation and Recovery (SAM) – 2012. *United States Environmental Protection Agency* (2017).

90. Bonanno, G. *et al.* - Translocation, accumulation and bioindication of trace elements in wetland plants. *Science of the Total Environment* **631–632**, 252–261 (2018).

91. Kovačević, M. *et al.* - Effects of high metal concentrations on antioxidative system in Phragmites australis grown in mine and flotation tailings ponds. *Plant and Soil* **453**, 297–312 (2020).

92. Ferreira, R. A. *et al.* - Phragmites sp. physiological changes in a constructed wetland treating an effluent contaminated with a diazo dye (DR81). *Environmental Science and Pollution Research* **21**, 9626–9643 (2014).